Finding new drugs for CNS diseases by targeting proteases: the case of matrix metalloproteinase-9 and prolyl oligopeptidase

Nuria Trallero Canela

UNIVERSITAT DE BARCELONA
Facultat de Farmàcia
i Ciències de l'Alimentació

Finding new drugs for CNS diseases by targeting proteases:

the case of matrix metalloproteinase-9 and prolyl oligopeptidase

Nuria Trallero Canela

Universitat de Barcelona

Facultat de Farmàcia i Ciències de l'Alimentació

PROGRAMA DE DOCTORAT EN BIOTECNOLOGIA

"Finding new drugs for CNS diseases by targeting proteases: the case of matrix metalloproteinase-9 and prolyl oligopeptidase"

Memòria presentada per Nuria Trallero Canela per optar al títol de doctor per la Universitat de Barcelona

Tesi doctoral dirigida per:

Dra. Maria Teresa Tarragó Clua

Dr. Roger Prades Cosano

Tutor:

Dra. Josefa Badia Palacin

Nuria Trallero Canela

Barcelona, 2023

Agraïments

Si ja he arribat a escriure aquestes paraules, vol dir que ja he arribat al final d'aquest llarg camí, en el qual hi ha hagut moltes persones que m'han ajudat.

Primer de tot, vull agrair a la Teresa i al Roger per donar-me l' oportunitat de poder fer aquesta tesi amb vosaltres i per tots els coneixements i suport que m'heu donat. He après moltíssim de vosaltres, tant professionalment com personalment. Després, a la Laura, per estar sempre allà des del principi (inclús molt abans de començar aquesta tesi) i per ensenyar-me i transmetre'm moltíssims coneixements. I després a la resta de l'equip d'Iproteos, un gran equip: el Pep, el Jesús, l'Ana, la Chiara, la Carlota i especialment la Sandra i l'Ariadna, que a més de ser unes grans companyes, heu estat unes grans amigues i una part d'aquesta tesi també es vostra. També vull agrair a altres grups del PCB, com a tots els membres del lab del Giralt (Adam, Aurelio, Salva, Cris Fuster, García i Díaz, Pep, Macarena, Monica, Martí i a tots els altres que me deixo) que sempre vau estar allà per ajudar i donar un cop demà quan era necessari, i a la Sònia i al Unai de UQC.

També vull donar les gràcies a totes les altres persones que m'han ajudat i m'han donat molts ànims, sobretot en aquesta última etapa tan llarga. Primer a amigues com la Sandra, l' Ana, l'Helena i la Claudia. Després a tota la gent d'Infinitec, en especial al Fran, gracias por ayudarme tanto y facilitarme las cosas. També al Javi perquè m'has ajudat molt i has estat una persona molt important per a mi. I finalment a la família, perquè sense vosaltres no hauria pogut acabar, gràcies al meu tiet i a la Mari Carmen, i sobretot als meus pares i al meu germà per tota la paciència i suport que m'heu donat.

ABSTRACT

Central nervous system (CNS) diseases are a broad category of conditions limiting health and the ability to function that affects nearly one in six people of the world's population. Proteases are involved in a large number of diseases, which difficult therapeutic treatment since it requires the design of highly selective molecules that inhibits or activate these enzymes in addition to have the capacity to cross the Blood-brain barrier (BBB). Over the last decades, several proteases have been identified as potential targets to treat some CNS related disorders. This is the case of the prolyl oligopeptidase (POP) and the matrix metalloproteinase type 9 (MMP-9), which have been related to the cognitive impairment associate with schizophrenia (CIAS) and epilepsy development respectively.

POP is a cytosolic serine endopeptidase that hydrolyses post-proline bonds of small peptides. It is ubiquitously expressed in the human body, but it has an increased expression and activity in the CNS. POP inhibition is known to have cognitive enhancing and neuroprotective effects in scopolamine-treated rats. An increase activity of POP has been described in plasma from schizophrenia patients but its mechanism of action is not well understood. POP has been suggested to be involved in protein-protein interactions in addition to its enzymatic role. In this regard, several studies suggest that POP interacts with other proteins expressed in neurons and accelerates alpha-synuclein protein aggregation. There are other studies reporting that Akt pathway could have some role in Schizophrenia patients.

Following bibliography evidences and previous experimental results obtained in the group, it has been performed a multiplex assay of this pathway and other related experiments to analyse the role of POP in the Akt pathway. In these experiments it has been confirmed that POP is involved in this pathway and that POP selective inhibition affects PP2A activity.

On the other hand, by means of immunoprecipitations and the western blot techniques, it has been analyzed the potential direct interaction of POP with some proteins such as alpha-tubulin, GAP43, alpha-synuclein or PP2A and its possible involvement in the

autophagic processes. All the experiments were performed in cells cultures or in mice in the presence or absence of the POP inhibitors IPR19 and IPR166, developed previously in the company.

Matrix metalloproteinases (MMPs) are a family of zinc dependent endopeptidases that play an important role in tissue remodelling in physiological and pathological conditions through cleaving extracellular matrix (ECM) proteins. The MMP subfamily of gelatinases is composed by the MMP-2 and MMP-9 which have reported to have a pivotal role in synaptic circuit remodelling, neuroinflammation and BBB maintenance. MMP-9 has been documented to drive the epileptogenesis process in several preclinical models of epilepsy, showing an up-regulation of the protease after a brain insult. High levels of MMP-9 have been also reported in human brain tissue of patients with epilepsy. It is well known that MMP-9 is involved in synaptic plasticity, learning and memory and is recognized as capable to degrade ECM proteins. Despite the robust evidence of the role of MMP-9 in the development of epilepsy and their potential use as a therapeutic target, currently there are no selective MMP-9 inhibitors because the high structural homology between MMPs, which has challenged its use as therapeutic target.

Prior to the start of the present thesis, a family of potent and selective gelatines inhibitors with the capacity to cross BBB were synthesized. These inhibitors, however, have low proteolytically stability in plasma and are not active after oral administration. In this thesis, I have been involved in a team who designed and synthesised new gelatinase inhibitors with a higher rat plasma stability maintaining selectivity, potency and permeability across the BBB to obtain a lead candidate. After the synthesis and several in vitro assays, the two most promising candidates were selected to perform a pharmacokinetics (PK) and solubility studies. Unfortunately, the pharmacokinetics were not satisfactory but first preliminary results of solubility and possible formulations were obtained along the present work.

RESUM

Les malalties del sistema nerviós central (SNC) són una àmplia categoria de condicions que limiten la salut i la capacitat de funcionar que afecta gairebé a una de cada sis persones de la població mundial. Les proteases estan implicades en un gran nombre de malalties, el que dificulta el tractament terapèutic ja que requereix el disseny de molècules altament selectives que inhibeixin o activin aquests enzims a més de tenir la capacitat de creuar la barrera hematoencefàlica. Durant les últimes dècades, s'han identificat diverses proteases com a dianes potencials per tractar alguns trastorns relacionats amb el SNC. És el cas de la prolil oligopeptidasa (POP) i la metaloproteinasa de matriu tipus 9 (MMP-9), que s'han relacionat amb el deteriorament cognitiu associat a l'esquizofrènia i el desenvolupament de l'epilèpsia.

La POP és una serina endopeptidasa citosòlica que hidrolitza els enllaços post-prolina de pèptids petits. S'expressa de manera ubiqua al cos humà, però té una expressió i activitat augmentades al SNC. Se sap que la inhibició de la POP té efectes neuroprotectors i de millora cognitiva en rates tractades amb escopolamina. També s'ha descrit un augment de l'activitat de la POP en el plasma de pacients amb esquizofrènia, però el seu mecanisme d'acció no s'entén bé. S'ha suggerit que la POP està implicada en les interaccions proteïna-proteïna, a més del seu paper enzimàtic. En aquest sentit, diversos estudis suggereixen que la POP interacciona amb altres proteïnes expressades a les neurones i accelera l'agregació de proteïnes alfa-sinucleïna. Hi ha altres estudis que informen que la via Akt podria tenir algun paper en pacients amb esquizofrènia.

Seguint les evidències bibliogràfiques i els resultats experimentals previs obtinguts en el grup, s'ha realitzat un assaig "múltiplex" d'aquesta via i altres experiments relacionats per analitzar el paper de la POP en la via Akt. En aquests experiments s'ha confirmat que la POP està implicada en aquesta via i que la inhibició selectiva de la POP afecta l'activitat de la PP2A.

D'altra banda, mitjançant immunoprecipitacions i la tècnica de "Western Blots", s'ha analitzat la possible interacció directa de la POP amb algunes proteïnes com l'alfa-tubulina, la GAP43, l'alfa-sinucleïna o la PP2A i la seva possible implicació en els processos

d' autofàgia. Tots els experiments es van realitzar en cultius cel·lulars o en ratolins en presència o absència dels inhibidors de la POP IPR19 i IPR166, desenvolupats prèviament a l'empresa.

Les metal·loproteïnases de matriu (MMP) són una família d'endopeptidases dependents del zinc que tenen un paper important en la remodelació dels teixits en condicions fisiològiques i patològiques mitjançant l'escissió de proteïnes de la matriu extracel·lular.

La subfamília MMP de gelatinases està formada per MMP-2 i MMP-9, les quals, tenen un paper fonamental en la remodelació del circuit sinàptic, la neuroinflamació i el manteniment de la BHE. S'ha documentat que la MMP-9 impulsa el procés d' epileptogènesi en diversos models preclínics d'epilèpsia, mostrant una regulació positiva de la proteasa després d'un insult cerebral. També s'han informat nivells elevats de MMP-9 en el teixit cerebral humà de pacients amb epilèpsia. És ben sabut que la MMP-9 està implicada en la plasticitat sinàptica, l'aprenentatge i la memòria, i també es reconeix que és capaç de degradar proteïnes de la matriu extracel·lular. Malgrat l'evidència sòlida del paper de la MMP-9 en el desenvolupament de l'epilèpsia i el seu potencial ús com a diana terapèutica, actualment no hi ha inhibidors selectius de MMP-9 a causa de l'alta homologia estructural entre les MMP, que ha desafiat el seu ús com a diana terapèutica. .

Previ a l'inici d'aquesta tesi, la companyia va desenvolupar una família d'inhibidors de gelatines potents i selectius amb la capacitat de creuar la barrera hematoencefàlica. No obstant això, aquests inhibidors tenen una baixa estabilitat proteolítica al plasma i no són actius després de l'administració oral. En aquesta tesi, he participat en un equip que ha dissenyat i sintetitzat nous inhibidors de la gelatinasa amb una major estabilitat del plasma de rata mantenint la selectivitat, la potència i la permeabilitat a través de la BBB per obtenir un candidat principal. Després de la síntesi i de diversos assajos *in vitro*, es van seleccionar els dos candidats més prometedors per realitzar proves de farmacocinètica i solubilitat. Malgrat que la farmacocinètica obtinguda no va ser la desitjada, es van obtenir uns primers resultats preliminars de solubilitat i possibles formulacions.

INDEX

ABBREVIATIONS

Abbreviations and acronyms

2-CTC: 2-chlorotrityl

ACN: Acetonitrile

AD: Alzheimer's disease

Akt: Protein kinase B

AUC: Area under the curve

BBB: Blood-brain barrier

BSO: L-Buthionine-sulfoximine

CIAS: Cognitive impairment associate with Schizophrenia

CL: Clearance

CL_{int}: Intrinsic clearance

CMA: chaperone-mediated autophagy

C_{max}: Peak plasma concentration

CNS: Central nervous system

co-IP: Co-Immunoprecipitation

DCM: Dichloromethane

DIC: *N,N'*-Diisopropylcarbodiimide

DIEA: *N,N*-Diisopropylethylamine

DMEM: Dulbecco's Modified Eagle Medium

DMF: *N,N*-Dymethilformmaide

DMSO: Dimethyl sulfoxide

DTT: Dithiothreitol

ECM: Extracellular matrix

EGF: Epidermal growth factor

Eq: equivalent

F: Bioavailability

Fmoc: 9-fluorenyl-methoxycarbonyl

GAP_{43}: Growth associated protein

GAPDH: Glyceraldehyde-3-phosphate dehydrogenase

GSK3b: Glycogen synthase kinase 3 beta

HDAC: histone deacetylase

HPLC: High-performance liquid chromatography

IGF1: Insulin-like growth factor 1

IP: Immunoprecipitation

ip: intraperitoneal

IRS-1: Insulin receptor substrate 1

LAMP-2A: Lysosomal associated membrane protein 2a

LC-MS/MS: Liquid chromatography–mass spectrometry

MMP: Matrix metalloproteinase

MMP-9: Matrix metalloproteinase type 9

MMPi: Matrix metalloproteinase inhibitors

MRT: Mean residence time

MT: Microtubule

mTOR: Mammalian target of rapamycin

N/E: not evaluated

NMe: N-mtehylated

NMM: N-methylmorpholine

PAMPA: Parallel artificial membrane permeability assay

PBS: Phosphate buffer saline

PCP: Phencyclidine

PD: Parkinson's disease

Pe: Permeability

PI:C: Polyinosinic:polycytidylic

PI3K: Phosphatidylinositol 3-kinase

PK: Pharmacokinetic

po: orally

POP: Prolyl oligopeptidase

PP2A: Protein phosphatase 2

RPE: Retinal pigment epithelium

sc: subcutaneously

SDS-PAGE: Sodium Dodecyl Sulfate Polyacrylamide Gel Electrophoresis

T: transport

*t*bu: tert-butyl

TFA: Trifluoroacetic acid

UV: Ultraviolet

VPA: Valproic acid

V_{SS}: Volume of distribution at steady state

WB: Western blot

WHO: World Human Organization

Amino acids

Alanine	Ala
Arginine	Arg
Asparagine	Asn
Aspartic Acid	Asp
Cysteine	Cys
Glutamic Acid	Glu
Glutamine	Gln
Glycine	Gly
Histidine	His
Isoleucine	Ile
Leucine	Leu
Lysine	Lys
Methionine	Met
Phenylalanine	Phe
Proline	Pro
Serine	Ser
Threonine	Thr
Tryptophan	Trp
Tyrosine	Tyr
Valine	Val

INTRODUCTION

GENERAL INTRODUCTION

1. Central Nervous System Diseases

The central nervous system (CNS) is one of the most complex systems of the human body responsible for controlling the body's most vital functions, including movement, sensation, perception, cognition, and behaviour. CNS diseases encompasses a broad category of conditions limiting health and the ability to function that affects nearly one in six people of the world's population according to the World Human Organization (WHO) (1). Several factors may account for the development of CNS disorders such as underlaying genetic mutations, metabolic dysregulation, infections, aging, stroke, tumours or environmental factors. Some of the most common CNS diseases include Alzheimer's disease, Parkinson's disease, multiple sclerosis and epilepsy. These diseases have a significant impact on a person's quality of life and are challenging to be treated. While most CNS diseases cannot be completely recovered symptoms can often be managed through a range of therapies such as drug prescription or surgical treatment.

The treatment of brain disorders continues to be a challenge because of the presence of the blood–brain barrier (BBB), a highly specialized and restrictive biological barrier that insulates the central nervous system (CNS) from the other parts of the body that provides an optimal environment for neuronal function and contributing the homeostasis of the CNS (2). The main components of this barrier are the brain endothelial cells that form the brain capillaries. These are supported by cells such as astrocytes and pericytes, which notably contributes to structure of the BBB capillaries (2) (Figure 1) The transport of compounds from the blood to the brain are hampered by the presence of tight junctions between endothelial cells that form the brain capillaries and the presence of these tight junctions accounts for restriction of the paracellular transport. The barrier is also featured by low vesicular transport, high metabolic activity and the presence of an extensive variety of efflux pumps in the lumen of brain capillaries that prevent many xenobiotics and hydrophobic compounds from accumulating in the CNS (2). Although several and promising drugs have been found to treat these disorders, the BBB presence is a limitation

for the therapeutic success (3–5). Currently, more than 98% of all small molecules and 100% of large-molecule pharmaceutical drugs are not able to cross the BBB (6).

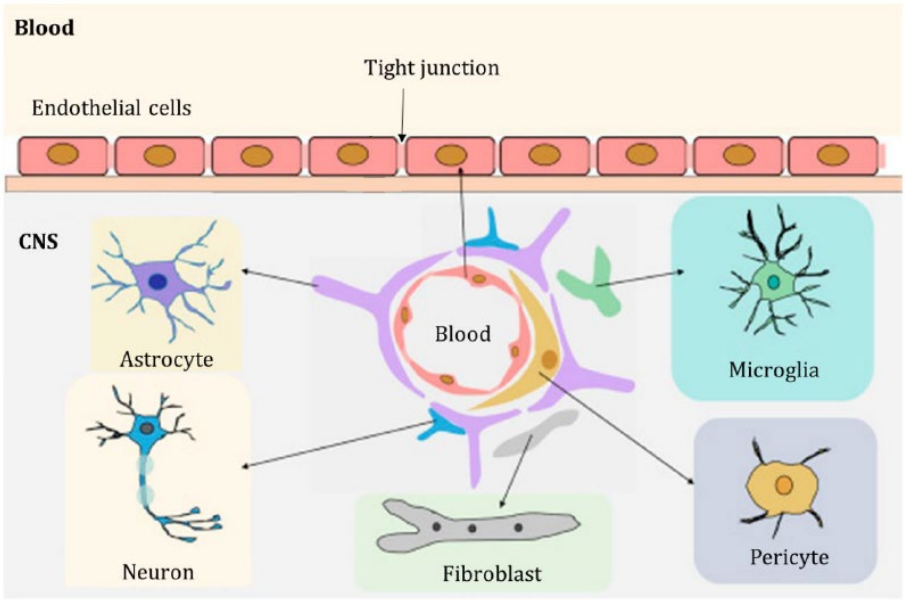

Figure 1. The composition of the BBB microenvironment (image from reference (7)

The pharmacological targets to treat some CNS disorders are proteases. Proteaes are enzymes that catalyze the breakdown of proteins into smaller peptides or amino acids that play a crucial role in many physiological processes (8). The most common strategy to reduce the protease activity is to identify a specific inhibitor, usually consisting in a small molecule, with the ability to block their active sit (8). This is the preferred strategy since protease inhibitors can be designed to be highly specific, blocking only the activity of the targeted protease. However, it is sometimes difficult to avoid side effects because the active sites of targeted proteases are very similar to those of the same family (8) and non related to CNS disorders. In recent years, several proteases have been identified as a promising therapeutics targets for the treatment of these diseases. This is the case of the prolyl oligopeptidase (POP) or the matrix metalloproteinase type 9 (MMP-9) to treat the cognitive impairment associate with Schizophrenia (CIAS) or epileptogenesis respectively.

2. Schizophrenia

Schizophrenia is a brain disorder that impairs mental function (9) and, according to the WHO, affects more than 24 million people worldwide (10). This disease exhibits heterogeneity and manifests various common characteristics among patients affected.

Schizophrenia's symptoms are classified into three broad categories: positive, negative and cognitive dysfunction. Positive symptoms, which are the most pronounced, are psychotic behaviours that include disorganization, hallucinations, delusions and thought disorders. Negative symptoms are associated with disruptions to normal emotions and behaviours and can be confused with depression or other mental conditions (11,12). Cognitive dysfunction are moderate to severe across several domains, including attention, working memory, verbal learning and executive functions. Cognitive impairment associate with schizophrenia (CIAS) imply an inadequacy of normal emotional responses and are characterized by apathy, anhedonia, and a general loss of motivation (11–13). These symptoms are common revealed between adolescence and early adulthood. Along this period, changes in the human lifestyle can promote the appearance of such symptoms that may require chronic medications since no treatment is yet available (12).

Even though there have been significant advances in understanding the biological underpinnings of the disorder and treating positive symptoms, there still remains an insufficient focus on crucial areas such as cognition and social cognition To treat the positive and negative symptoms of schizophrenia there are antipsychotic and antidepressant drugs that limit the effects on cognition deficits but in some cases their side effects may even aggravate some of these deficits. The antipsychotics drugs licensed for the schizophrenia treatment are based on dopamine D2 receptor antagonist but have small effects on cognition function (14). Other psychotropic drugs with anticholinergic effects have a detrimental effect on cognitive function, but reducing the dose to mitigate extrapyramidal side effects has been shown to improve cognitive function. (15). Another strategy that has shown potential is psychological treatments to treat the impairments but have less established evidence (16). Although there are new strategies for treating the positive and negative symptoms of schizophrenia, such as presynaptic neuronal activity,

acetylcholinesterase inhibition or cannabidiol treatment, it has not been clearly demonstrated that these treatments also help to treat CIAS (17).

Therefore, there is not any specific treatment for CIAS (18), despite the fact cognitive impairment is present in over 80% of patients with schizophrenia and is an important determinant of functional disability and indirect costs of the disease. (13).

In recent years, research persuading the identification new pro-cognitive targets has increased (19). Among the new targets, POP has emerged as an innovative candidate for the treatment of CIAS and other mental diseases like Parkinson (18).

3. Prolyl oligopeptidase

Prolyl oligopeptidase (POP, EC3.4.21.26), also known as prolyl endopeptidase (PREP or PO), is an enzyme that has been suggested to be involved in several CNS diseases such as neurodegenerative diseases, mood disorders and cognitive disorders (20–22). POP is a cytosolic serine protease (81kDa) that hydrolyses post-proline bonds of small peptides with less than 30 residues long (23). POP was discovered in the early 1970s in the human uterus and was described as oxytocin-hydrolysing enzyme (24). In later research it was observed that POP has the capacity to metabolize several neuropeptides such as the substance P, neurotensin, arginine-vasopressin and thyrotropin-releasing hormone, among other short peptides involved in learning and mnemonic process. This catalytic activity, however, has only been observed *in vitro* (25,26). A natural *in vivo* ligand of POP has not still been reported in recent research.

3.1. Structure of POP

The first crystallographic structure of POP was obtained by Fulop *et al.* from porcine muscle (27). It was described as a monomeric protein that has an overall cylindrical shape formed by two domains: the α/β-hydrolase and the β-propeller that are linked by a pair of hinge polypeptide chains (27). The catalytic domain is a typical α/β-hydrolase peptidase domain in which the catalytic triad is composed by Ser554, His680 and Asp641 (28). The structural domain consists in a seven-bladed β-propeller with non-conventional properties

that acts as an empty cylinder restricting the size and orientation of the substrates (27). Figure 2 shows the open conformation of the porcine POP homology model.

Molecular dynamics studies suggest that POP is a dynamic enzyme showing an equilibrium between open and close conformation. This conformational equilibrium can be shifted by direct active site POP inhibitors (16,17).

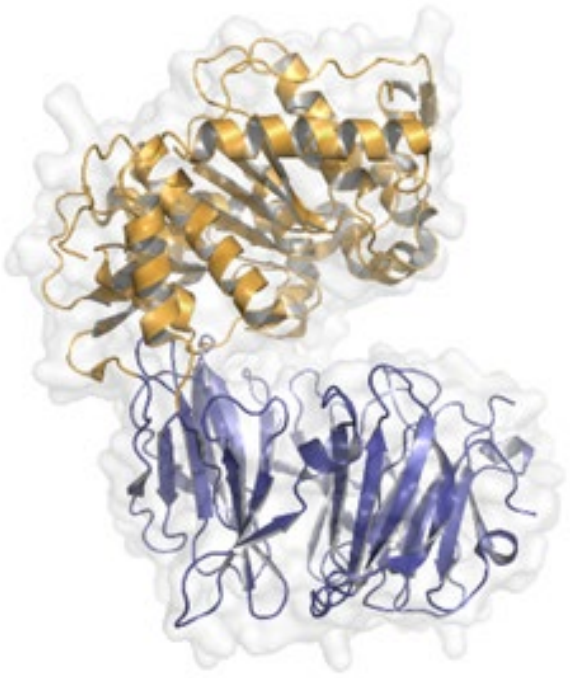

Figure 2. Open conformation of the porcine POP homology model of *Aemonas punctata* POP (PDB entry 3IUJ). β-propeller is shown in blue and α/β-hydrolase domain in orange.

3.2. Biological function of POP

Despite POP is ubiquitously expressed in the human body, an increased expression and activity is observed in the brain tissue, particularly in Purkinje cells and in pyramidal neurons of the cortical layers II to VI and the hippocampal CA1 (31–33) Most *in vitro* POP substrates are small proline-containing neuropeptide or peptide hormones present in the brain, such as substance P, vasopressin, neurotensin or α-melanocyte stimulating hormones (23,26). Moreover, the presence of proline protects these substances from general proteolytic degradation. It is for this reason that the first hypothesis on the *in vitro* role of POP proposed was a specific prolyl hydrolytic function as the main mechanism of

action. There are several studies suggesting that POP activity is altered in patients that suffers from Alzheimer disease, Lewy body dementia, Parkinson's disease, Huntington disease or schizophrenia among others (34). A dysregulation of POP activity has also been found in the serum of patients suffering mood disorders as depression or bipolar disorder (35). In addition to this, experimental data showed that POP inhibition has neuroprotective, anti-amnesic and cognition-enhancing properties in scopolamine-treated rats, whereas it decreases extracellular acetylcholine concentrations in the cortex and hippocampus of rats (36,37). These observations provided the first insights of POP involvement in brain functions. These findings stimulated the development of some POP inhibitors for the treatment of Alzheimer's disease (AD) (38). However, the development of some of these drugs were stopped in clinical stages. The failures of disease-modifying treatments for AD can likely be attributed to several factors. These include the delayed initiation of treatments during AD progression, incorrect drug dosages, incorrect selection of treatment targets and an inadequate understanding of the complex pathophysiology of AD which may need the combination of drug treatments (39).

3.3. POP mechanism of action

It was described by Di Daniel *et al*. (40) the potential role of POP in protein-protein interactions such as with growth associated protein (GAP43), independently of its catalytic action. It was proposed that POP regulates synaptic functions independently of its peptidase activity. According to this, the action of POP inhibitors the action of POP inhibitors could be to induce changes in the tertiary structure of the enzyme thus modifying its protein-protein interactions and not to inhibiting its catalytic activity.

GAP43 is expressed in neurons and is involved in neuronal growth cone formation, axon guidance and calcium-dependent synaptic plasticity. Although the interaction of POP and GAP43 is weak and transient, a clear co-localization of the two proteins has been observed in HeLa cells (40,41).

POP was also reported to be an interactor of α-synuclein, an intrinsically disorder cytosolic protein that aggregates into fibrils. These fibrils are found in Lewy bodies of

Parkinson's patients. It has been suggested that POP/α-synuclein interaction could accelerate the aggregation of α-synuclein (42–44). This process is reversed by the inhibition of POP in preclinical Parkinson models (42,43).

Another POP interaction that has been also described is with α-tubulin suggesting that POP can be involved in processes related to intracellular trafficking and vesicle sorting (45) and glyceraldehyde-3-phosphate dehydrogenase (GAPDH), an interaction that seems to have a key role in genotoxic stress-induced nuclear GAPDH translocation and, consequentially, in cell death (34). It is also known that the pharmacological inhibition or gene deletion of POP counteracts the morphological changes induced by lithium or valproic acid (VPA), leading to changes in gene expression and potentially affecting processes such as neuroplasticity and neuroprotection. and Carbamazepine can also lead to such inhibition in neurons through a mechanism that involves the inositol triphosphate pathway (46). Despite the described findings, more research is needed to elucidate the *in vivo* role of POP.

In recent years, several studies have described the role POP in regulating the activity of several key signalling pathways, including the glycogen synthase kinase 3 beta (GSK3b) and protein kinase B (Akt) pathways (47,48).The phosphatidylinositol 3-kinase (PI3K)/AKT/mammalian target of rapamycin (mTOR) pathway is a signalling cascade that regulates several cellular processes such as cell growth, proliferation, migration, survival, metabolism, apoptosis and autophagy. Its dysfunction has been proposed as the basis of neurodevelopmental and neuropsychiatric diseases such as autism spectrum disorder, epilepsy, CNS tumours, neurodegenerative disorders and several brain malformations (49,50). Schizophrenia has been also related to this pathway (51,52).

These studies suggest that POP may play important roles in the regulation of intracellular signalling pathways, including the GSK3b and Akt pathways, cell survival signalling pathways, cell differentiation, and cell proliferation. Further research is needed to fully understand the molecular mechanisms by which POP regulate these pathways and their potential as therapeutic targets in various diseases.

3.4. POP inhibitors

As explained in the previous sections, the role of POP in the mentioned diseases is not well understood. Several preclinical studies in well-established schizophrenia-like mice models treated with POP inhibitors have demonstrated the memory and cognition-enhancing properties of POP inhibitors (37,53,54). It is hypostatized that the therapeutic benefit observed in these models are due to the blockage of the conformational dynamics of POP rather than the inhibition of the proteolytic activity of the enzyme (55).

The first POP inhibitor was discovered in 1977 with proline-containing chloromethyl ketone-based compounds. Since then, numerous POP inhibitors from a wide diverse origin have been described: natural products such as berberine (56) or synthetised as small molecules, peptides and peptidomimetics (57–59) .

In the early 1980s, it was developed POP inhibitor benzyloxycarbonyl-prolyl-prolinal (ZPP, Figure 3) for the treatment of neurotic pain and as anti-HIV agent (60,61). Despite the highest development phase reached by this inhibitor was preclinical, ZPP is the reference scaffold for the development of many POP inhibitors and were obtained through modifications in several positions of the original molecule. The pharmacophore of these inhibitors is described as a function of the three well-defined enzymatic cavities of POP (S_1, S_2 and S_3) involved in the interaction with the inhibitor (62,63). Therefore, the P_1, P_2 and P_3 positions describe the pharmacophore of the POP inhibitor (Figure 3).

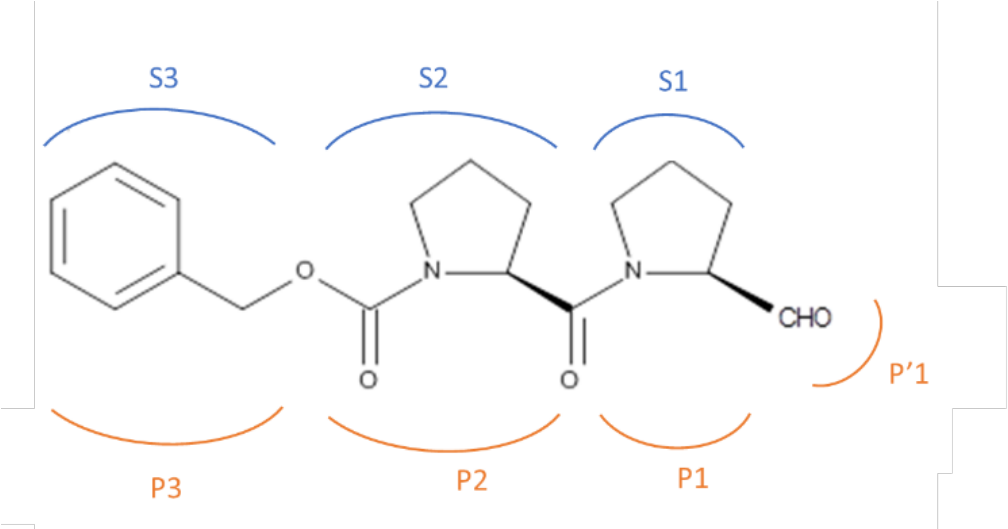

Figure 3. Z-prolyl-propinal structure showing the general scheme of peptidomimetic inhibitor positions (P1, P2 and P3) and the complementary binding sites of the enzyme (S1, S2 and S3)

A common feature of POP inhibitors is the presence of a five-member ring with electrophilic moieties acting as a warhead, covalently interacting with the catalytically active site Ser554 at P1 and specifically fits into S1 (59). The use of highly reactive groups at this position may affect the stability of the inhibitors in serum and cause unspecific binding, thus affecting inhibitor's efficacy and selectivity. The S2 region exhibits relatively lower definition and lacks the same level of steric or electronic requirements compared to S1. Consequently, a broad range of structures, including linear amino acids (both charged and uncharged), proline and simple or fused rings, have been investigated at the P2 position (59). Modifications at P2 can determine the selectivity and potency of the inhibitor. Lastly, S3 is a spacious cavity that can contain an aliphatic spacer attached to a bulky moiety, usually aromatic rings. Despite the large size of S3, a relevant impact on the potency of the inhibitor can produce subtle modifications at P3 (59).

POP inhibitors reported with cognition-enhancing properties and have been tested in animals or have reached clinical trials. Such inhibitors are JTP-4819, KYP-2047, S-17092, ONO-1603, Z-321 and Y-29794 (see **¡Error! No se encuentra el origen de la referencia.**). The chemical structures of those promising drug inhibitors are depicted in **¡Error! No se encuentra el origen de la referencia.**. as it can be easily seen, the latest phase reached amongst them has been Phase II for JTP-4819 and ONO-1603 (18).

Table 1. POP inhibitors structure developed for CIAS treatment

Clinical phase reached	POP inhibitor	Institution	Chemical Structure
Preclinical	KYP-2047	University of Eastern Finland	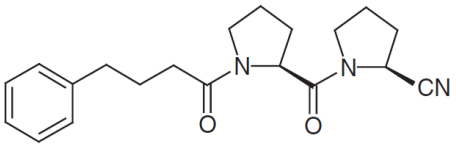
	Y-29794		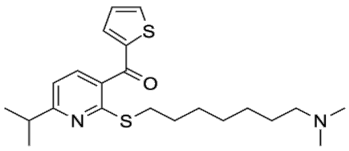
Phase I	S-17092	Servier	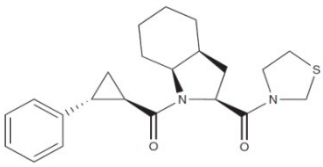
	Z-321	Zeria	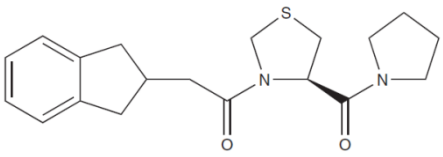
Phase II	JTP-4819	Mitsubishi Tanabe Pharma/Japan Tobacco	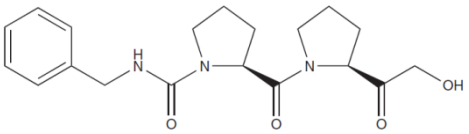
	ONO-1603	Ono	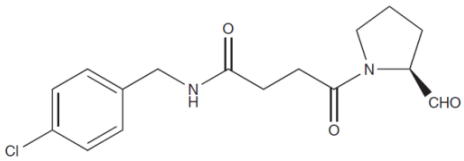

In 1990, Zeria developed Z-321 for treatment of Alzheimer's disease and dementia. The pharmacokinetics and toxicology of Z-321 were tested in humans (18), but unfortunately no cognitive enhancement or learning improvements of this molecule were reported.

In 1994, Mitsubishi Tanabe Pharma and Japan Tobacco described JTP-4819. Studies revealed the anti-amnesic, memory enhancing and improvement in spatial memory effect (64–66). However, the low reproducible results, poor dose dependency and non-predictable behaviour of POP inhibition were incoherent with a simple direct effect (54). Also, it showed poor BBB permeability (59).

Years later, in 2000, the University of Eastern Finland developed KYP-2047 as a POP inhibitor for the treatment of cognition disorders. The results were not as expected because it was detected inconsistencies between the levels of several neuropeptides and IP_3 in response to treatment with this inhibitor (42). In other studies, no significant evidence of mnemonic improvement was observed; in fact, only a slight enhancement of motor skills (67).

In 1998, Ono started investigations on ONO-1603. This POP inhibitor was the first to be reported to prevent age-induced apoptosis of cerebellar granule cells, demonstrating the neuroprotective effects of POP inhibition (68).

In 1996, S-17092 was developed by Servier. This molecule, a potent POP inhibitor increased the performance of cognitive tasks in monkeys with induced Parkinson's disease (69). Besides, it showed cognition-enhancing properties in healthy elderly subjects and a clear dose-dependency. Moreover, no adverse effects were detected. Later studies suggested additional slight mood-stabilizing properties for this compound (70).

POP inhibitors are believed to faile in clinical trials because the lack of efficacy in Alzheimer diseases, a complex disease featured by neurodegeneration and neuronal death with very challenging clinical trials designs due to the lack of biomarkers to stratify patients in the early phases of the disease. CIAS is believed to be a more appropriate indication for POP inhibitors because neurodegeneration and neuronal cell death is not observed. For this reason, it was decided to develop new POP inhibitors for the treatment of the cognitive symptoms of schizophrenia.

Iproteos, S.L. developed the POP inhibitors IPR19 and IPR166 with the capacity to cross BBB for the treatment of CIAS. The efficacy of IPR19 was demonstrated by the acute

administration in three well-established schizophrenia-like mice models reversed the cognitive performance deficits of the three mice models in the novel object recognition test, T-maze, and eight-arm radial maze. Also, the compound ameliorates deficits of the prepulse inhibition response (37).

4. Matrix metalloproteinases

Matrix metalloproteinases (MMPs) are part of a super family of more than 20 zinc-dependent endopeptidases. These proteolytic enzymes are capable of degrading and remodelling proteins of extracellular matrix (ECM) and basement membrane. Other evidences suggest that MMPs participates in a range of physiological processes such as inflammation, immunity, neurite growth and bone remodelling through processing bioactive molecules including cell surface receptors, apoptotic ligands, pro-neurotrophic factors and cytokines (71). It has been described that MMPs are implicated also in several pathological conditions such as cancer, chronic inflammatory or neurodegenerative diseases (72).

4.1 Structure

There are five MMPs subfamilies and they have been classified according to their domain organization: matrilysins, stromelysins, collagenases, gelatinases, membrane-type MMPs and furin-activating. All of them have a *N*-terminal signal peptide directing them to the secretory pathway and a pro-peptide domain followed by a *C*-terminal catalytic domain composed by three histidine residues that coordinate with the zinc ion in the active site. The pro-peptide domain contains a cysteine switch that forms a complex with the catalytic zinc in a catalytic domain inhibiting their enzymatic activity. Matrilysins (MMP-7 and MMP-26) have only the minimal domain. The rest of MMPs have a hinge-region that acts as a linker with an hemopexin-like domain at the *C*-terminal. The difference between stromelysins (MMP-3, MMP-10 and MMP-11) and collagenases (MMP-1, MMP-8 and MMP-13) with gelatinases (MMP-2 and MMP-9) is that gelatinases contain three fibronectin II-like repeats in the catalytic domains. Furthermore, MMP9 is the only MMP that has a heavily O-glycosylated hinge region. Furin-activating (MMP-11, MMP-21 and MMP-28) have a furin-activating motif at the *C*-terminal end of their pro-peptide

domains. Also, all membrane-anchored MMPs (MT-MMPs, MMP-14, MMP-15, MMP-16, MMP-17, MMP-23, MMP-24 and -25) contains a transmembrane domain for binding to the cell membrane. Additionally, the *C*-terminal of MMP-23 contains cysteine array (Ca) and immunoglobulin (Ig)-like domain replacing hemopexin domain in the *C*-terminal catalytic domain (71,73).

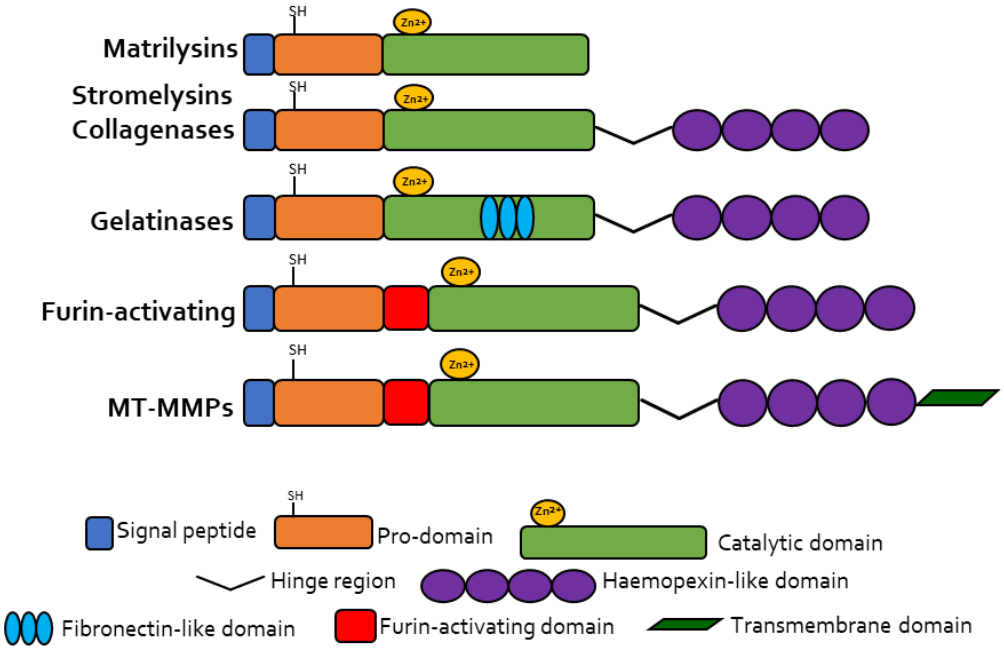

Figure 4. Structural domains of MMPs.

4.2 Activity regulation

MMPs are important regulators for tissue homeostasis and immunity in the network of multidirectional communication within tissues and cells for their extensive substrate spectrum. Therefore, catalytic activity of MMPs is highly controlled at four different levels: 1) gene expression regulation; 2) extracellular localization and tissue or cell type of MMP release; 3) pro-enzyme activation by removal of the pro-domain; and 4) inhibition by specific inhibitors.

MMPs are synthesized as inactive pro-enzymes (zymogens) with a pro-domain which has to be removed for activation. This activation takes place through "cysteine switch" where the free cysteines interact with the catalytic zinc ion when there is a conformational

change. MMP activity can be regulated by the endogenous tissue inhibitor of metalloproteinases (TIMPs) (74,75).

5. Epileptogenesis and MMP-9

Epilepsy is a neurological disorder characterized by recurrent spontaneous abnormal electrical discharges in the brain (seizures) affecting consciousness, perception and motor activity of the patient and affects around 2% to 4% people worldwide (76). There are several commercially available antiepileptic drugs for the management of the seizures that ameliorate the intensity of the seizures. These drugs, however, are not able to slow down the progression of disease or to ameliorate the disorder. Moreover, over 30% of people with epilepsy do not respond to current antiepileptic drugs. In these cases, as an alternative surgery to extirpate the seizure trigger area can be recommended. For these reasons, in the last years, research has been focused in to treat epileptogenesis (77).

Epileptogenesis is the process by which a normal brain develops various alterations in structure and physiology that increase seizures susceptibility and enhance the probability to have spontaneous recurrent seizures. This process can be initiated by several causes such as stress, traumatic brain injury, infection, cancer or genetic background. In general, the research on antiepileptogenic drugs is focused in to prevent the long-term consequences in epilepsy (78).

As previously mentioned, MMP-9 is a gelatinase and one of the most complex proteases of MMP family for its different domains which is composed. Due to its structure complexity, this gelatinase can bind to various substrates such as TIMPs, gelatin or precursors growth factors among others (71,72) . It has been described that various MMP-9 substrates are associated with a number of processes in CNS, such as epilepsy, Alzheimer and Parkinson disease (79).

The expression and activity of MMP-9 in the hippocampus, cerebral cortex and cerebellum is well described and it is related with processes such as synaptic plasticity, learning and memory (80). Over the last years, growing evidences have pointed out MMP-9 as a key player in epileptogenesis, nominating this protease as a highly interesting

therapeutic target for the treatment of epileptogenesis (81). In this regard, it has been observed an upregulated MMP-9 activity in animal models of epilepsy and in humans after seizure (79–81). This upregulation of MMP9 activity in brain tissue triggers neuronal death, aberrant synaptic plasticity and neuroinflammation, which contribute to the progression of epilepsy and exacerbate the occurrence of seizures (82). In contrast to this, MMP-9 deficiency mice are less sensitive to epilepsy inducing agents' seizures, whereas MMP-9 overexpressing rats are more sensitive to these agents (82,83).

5.1 MMP-9 inhibitors for CNS

The development of MMP inhibitors (MMPi) for the treatment of some diseases has been on the pharmaceutical pipeline for some decades without success. The first inhibitors were designed to regulate the MMP activity in cancer because of the increased activity of MMPs in the angiogenesis process, here we found, for example the broad-spectrum inhibitors Batimastat (84), Marimastat (84) or Ilomastat (85) (2). The first drug development strategies consisted in the use of peptidomimetics with a hydroxamic acid moiety as zinc-binding group to promote the chelation of this ion located in the active site of the enzyme (86). This first-generation of MMPi, despite showing a high inhibition potency (nanomolar range), did not have specificity for a give MMPs, hence these were not selective inhibitors. Because of their poor specificity, strong side-effects were reported during the clinical trials, which accounted for the halt down of their development in clinics. Moreover, these molecules had low solubility, low oral bioavailability and a high toxicity (87).

Table 2. MMP inhibitors discussed in this section. Structure and inhibitory potency (IC50 or Ki values).

Inhibitor	Structure	MMP inhibition (IC50/*K_i)
Batimastat	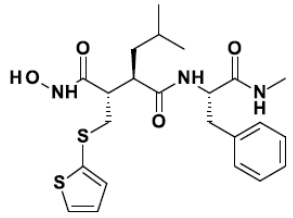	MMP-1= 3 nM MMP-2= 4 nM MMP-3= 20 Nm MMP-7= 6 nM MMP-8= 10 nM MMP-9= 1 nM
Marimastat	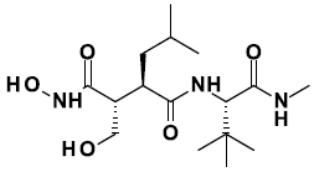	MMP-1= 5 nM MMP-2= 6 nM MMP-3= 200 Nm MMP-8= 2 nM MMP-9= 3 nM MMP-14= 2 nM
Ilomastat	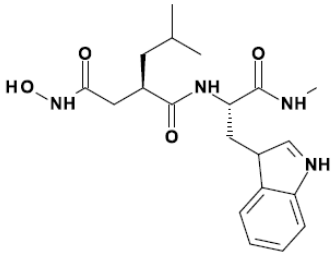	MMP-1*= 0.4 nM MMP-2*= 0.5 nM MMP-3*= 27 Nm MMP-8= 3.7 nM MMP-9*= 0.2 nM MMP-14*= 13.4 nM

Years after a second-generation of MMPi was developed using other zinc-ion chelating moieties with the aim to treat diseases such as arthritis or sepsis. Unfortunately, the new molecules were not reach clinical phases neither for the same reasons than previous generation of MMPi (87).

The design of a selective and potent MMP-9 inhibitor is highly challenging because the structural homology of MMP family members. Furthermore, for CNS conditions, such as epileptogenesis, the molecules must cross the BBB.

Previously, it was developed a family of potent and selective gelatinase (MMP-2 and MMP-9) inhibitors which have the capacity to cross BBB but are not active after good oral administration (88).

4. Perspectives

In the last years, POP and MMP-9 have been identified as a promising therapeutics targets for the treatment of CNS diseases such as CIAS or epileptogenesis, respectively.

For POP, although very promising results have been found for POP inhibitors as cognition enhancers in animal models the evidence by which they have succeeded is not well described. To gain insight into POP mechanism of action different kinds of experiments have been performed in this thesis. On the one hand, several studies have been proposed to try to clarify the possible role of POP in the Akt metabolic pathway. On the other hand, different experiments have been carried out to try to identify or confirm possible direct interactors of POP. And with all these results, to try to understand better the role of this protease in the different CNS diseases with which it has associated. Knowing the POP mechanism of action is crucial for the clinical development of its inhibitors as it may help to develop more effective and targeted therapies.

Related MMP-9, a potent and selective MMP-9 inhibitor was designed prior the accomplishment of this work but is not active after oral administration. For this reason, it was necessary a design and synthesis new candidates with a higher rat plasma stability maintaining selectivity, potency and permeability to obtain a lead oral candidate for non-regulatory clinical phase. Obtaining a molecule with these characteristics, in addition to achieving an unmet medical treatment for epileptogenesis, if it can be administered orally makes the treatment higher compliance with the patient.

OBJECTIVES

In the last years, several proteases have been identified as a promising therapeutics targets for the treatment of CNS diseases. This is the case of POP and MMP-9 to treat CIA) or epileptogenesis, respectively.

For POP, it is known that its inhibition ameliorates the cognitive impairment in amnesia and schizophrenia-like preclinical models but their mechanism of action is still unclear, although there is some data suggesting that it may be involved in the Akt signaling pathway and protein-protein interactions. Therefore, our first goal of the present work is to elucidate the mechanism of action of POP.

Related to MMP-9, a potent and selective MMP-9 inhibitor was designed prior the accomplishment of this work but was not active after oral administration. Hence, our second goal is to develop and optimized MMP-9 inhibitor suitable for oral administration.

Thus, to accomplish our goals, the present thesis is organized based on the following objectives:

1 To elucidate the role of POP in some metabolic pathways:
   - 1.a Study the effects of POP inhibition in proteins of the Akt signaling pathway in mice brain extracts.
   - 1.b Analyze the effects of POP inhibition in proteins of the Akt metabolic pathway in cell cultures.
   - 1.c Study the effects of POP inhibition in proteins of the Akt metabolic pathway in brain extracts from schizophrenia-like mice models.
   - 1.d Study the effects of POP inhibition in PP2A protein and HDAC.

2 To identify the main protein interactions of POP:

2.a Set-up immunoprecipitation (IP) technique for POP.

2.b Validate POP interactors described in bibliography by means of co-IP.

2.c Perform an interactome analysis to identify new POP interactors of active and inhibited POP and confirm the most interesting candidates by co-IP technique.

2.d Study the interaction of POP with PP2A by co-IP.

2.e Study the involvement of POP in autophagic processes.

3 To obtain an optimized MMP-9 inhibitor for oral administration:

3.a Synthesize and evaluate the designed compounds regarding potency and selectivity for MMP-9.

3.b Test the *in vitro* BBB permeability of the compounds.

3.c Study the *in vitro* microsomal and plasma stability of compounds.

3.d Calculate the pharmacokinetics parameters of selected compounds in rats.

RESULTS AND DISCUSSION

The results obtained during the thesis are divided into three chapters. First two refer to the work devoted to POP and the third to MMP-9 inhibitors.

*CHAPTER 1: **Implication of POP in metabolic pathways***

1.1. Introduction

Schizophrenia is a prevalent complex trait disorder, and accumulating evidence has indicated the involvement of the Akt/GSK3 signaling pathway in the pathogenesis of this disorder (51,52). Akt-1 has been identified as a gene related candidate for being susceptible to have schizophrenia because there is evidence that level of Akt protein and its kinase activity decreased significantly both in white blood cells and in post-mortem brain tissue of schizophrenic patients (89). In the same line of these findings, alterations in the upstream and downstream pathways of Akt have also been found in many psychiatric disorders (51,52). Antipsychotic drugs as clozapine modify the Akt signaling pathway in a variety of conditions relative to schizophrenia. It is thought that the reduced activity of PI3K/Akt signaling pathway could, at least, partially explain the cognitive impairment, synaptic morphologic abnormality, neuronal atrophy and dysfunction of neurotransmitter signaling in schizophrenia (51).

Early studies found that POP regulates IRS-1 which is critical for PI3K/AKT/mTOR signaling in pancreatic cancer cells (48).These studies suggest that POP may play important roles in the regulation of intracellular signalling pathway GSK3b and Akt and for these reasons it has been studied the role of POP in Akt signaling pathway in this thesis.

Another protein from the Akt pathway studied is protein phosphatase 2 (PP2A). It is an enzyme that plays a critical role in the regulation of the cell-cycle (90). Its serine/threonine phosphatase activity has a broad substrate specificity and diverse cellular functions. It is known that phosphorylation of Akt at regulatory residues Thr-308 and Ser-473 leads to its full activation, hence PP2A negatively regulating Akt activity. PP2A preferentially dephosphorylates phospho-Thr-308 rather than phospho-Ser-473 (90).

Lithium and valproic acid are effective mood-stabilizing treatments for bipolar affective disorder (91). It has been proposed that inositol depletion and GSK3 inhibition are common outcomes of both drugs and may explain their efficacy (91). Moreover, it has been reported that POP inhibition or the depletion of POP gene counteracts the effects of lithium and valproic acid (VPA) (91,92), thus, suggesting that POP may also be involved in the action of these compounds.

1.2 Akt pathway

Previous internal works has suggested that the proteins expressed in mouse cortex samples treated with the POP inhibitor IPR19 (an inhibitor analogous to IPR166) are almost the same as proteins expressed in control samples. Changes in post-translational modifications, such as phosphorylation were not assessed. Considering these results and the reported implication of POP in the Akt signaling pathway (48), the phosphorylation state of selected proteins from Akt pathway was performed (Figure 5).

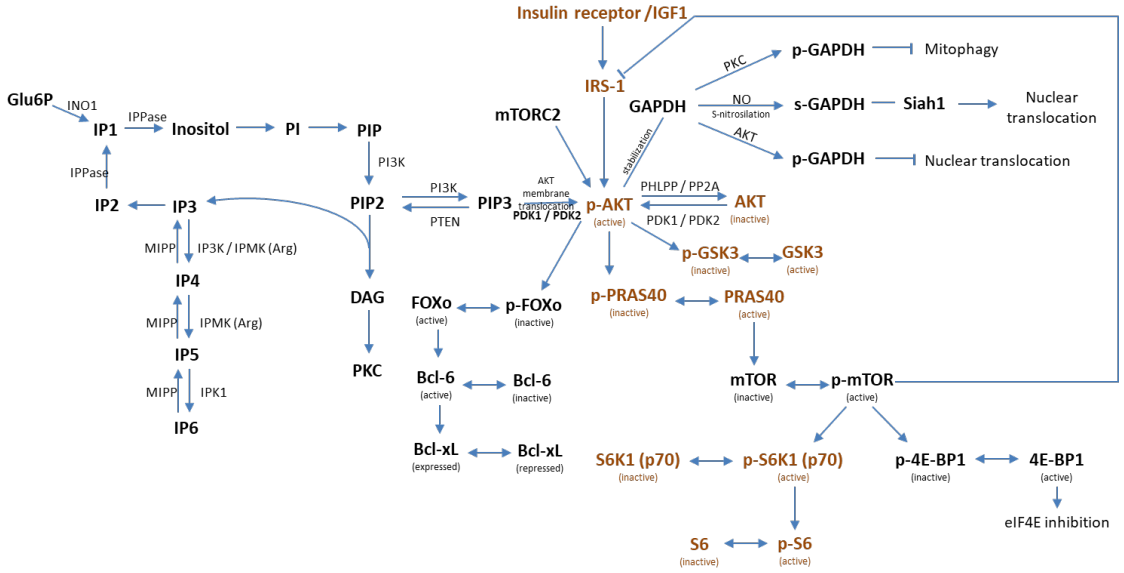

Figure 5. Scheme of Akt and Inositol signaling pathway. In brown are highlighted the selected proteins for the multiplex assay. IGF1: Insulin-like growth factor 1; IRS-1: Insulin receptor substrate 1.

The m*ultiplex assay* kit of total protein and phosphorylated Akt, GSK-3β, IGF-1R, IR, IRS-1, p70S6K and PRAS40 protein was the selected approach for this study.

1.2.1 Multiplex assay

Multiplex Bead Immunoassay Kit allows the quantitation of different proteins of a single sample in same experiment. This technique is a solid phase protein immunoassay that uses spectrally encoded antibody-conjugated beads as the solid support (Figure 6). The assay was performed in a 96-well plate format and analysed with a Luminex® 100™ instrument which monitors the spectral properties of the capture beads while simultaneously measuring the quantity of associated fluorophore.

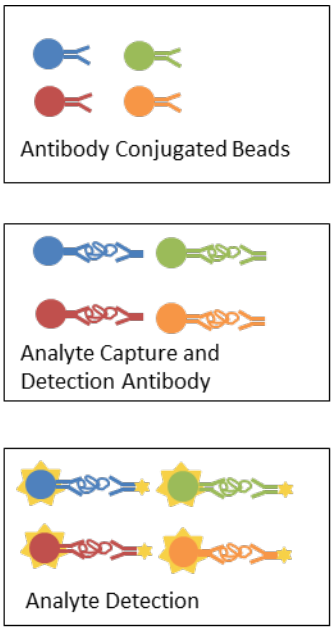

Figure 6. Principle of Multiplex assay

Two different kits (Akt Total and Akt Phospho Magnetic 7-PLEX Panels) were selected for the simultaneous quantitative determination of total and phosphorylated protein. In these experiments, it was analysed half-brain cortex homogenates from adult male C57/Bl6J mice treated with IPR19 (n=8) and untreated (vehicle)(n=8) in duplicate. The animals were injected intraperitoneal (ip) with the vehicle (to) or IPR19 (5 mg/kg, 5% Tween80 in PBS). After, at predetermined time points (45 min and 6 h) animals were euthanized by cervical dislocation. Previous cervical dislocation (6 min before), the animals were anesthetized with chloral hydrate (400 mg/kg).

Phosphoproteome results shown in Figure 7 suggest that samples obtained after 45 min of the injection, had not not significative differences between IPR19 treated and vehicle treated samples. After 6 h of the injection, significative differences were found in the levels of the proteins p-IR (mean 0,57 ± SD 0,02 in IPR19 vs mean 0,44± SD 0,02 in control samples, p=0,0005) and p-IRS (mean 1,09 ± SD 0,03 in IPR19 vs mean 0,86 ± SD 0,05 in control samples, p=0,0024) (Figure 5B and E). An increase in the phosphorylation levels of Akt and p70s6K in the IPR19 treated samples were also found although this difference was not statistically significative (Figure 7A and F).

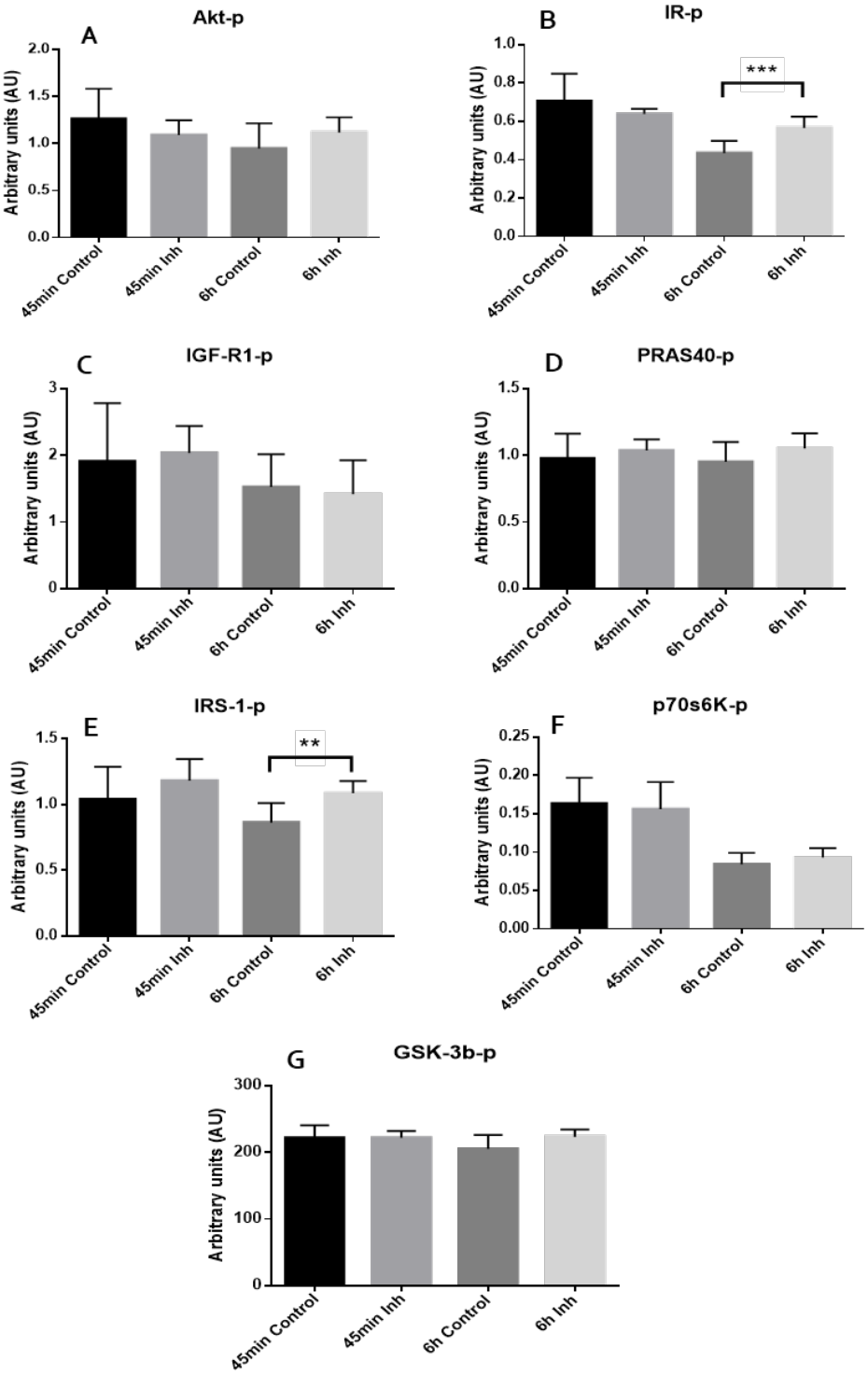

Figure 7. Levels of different selected phosphorilated proteins analysed. n=8. Results are shown as the mean ± SEM of the values obtained from the n independent samples. **B)** *** p=0,0005 6h control vs. 6h IPR19 (Student's t-test) **E)** ** p=0,0024 6h control vs. 6h Inh (Student's t-test)

Regarding the levels of total protein (Figure 8), the group of samples obtained after 45 minutes of the injection showed a significative difference in PRAS40 protein levels (mean 1,46 ± SD 0,16 in IPR19 vs mean 0,84 ± SD 0,05 in control samples, p=0,0077) (Figure 8D). POP inhibitor IPR19 decreases PRAS40 phosphorylation levels since the ratio between p-PRAS40/PRAS40 at 45 min is lower in IPR19 treated samples than in control. These differences, however, were not observed for the animals euthanized 6 h post treatment. Although differences in p-IR and p-IRS protein were observed, when p-IR/IR and p-IRS/IRS ratios are calculated, no differences between treated and untreated samples were observed, thus, suggesting that the phosphorylation levels were the same.

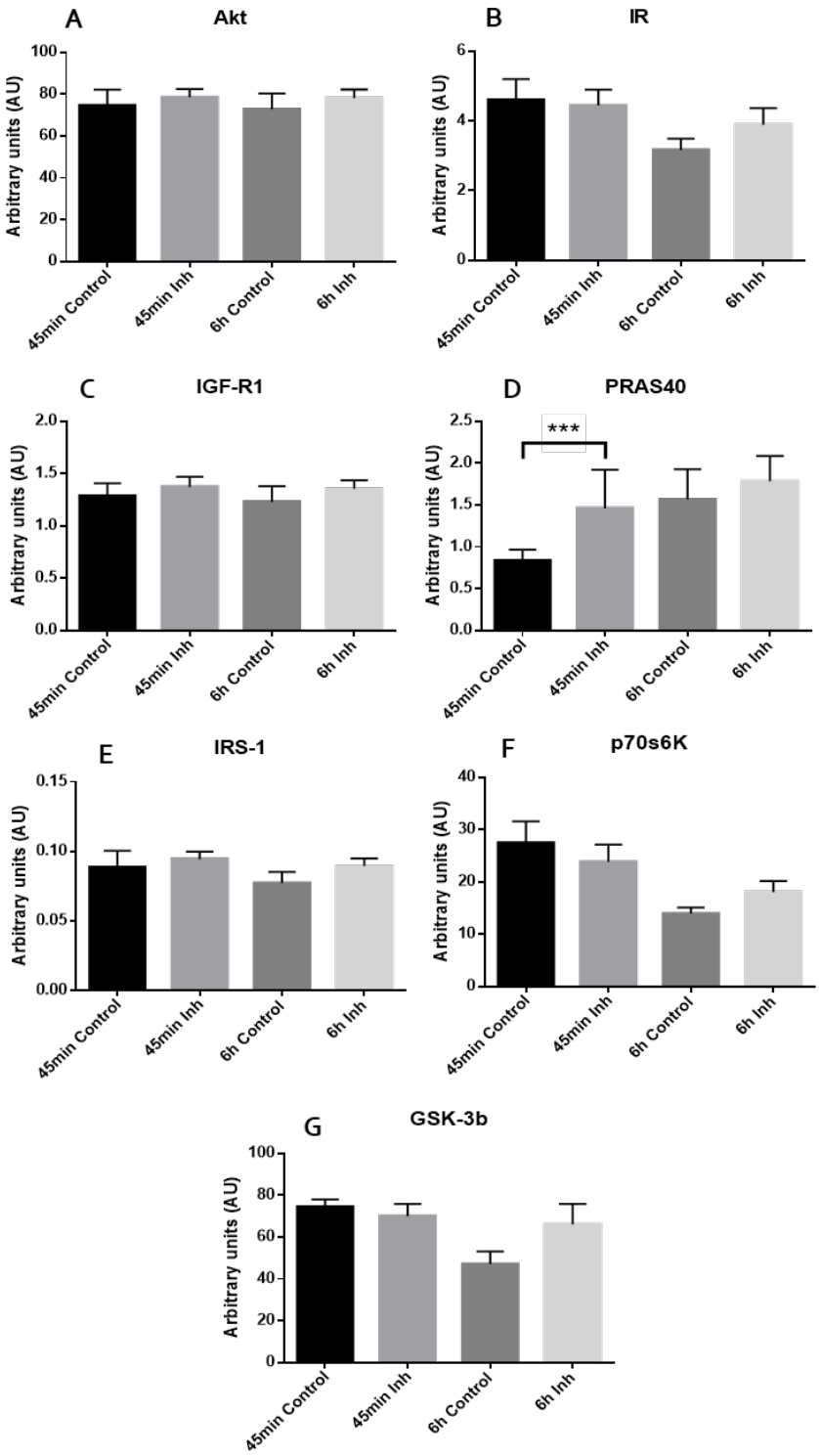

Figure 8. Levels of different selected total proteins analysed. n=8. Results are shown as the mean ± SEM of the values obtained from the n independent samples. **D)** *** p=0,0077 45min control vs. 45min IPR19 (Student's t-test)

These results led to the hypothesis that POP was involved in the Akt pathway. So as to confirm this conjecture, more experiments were carried out. Western blot analysis of different IPR166 treated and untreated samples were performed to assess differences in phosphorylation levels of some key proteins of Akt pathway such as Akt, PRAS40 and S6. The samples used for these experiments were extracts of SH-SY5Y and Retinal Pigment Epithelium cells and brain homogenates from different schizophrenia-like mice models.

1.2.2 Cell extract samples

To elucidate the possible effect of the POP inhibitor on the Akt pathway, the *in vitro* assays had been performed in different cell lines. Cells were stimulated with different compounds to cause a cellular damage, thus, activating in a direct or indirect manner the Akt pathway. After this treatment cells were lysed and the protein extracts were analysed by Western blot. The WB technique is a method used to detect specific protein from among a mixture of proteins previously separate based on their molecular weight. First, to separate the sample's proteins by mass, a Sodium Dodecyl Sulfate Polyacrylamide Gel Electrophoresis (SDS-PAGE) must be performed. The principle of SDS-PAGE is that when proteins are separated by electrophoresis through a gel matrix, smaller proteins migrate faster due to less resistance from the gel matrix. The separated proteins are then transferred from the gel onto a blotting membrane, and this membrane is exposed to an antibody specific to the target protein, and binding of the antibody is detected using a radioactive or chemical tag. The procedure is described in Material and Methods section of the present work (section 4.2).

1.2.2.1 SH-SY5Y cells

SH-SY5Y cells are human cells from neuroblastoma. This cell line is one of the preferred models for the study of neurological disorders and it has been reported that expresses POP (93). Several experimental conditions such as different incubation times and drug concentrations were carried out in order to find an optimized protocol to quantify the protein levels of Akt, pAkt, PRAS40 and pPRAS40 by Western blot. Cells were stimulated to cause a cellular damage (mimicking the cellular damage in CIAS' patients) with L-Buthionine-sulfoximine (BSO) or dizocilpine (MK-801) to activate in an indirect

manner the Akt pathway. BSO is a glutathione-synthesis inhibitor that activates oxidative stress through irreversibly inhibiting γ-GCSc (γ-glutamylcysteine synthetase) and activates Akt pathway increasing Akt levels(94). MK-801 is a non-competitive antagonist of the N-Methyl-D-aspartate (NMDA) receptor that its administration induces schizophrenia-like structural changes in the rat brain (95) and it is used in *in vitro* assays too.

The protein levels of Akt, pAkt, PRAS40 and pPRAS40 were studied by Western blot in samples treated or untreated with IPR166. The most relevant conditions are depicted in Figure 10.

1) 2 μM of IPR166 (in 1 % Dimethyl sulfoxide (DMSO)) preincubated with SH-SY5Y cells for 2 h and additional incubation of 48 h with 10 mM BSO.

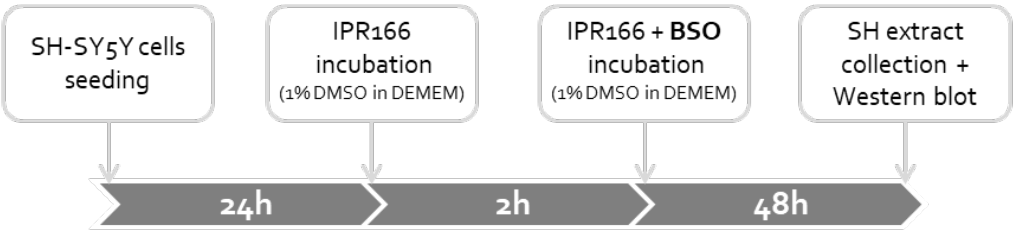

2) 2 μM of IPR166 (in 1 % DMSO) preincubated with SH-SY5Y cells for 2 h and additional incubation of 24 h with 10 mM BSO.

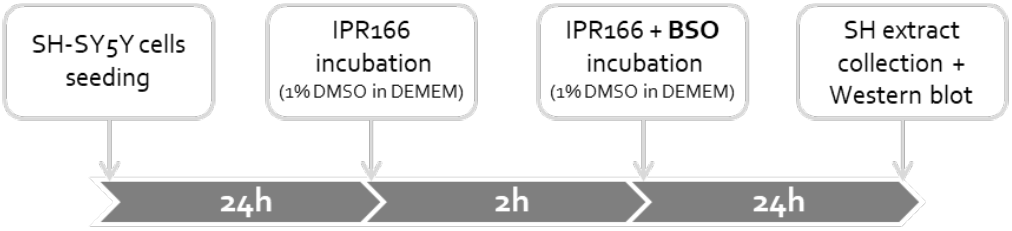

3) 2 μM of IPR166 (in 1 % DMSO) preincubated with SH-SY5Y cells for 2 h and additional incubation of 24 h with 10 μM dizocilpine (MK-801).

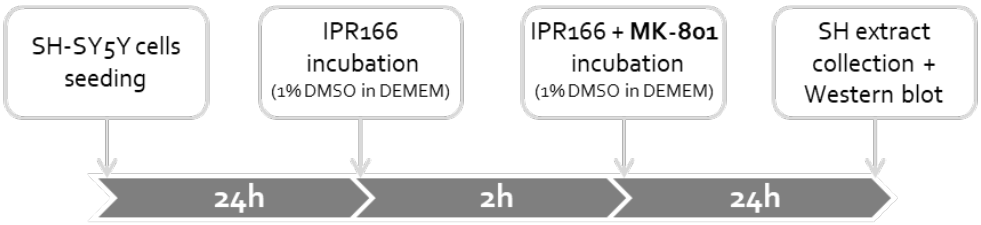

Figure 9. Scheme of different treatments performed in SH-SY5Y cells.

After several attempts testing these conditions, results did not lead to a conclusion due to the high variability obtained between replicates. However, the tendency seems to be that IPR166 does not alter the levels of Akt, pAkt, PRAS40 and pPRAS40 as can be observed in the **Figure *10*** and **Figure *11***.

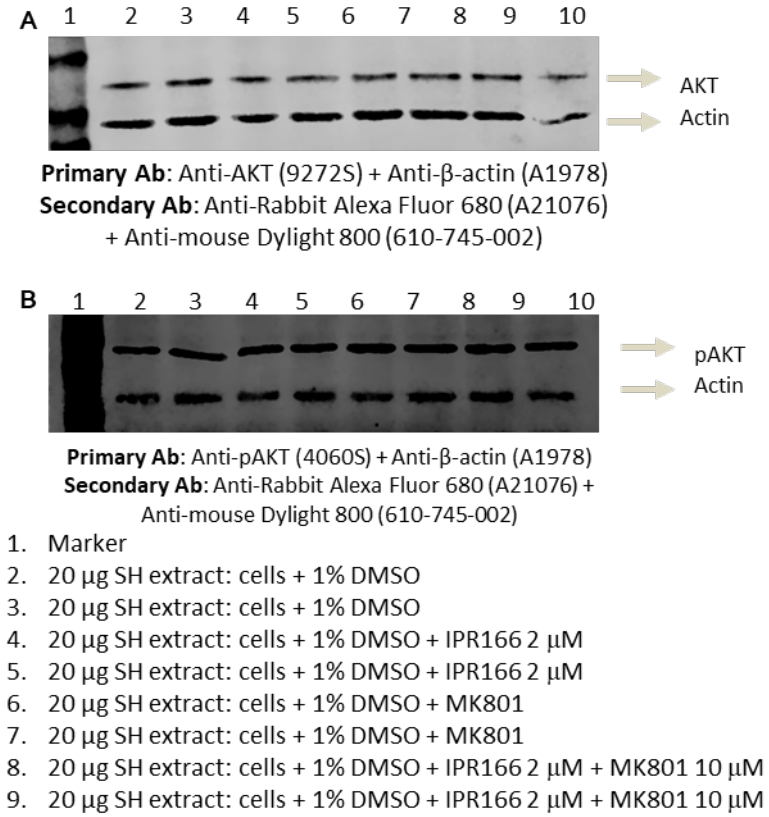

Figure 10. Western blot film of Akt and pAkt levels. **A)** Membrane incubated with anti-Akt antibody obtained from SH-SY5Y cells treated with the condition number 3. Treated with or without IPR166 POP inhibitor and with or without MK801. **B)** Membrane incubated with anti-Akt antibody obtained from SH-SY5Y cells treated with the condition number 3. Treated with or without IPR166 POP inhibitor and with or without MK801.

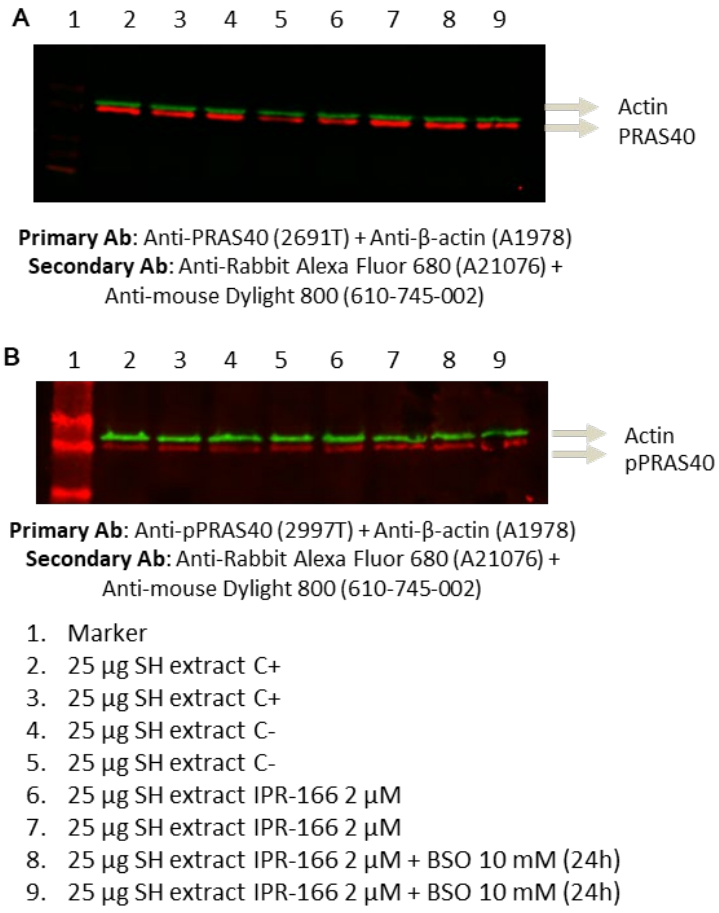

Figure 11. Western blot film of PRAS40 and pPRAS40 levels. **A)** Membrane incubated with anti-PRAS40 antibody obtained from SH-SY5Y cells treated with the condition number 2. Treated with or without IPR166 POP inhibitor and with or without BSO. **B)** Membrane incubated with anti-pPRAS40 antibody obtained from SH-SY5Y cells treated with the condition number 3. Treated with or without IPR166 POP inhibitor and with or without BSO.

1.2.2.2 RPE cells

Considering the poor results obtained in SH-S5Y5 cells extracts a retinal pigment epithelium (RPE) cell line, gently provided by Dr Agell (Hospital Clínic de Barcelona) was selected because it had been widely reported in similar experiments (96). Cells were treated with IPR166 and stimulated with epidermal growth factor (EGF), an activator of Akt pathway, including Akt (97).

The experimental conditions carried out in this study are summarized in Figure 12.

1) 2 µM of IPR166 (in 1 % DMSO) preincubated with RPE cells for 1 h and additional incubation of 10 min with 12.5 µM Epidermal Growth Factor (EGF).

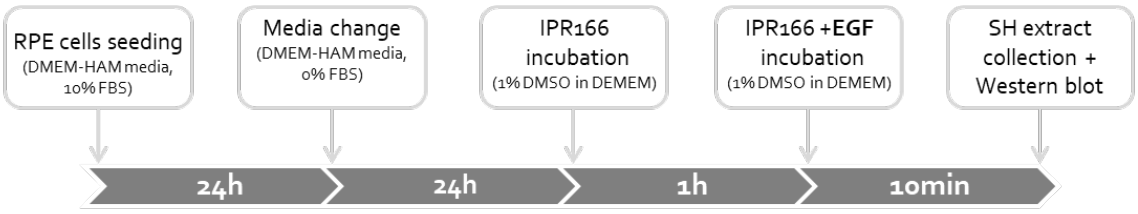

Figure 12: Scheme of treatment performed in RPE cells.

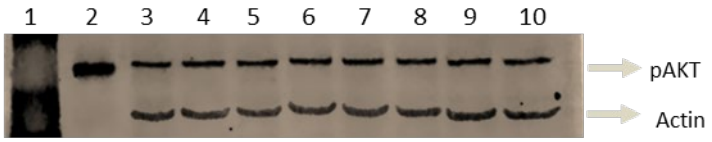

Primary Ab: Anti-pAKT-Ser473 (4060S) + Anti-β-actin (A1978)
Secondary Ab: Anti-Rabbit Alexa Fluor 680 (A21076) + Anti-mouse Dylight 800 (610-745-002)

1. Marker
2. pAKT control
3. 30 µg RPE cell extract: cells + 1% DMSO + 0,05 ug/mL EGF
4. 30 µg RPE cell extract: cells + 1% DMSO + 0,05 ug/mL EGF + 2 uM IPR-166
5. 30 µg RPE cell extract: cells + 1% DMSO + 0,05 ug/mL EGF
6. 30 µg RPE cell extract: cells + 1% DMSO + 0,05 ug/mL EGF + 2 uM IPR-166
7. 30 µg RPE cell extract: cells + 1% DMSO + 0,05 ug/mL EGF
8. 30 µg RPE cell extract: cells + 1% DMSO + 0,05 ug/mL EGF + 2 uM IPR-166
9. 30 µg RPE cell extract: cells + 1% DMSO + 0,05 ug/mL EGF
10. 30 µg RPE cell extract: cells + 1% DMSO + 0,05 ug/mL EGF + 2 uM IPR-166

Figure 13. Western blot film of pAkt levels. Membrane incubated with Anti-pAkt antibody obtained from treated RPE cells with or without IPR166 POP inhibitor.

As shown in Figure 13, no differences were observed in pAkt levels between IPR166 treated (lane 4, 6, 8 and 10) and non-treated cells (lane 3, 5, 7 and 9), thus concluding that POP inhibition is not affecting pAkt levels in RPE cells.

1.2.3 Mice brain extract samples

After the inconclusive results for the Akt and pAkt levels in cell extracts, it was decided to repeat the experiments with mice brain homogenates because, it is a different kind of sample where to perform the studies, and the positive results obtained from *in vivo* samples, then are more translational.

1.2.3.1 Phencyclidine Mice model

The phencyclidine (PCP) model is a mouse model with behavioural responses that resemble the symptoms of schizophrenia. The treatment the adults' rodents with phencyclidine impairs different behavioural effects than the control ones (98). Specifically, the study analyses the activity of three different doses of IPR166 at 5 mg/kg, 2.5 mg/kg and 1mg/kg orally (po) diluted in Tween80 5% in saline or vehicle (5% Tween80 in saline) po administered in old male CD-1 mice 60 minutes before the euthanized. Cognitive deficit was induced by 3 mg/kg PCP given subcutaneously (sc) 30 min prior being euthanized. Five treatment groups were used in this study: saline/ vehicle, PCP/vehicle, PCP/ 5 mg/kg IPR166, PCP/ 2.5 mg/kg IPR166 and PCP/ 1 mg/kg IPR166.

After the corresponding treatment, animals were sacrificed and brains were extracted and homogenized according to the protocol described in the Material and Methods section of this thesis (section 2.4). The Akt and pAkt level were also analysed by WB Table 2 shows the Akt and pAkt levels registered using actin levels as protein for normalization. Some samples were quantified in duplicate or triplicate due to experimental organization and in order to optimize all available wells in each SDS-PAGE gel.

Table 3. Western blots results of relative levels of Akt and pAkt of different mice brain extracts samples

		Replicate 1		Replicate 2		Replicate 3	
Sample number	Treatment	pAKT	AKT	pAKT	AKT	pAKT	AKT
1	IPR166 5 mg/PCP	0,36	3,16				
2	IPR166 5 mg/PCP	0,72	3,82				
11	IPR166 5 mg/PCP	0,55	8,90				
18	IPR166 5 mg/PCP	0,83	7,49				
19	IPR166 5 mg/PCP	0,35	6,30	1,38	6,68		
5	IPR166 2.5 mg/PCP	0,54	3,33				
6	IPR166 2.5 mg/PCP	0,58	4,55				
13	IPR166 2.5 mg/PCP	0,42	8,92				
22	IPR166 2.5 mg/PCP	0,30	6,69	0,89	5,90		
23	IPR166 2.5 mg/PCP	0,49	5,22	2,31	13,06		
9	IPR166 1 mg/PCP	0,51	4,59				
16	IPR166 1 mg/PCP	0,69	8,61				
17	IPR166 1 mg/PCP	0,39	6,38				
10	IPR166 1 mg/PCP	0,50	5,98	1,25	13,09		
25	IPR166 1 mg/PCP	0,80	9,71	1,72	13,32		
3	IPR166 vehicle/PCP	0,70	4,80				
4	IPR166 vehicle/PCP	0,54	4,19				
12	IPR166 vehicle/PCP	0,28	5,21				
20	IPR166 vehicle/PCP	0,37	4,60				
21	IPR166 vehicle/PCP	0,36	6,52	1,35	5,32		
7	IPR166 vehicle/saline	-	4,99	0,64	5,71	0,03	7,57
8	IPR166 vehicle/saline	-	5,49	0,60	8,73	0,15	7,04
14	IPR166 vehicle/saline	0,46	7,41				
15	IPR166 vehicle/saline	0,31	5,45				
24	IPR166 vehicle/saline	0,53	6,08	1,49	7,97		

As it can be observed in Table 3, the obtained results have a great variability between samples and replicates, thus, differences observed were not statistically significant. There are two hypothesis by which these difference are observed: *in vivo* samples were handled, thus, leading to an intrinsic variability between individuals and phosphate groups of the samples were lost very quickly with handling. An example of a WB membrane of the analysis of both proteins is shown in Figure 14.

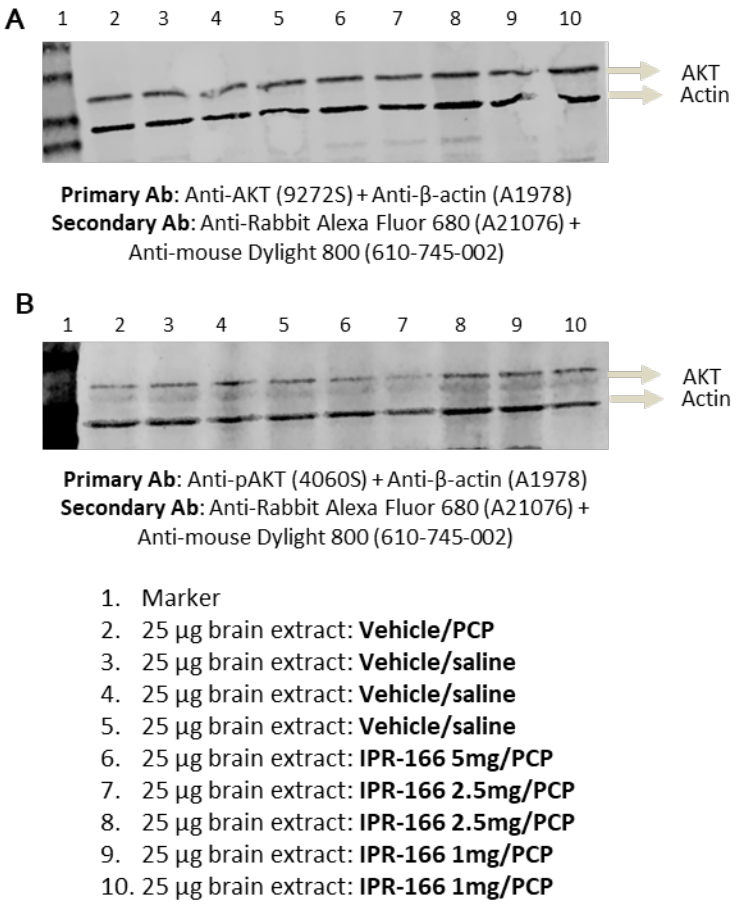

Figure 14. Western blot results of Akt and pAkt levels. Membranes incubated with **A)** Anti-Akt antibody and **B)** Anti-pAkt antibody obtained from mice brain extracts treated with or without IPR166 POP inhibitor.

1.2.3.2 Polyinosinic:polycytidylic (PI:C) mice model

The polyinosinic:polycytidylic (PI:C) mice model is a validated animal model of cognitive deficits of schizophrenia based in the treatment of the pregnant mouse with the viral mimic polyinosinic:polycytidylic acid , which mimics viral infection during pregnancy and elicits in the offspring schizophrenia-like neurochemical, morphological and behavioural changes that resemble those in other rodent models of psychosis (99,100). Bacterial or viral infections during the second trimester of gestation increase the likelihood that the offspring will go on to develop schizophrenia in adulthood. It is thought that an increase in pro-inflammatory cytokines in response to infections are able to alter fetal neurodevelopment in a way that increases vulnerability to the disease (101–103).

Prof. Javier Meana, Dr. Leyre Urigüen, Dr. Eva Munarriz and team from Universidad del País Vasco (UPV/EHU) assessed Akt, pAkt, S6, pS6, PRAS40 and pPRAS40 levels in different mice brain extract samples. Experiments were conducted using C57/BL6 mice. On day 9.5 of pregnancy, female mice received ip injection of polyinosinic:polycytidylic acid (7.5 mg/kg i.p.) or saline. Offspring were separated from their mothers after three weeks. Subsequent experiments were performed in adult (8–10 weeks at the beginning) male mice. Specifically, the study analyses the activity of a single dose of IPR166 at 5 mg/kg ip diluted in Tween80 5% in saline or vehicle (5% Tween80 in saline) ip. Four treatment groups were used in this experiment: saline/ vehicle, saline/ IPR166, (PI:C) /vehicle and (PI:C))/ IPR166. After the corresponding treatment, animals were euthanized 30 minutes post-treatment and the brains were extracted and homogenized according to the protocol described in Material and methods section of this thesis (section 2.4).

In order to analyse the protein levels by Western blot, samples from different mice with the same administration treatment were pooled as there was not enough mouse brain sample from each animal to carry out the experiments.

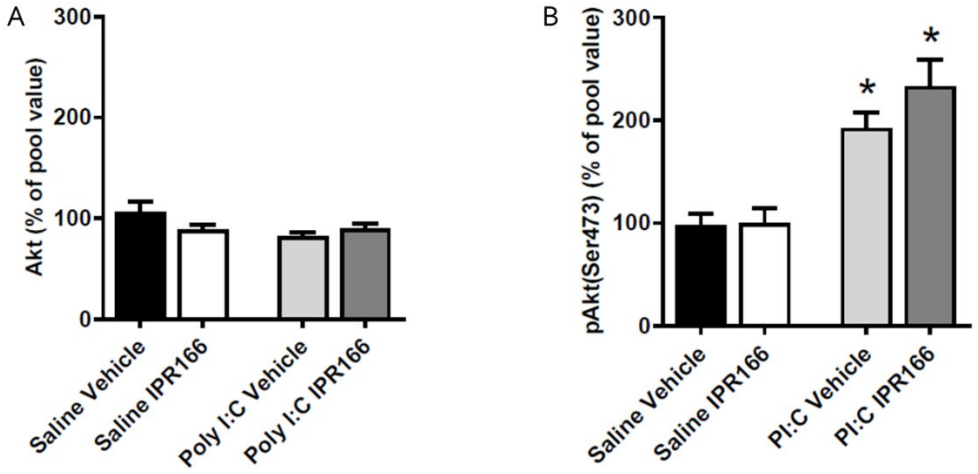

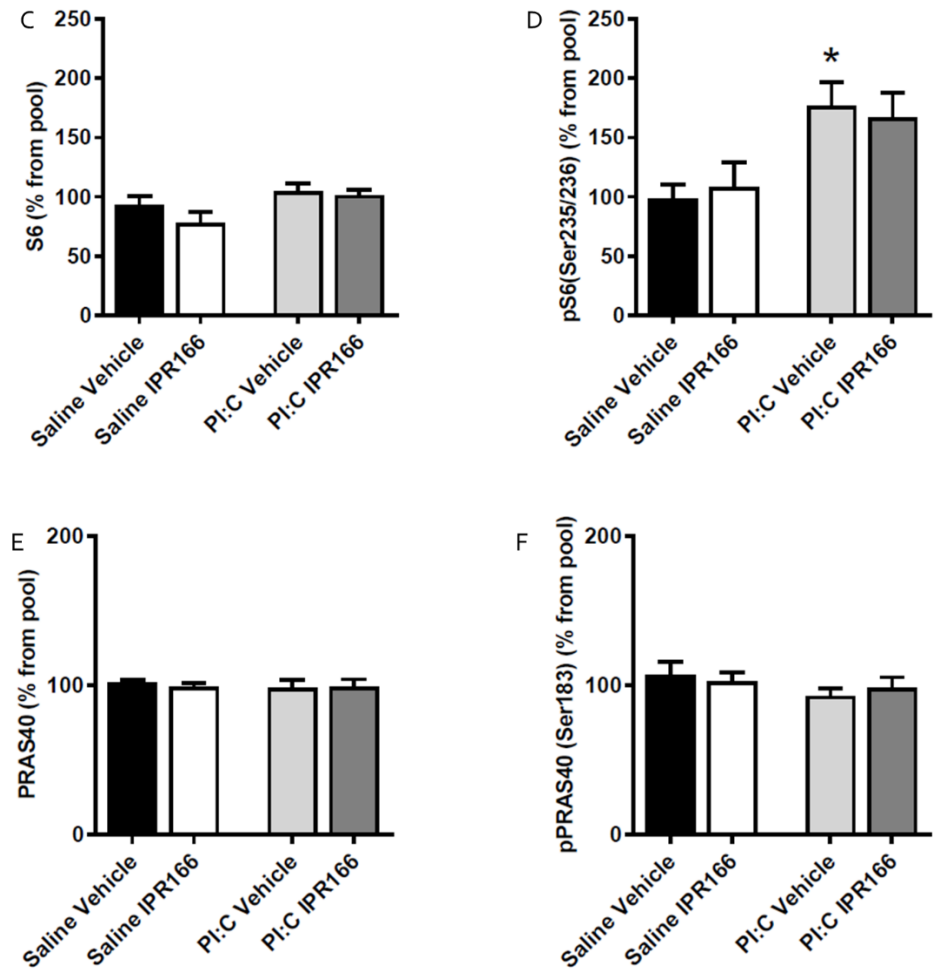

Figure 15. Western blot results of relative levels of different protein of mice brain extracts samples.

Figure 15 indicates that PI:C mice have increased pAkt and pS6 levels than control mice (Saline). According to total protein levels, these differences were not observed. Interestingly, it was observed that PI:C mice treated with IPR166 maintained the same high levels of pAkt as those treated with vehicle, but when pS6 levels were analysed, it was observed that the treatment with IPR166 reduced the expression of this protein to levels like those of the control animals. Thus, it seemed that POP inhibition restored pS6 levels in this schizophrenia mice model. The protein level differences were neither observed in PRAS40 samples nor pPRAS40.

Obtaining these results in PI:C mice model were very relevant because the offspring had the damage and were likely to developed schizophrenia in their adulthood, therefore, this makes it as close to a brain as possible with CIAS.

In summary, after all these experiments, it seems that POP could be related to Akt pathway, but the obtained results are not fully conclusive. More research in this area should be performed.

1.2.4 PP2A activity

Some experiments evaluating whether POP is somehow involved in PP2A activation were performed. SH-SY5Y cells were treated with POP inhibitor IPR166 to analyse if PP2A activity was modified. This phosphatase is one of the reported Akt inactivators.

PP2A Immunoprecipitation Phosphatase Assay Kit utilizes the Malachite Green and contains components that have been matched to optimize sensitivity and range of detection of PP2A. The performed experiment consisted in an immunoprecipitation (IP) of PP2A from SH-SY5Y cell lysates and the subsequent assessment of its activity. The activity was measured through the quantification of the dephosphorylation of the phosphopeptide (K-R-pT-R-R), which is substrate of PP2A. After some experiments to optimize the protocol, the cells were treated with 2 μM IPR166 for 1h and the cell lysate was extracted. Detailed experimental conditions can be found in Material and Methods section of this thesis (section 4.4).

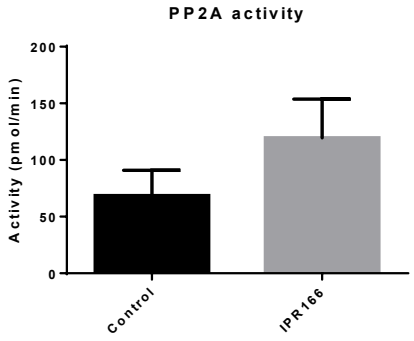

Figure 16. PP2A activity levels in pmol/min. Results obtained from enzymatic activity after treated and untreated with IPR166 SH-SY5Y cells. n=3. Results are shown as the mean ± SEM of the values obtained from the n independent samples. No significant differences have been observed between assayed conditions. (Student's t-test)

Although Figure 16 shows that there was a tendency in which POP inhibition increase PP2A activity in SH-SY5Y cells, this increase was found to be statistically non-significant (n=3, p-value=0,096). To confirm these results, the experiment should be performed with a higher number of samples.

To investigate whether POP caused this modification on PP2A activity thought a direct interaction of both proteins, a co-immunoprecipitation (co-IP) POP-PP2A was performed (See Chapter 2: POP interactors, section 2.5). The results were analysed by Western Blot and indicated that POP was modulating PP2A activity somehow that does not imply a direct interaction between them.

It has been observed that in presence of POP inhibitor IPR166, PP2A activity is higher than at basal conditions. Considering that PP2A is a phosphatase that dephosphorylates Akt, it could seem logical that a decrease in pAkt levels could also observed in presence of IPR166 as in the previous experiments.

In 2020, Svarcbahs, Myöhänen *et al*. (104) reported a study where POP was identified as a negative regulator of PP2A. The publication described the performance of different experiments with PP2A complex and confirmed that the inhibition of POP with a small inhibitor could activates PP2A. Moreover, the study confirmed that the deletion of POP had a similar effect while POP overexpression or restoration inhibited PP2A from cell

cultures to *in vivo* (104). Therefore, this study confirms our PP2A activity-POP inhibitor preliminary results.

1.3 Histone deacetylase pathway

As mentioned before, POP inhibition or the depletion of POP gene counteracts the effects of lithium, carbamazepine and valproic acid (VPA) (91,92), three effective mood stabilizers whose mechanism of action is related with inositol depletion. VPA has also been described as histone deacetylase (HDAC) inhibitor (105). Thus, it was studied if POP inhibition had also an effect over HDAC activity. This activity was measured *in vitro* using a commercial assay kit (HDAC Activity Assay kit). HeLa Nuclear extracts were treated with 0.5 and 1 μM POP inhibitor IPR166 in triplicate and HDAC activity was assessed as described in Materials and Methods section of this thesis (section 4.5).

Results obtained are depicted in Figure 17. This figure shows that POP inhibition is not affecting HDAC activity because there were no differences observed between IPR166 treated and non-treated (C+) cell extract. Therefore, it seemed that POP inhibition had no relation with HDAC activity even though POP inhibition reverts the effects of VPA (91).

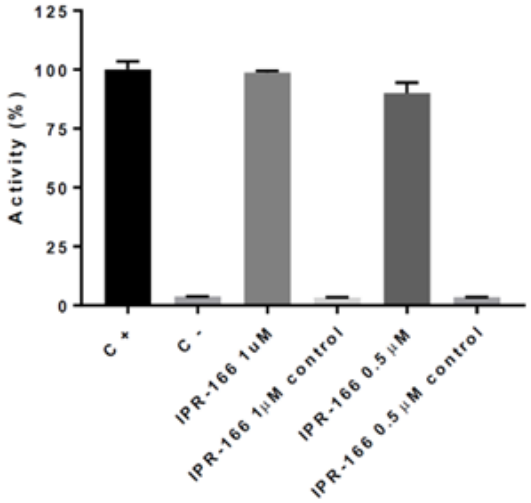

Figure 17. Percentage of HDAC activity in HeLa Nuclear extracts treated with 0.5 and 1 μM IPR166. n=3. Results are shown as the mean ± SEM of the values obtained from the n independent samples. No significant differences have been observed between assayed conditions.

1.4 Summary of the chapter

Even though the role of POP and its mechanism of action in some diseases that cause cognitive impairment have not been elucidated, there were some indications in the bibliography and in previous results from the company that it may be involved with Akt metabolic pathway. For this reason, it was decided to perform assays to try to obtain evidence that POP activity directly affects Akt protein or some other protein (and their phosphorylation versions) of this metabolic pathway. To carry out these experiments, cellular and in vivo models have been used, including cognitive deficits' validated mice models. Although positive results have been obtained, such as POP inhibition decreases pAkt levels, these have not been a hundred per cent confirmed. Further experiments should be carried out to confirm these results.

Experiments have also been carried out to look at the relationship of the PP2A protein with POP and our results have subsequently been validated with other studies carried out by other groups.

CHAPTER 2: ***POP interactors***

2.1 Introduction

During last years, there have been a growing interest in elucidating POP's interactors because their potential involvement in POP's biological role in physiological and pathological conditions. In this regard, several POP interactors have been described, such as α-synuclein, GAP43 or GAPDH among others (40,45,106,107). To shed light about these interactions, several experimental techniques such as yeast-two-hybrid, immunoprecipitation, protein complex co-immunoprecipitation or enzyme-linked immunoassay assays have been used (40,41).

The objective of this chapter is to confirm the POP interactors reported in the literature. For this purpose, we selected immunoprecipitation (IP) as a technique to isolate POP (and interactors) from cell extracts. This isolation or purification step was followed by interactome mass spectrometry analysis to validated reported POP interactors and, additionally, investigate the effect of POP inhibitors IPR19 and IPR166 on POP's interactome.

IP is a technique suitable for the isolation of a particular protein from complex mixtures such as cell culture extracts. The assay is based on the immobilization of antibodies (against the target protein) on beads from different materials, which are mixed with the cell extract. Afterwards, the beads are recovered from the mixture and the "fished" targeted protein is dispatched from the beads.

In order to detect POP interactors, the first step was to optimize the IP experimental conditions to isolate POP from the cell extracts.

2.2 Immunoprecipitation optimization

Immunoprecipitation can be done using three approaches: direct method (pre-immobilized antibody approach), indirect method (the specific antibody for the selected protein is added directly to the antigen sample) (Figure 18) or mixed method (the antigen sample, the specific antibody and the beaded support are all incubated together at the same time) (Figure 19). In the direct method, the antibodies are covalently attached (cross-linking technique) to the beads in advance, providing a better control on antibody binding.

This approach allows to avoid antibody elution and interferences during the subsequent analysis steps. In the indirect method antibodies are incubated with the antigen before beads are added to the cell extract mixture. This approach is usually considered to be more friendly because has fewer steps. However, this approach is only suitable when antibodies do not interfere with following steps.

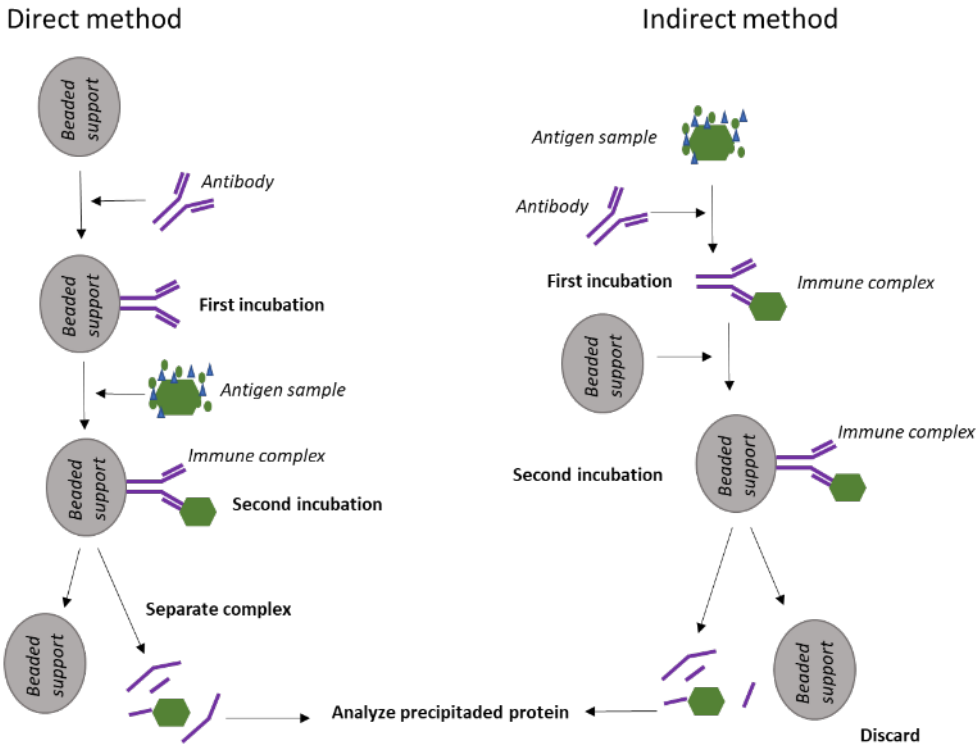

Figure 18. Scheme of Direct and indirect IP method

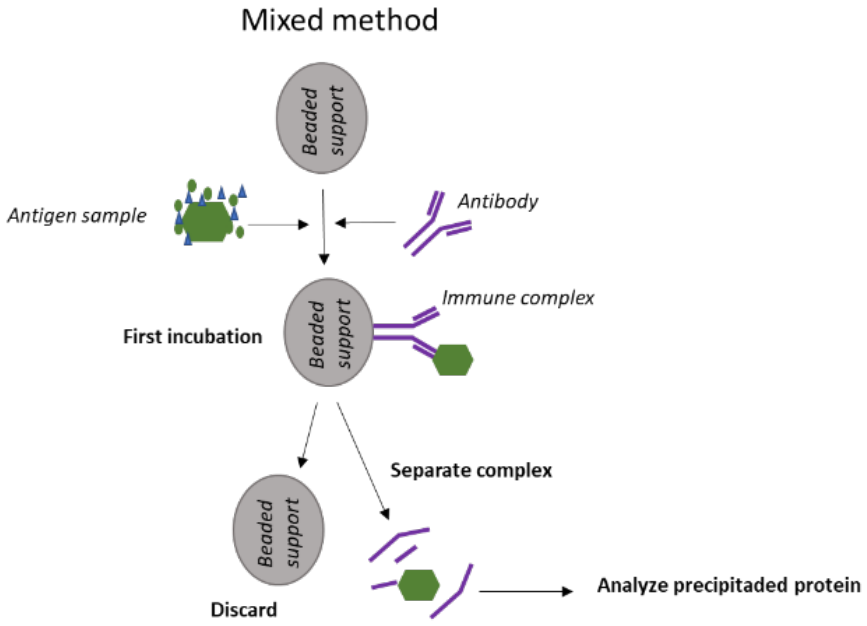

Figure 19. Scheme of mixed IP method

In this technique, several experimental parameters can have a big impact on the outcome of the method. Some of them are the type of beads (magnetic, sepharose or agarose), the selected antibody and dilution, buffers, time and temperature of incubation, antibody loading or the amount of extract used in the assay. Other factors that can impact the performance of the IP is the source of the samples (in the case of this study from SH-SY5Y cells and mice brain homogenates) and the incubation or not of the cell cultures with protein-protein interactions disruptors, In the case of this study with the POP inhibitors IPR19 and IPR166.

As mentioned before, after the IP procedure, the performance of the technique was assessed by means of a WB analysis using POP as a target protein. Prior to the WB analysis, the beads fraction were separated from the supernatant by centrifugation. Afterwards, "fished" POP was detached from the beads using a mixture of Laemmli buffer, dithiothreitol (DTT) and Phosphate buffer saline (PBS). The protein fraction of this operation was loaded into the polyacrylamide gel. The supernatant and recombinant POP (as molecular weight marker) were used as controls in the WB gel. The complete procedure is explained in Materials and Methods Section (section 3). As a negative control, during the

IP an antibody that recognizes β-actin was also used. The experiments were performed in SH-SY5Y cell cultures and mice brain extracts.

The parameters and reagents tested to optimize and enhance the IP performance are described in Table 4. The parameters for optimization were selected and optimized according to the instructions from kit manufacturers, bibliography, and our own experimental observations.

Table 4. Different conditions of IP parameters tested

Beads	Sepharose A beads (Sigma-Aldrich)
	Magnetic beads
	Sepharose beads (Merck)
	Agarose A beads
	From Merck PP2A Kit
Antibody	N-terminal region (Abcam)
	N-terminal region (Abcam)
	N-terminal region (Sigma-Aldrich)
	β-propeller region (Abcam)
	In-house produced antibody
	N-terminal region (Santa Cruz Biotechnology)
Incubation time	1h30min
	4h
	O/N
Temperature	Room temperature
	4ºC
Incubation Buffer	Ser/Thr assay buffer
	Assay buffer (50mM Tris-HCl, pH 7.0, 0.1mM $CaCl_2$)
	PBS
Washing buffer	PBS

	50mM Tris-HCl, pH 7.5 (TBS)
Amount of protein	3000 µg
	1500 µg
	1000 µg
	500 µg
	150 µg
Order incubation	Direct Method
	Indirect Method
	Mixed

After an initial set of experiments, the optimal conditions for experiments involving POP were: beads from Merck (PP2A kit), incubation for 1,5 h at 4ºC, mixed approach and N-terminal antibody from Abcam. The selected buffer for washings was TBS. The detailed experimental conditions are described in Material and Methods. (section 5.1).

As it can see in Figure 20, the antibody that recognizes the POP N-terminal region from Abcam (Figure 20, lane 5) works better than the one from other vendors that recognizes other regions of the target protein such as the β-propeller region (from Abcam) (Figure 20, lane 1). This antibody is thought to work better than the other ones because the region responsible of recognizing is more accessible when the protein is folded.

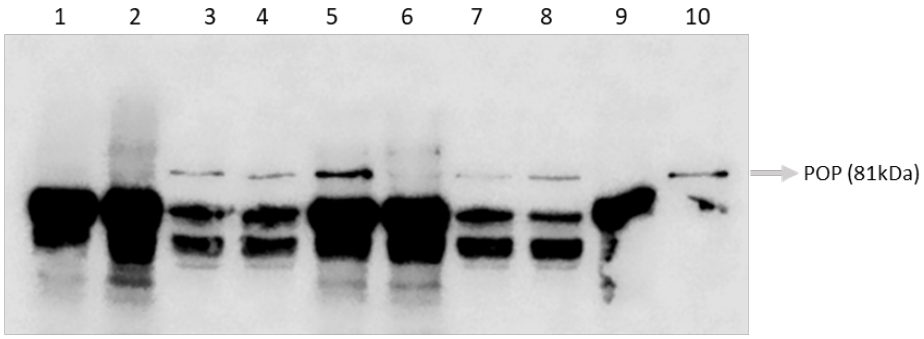

Primary Ab: Anti-POP (ab58988)
Secondary Ab: Anti-Rabbit (P0448)

1. 20 µL POP_beta-propeller IP (from cells control)
2. 20 µL POP_beta-propeller IP (from cells treated with IPR166)
3. 20 µL POP_beta-propeller IP **SN** (from cells control)
4. 20 µL POP_beta-propeller IP **SN** (from cells treated with IPR166)
5. 20 µL POP_N-term IP (from cells control)
6. 20 µL POP_N-term IP (from cells treated with IPR166)
7. 20 µL POP_N-term IP **SN** (from cells control)
8. 20 µL POP_N-term IP **SN** (from cells treated with IPR166)
9. 20 µL actin IP
10. 10 ng POP

Figure 20. Western blots film of POP Ips testing different antibodies in SH-SY5Y cells extracts. Membrane incubated using an antibody to detect POP protein.

An interesting observation is that the treatment of the cell cultures with 2 µM IPR166 for 1 h reduced considerably POP recognition capacity (Figure 20, lane 5 and 6). This is likely caused by the binding of the inhibitor to the protein, inducing a conformational change in the protein that challenge the binding of the antibody.

After optimizing the experimental parameters in SH-SY5Y cells extract, the performance of the optimized method was tested in mice brain homogenates (Figure 21). As it can be observed in Figure 21, lane 2, it has been demonstrated that, under these experimental conditions, POP IP does not work in mouse brain homogenates. Figure 21, lane 4 shows that POP IP using SH-SY5Y cell extract works.

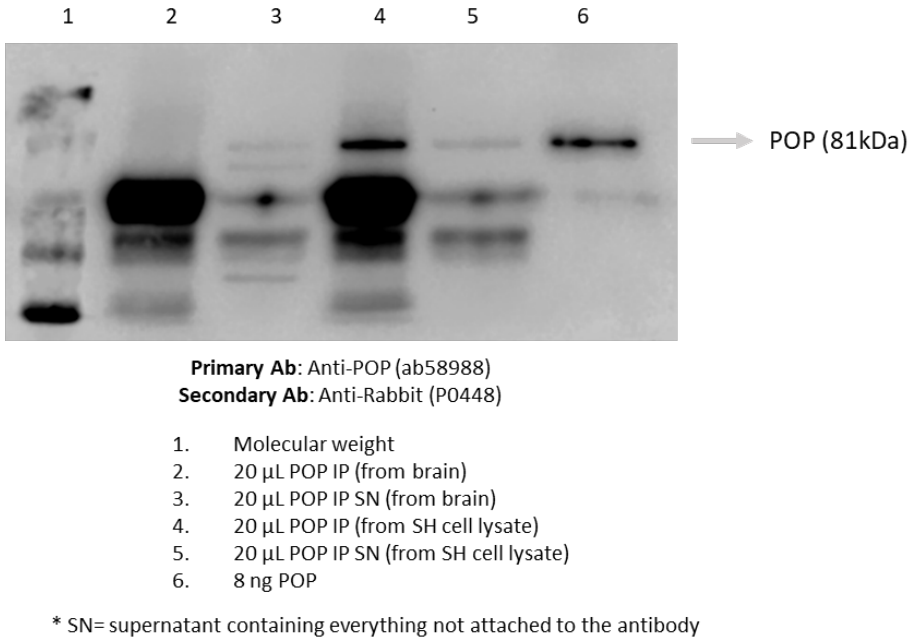

Figure 21. Western blots film of POP IP in SH-SY5Y neuroblastoma and with mouse brain extract. Membrane incubated Anti-POP antibody

Due to the results in brain homogenates, it was explored whether the POP antibody used for the WB (poor or no detection of POP) or the components used during the IP procedure (*i.e.* buffers, salt concentration, presence of lipids, etc) could be the reason behind the lack of POP recognition. Figure 22A, lanes 6 and 7, in which mouse brain homogenates were loaded, demonstrated that POP detection was effective. In Figure 22B, it is shown (lane 1) that when the brain homogenates are mixed with human recombinant POP as control, the IP performance was positive.

As a conclusion, POP IP from mouse brain homogenates probably did not work due to the impossibility of the POP antibody (the one used to perform the IP) to detect native mouse POP, although this antibody does recognize native POP from human and from SH-SY5Y cells. Another hypothesis may be that there is not enough POP in the mice brain samples and therefore this technique does not have enough detection capacity for this protein in this kind of samples.

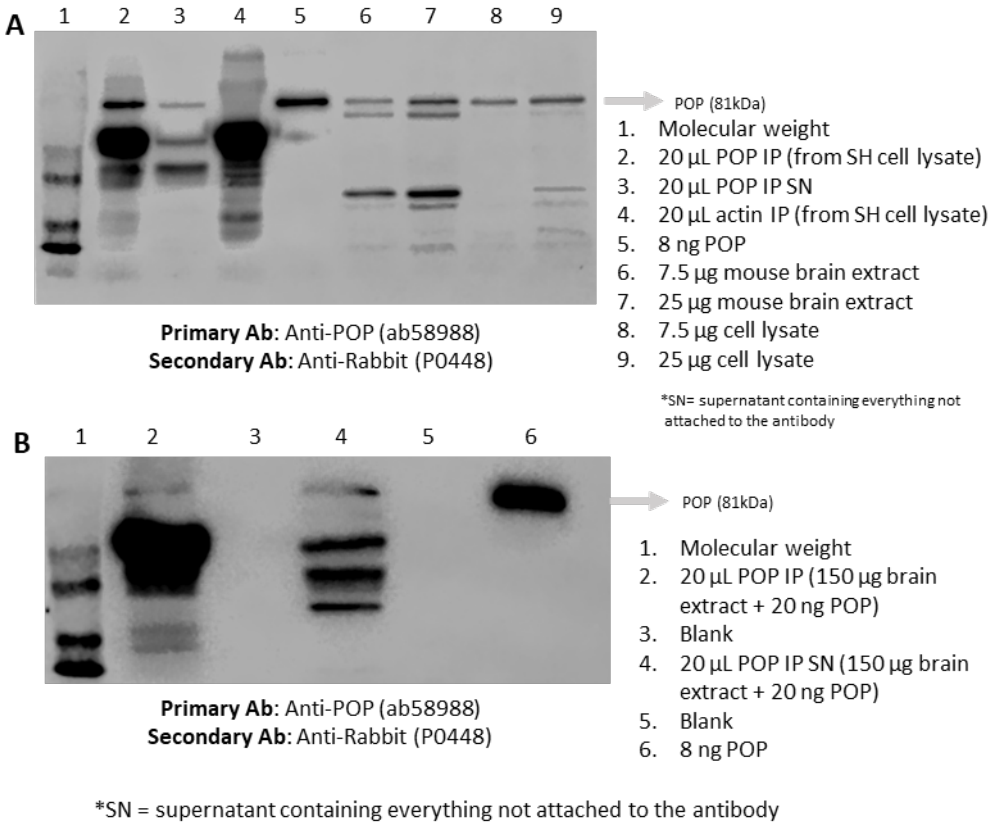

Figure 22. A) Western blots film of POP IP with SH-SY5Y neuroblastoma cells extracts and direct POP detection form mouse brain homogenates. Membrane incubated Anti-POP antibody. **B)** Western blots film of POP IP with mouse brain homogenate with recombinant POP as internal control. Membrane incubated Anti-POP antibody.

2.3 Confirmation of POP interactors

Once the IP was optimized and the best conditions were obtained for the POP protein, the optimization of protein complex co-immunoprecipitations (co-IPs) using SH-SY5Y cell extracts was performed to confirm some interactors that have been previously described. Co-IP is a technique, similar to IP, that can be used to identify physiologically relevant protein-protein interactions. After performing a standard IP for a target protein, POP in our case, the POP protein interactor candidate to be validated was detected by WB (Figure 23)

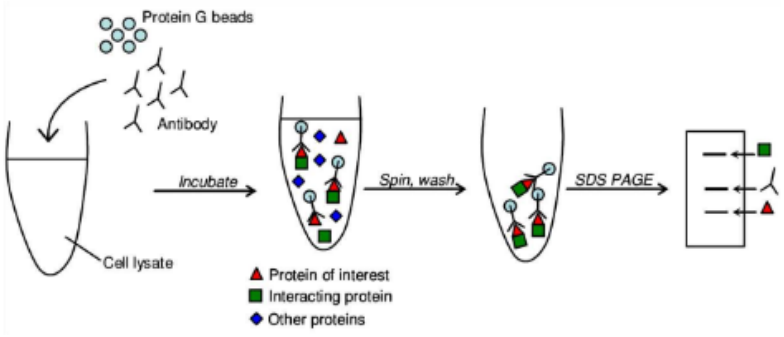

Figure 23. Scheme of the Co-IP (image from reference (108)

The main POP interactors described in the literature are the cytosolic proteins α-synuclein, GAPDH and GAP43 (40,45,106,107). The selected proteins to perform the co-IP and try to confirm their direct interaction with POP were α-synuclein and GAP43. The fibrillary aggregation of α-synuclein protein in the cytoplasm of neurons and glia is the main feature of synucleinopathies, including Parkinson's disease (PD), Lewy body dementia and multiple-system atrophy, among others (109). The contribution of POP to enhancing α-synuclein aggregation was reported for the first time by Brandt et al. in 2008 (110). Since then, it has been shown that POP co-localizes with α-synuclein in the substantia nigra of PD patients (43) and later that both proteins directly interact between them. This interaction was revealed through microscale thermophoresis and surface plasmon resonance studies (111).

Among other CNS-related functions, GAP43 is involved in growth cone formation and axon guidance (112,113) although the underlying molecular mechanism is still not well understood. This finding suggests that POP is also related to growth cone development. In this regard, Di Daniel et al. (40) proposed that this function of POP might be explained by its interaction with GAP43. Di Daniel demonstrated the interaction between POP and GAP43 using co-immunoprecipitation and yeast two-hybrid assays (40). Years later, this study was questioned by Szeltner et al., (41) who reported partial co-localization of POP and GAP43, without strong physical direct interaction. In this regard, these authors reported a weak and transient interaction between the two proteins, as demonstrated by

a glutaraldehyde cross-linking assay (41). Despite this contradiction, it is still plausible that POP participates in growth cone development via direct or indirect interaction with GAP43.

After some experiments to optimize the experimental conditions for the targeted proteins, it was obtained the following results: the GAP43-POP interaction detection, it was performed by means anti-GAP43 IP and, after, detection anti-POP in the WB (

Figure 24A) and vice versa , i.e., anti-POP IP and, after, detection anti-GAP43 in the WB (

Figure 24B).

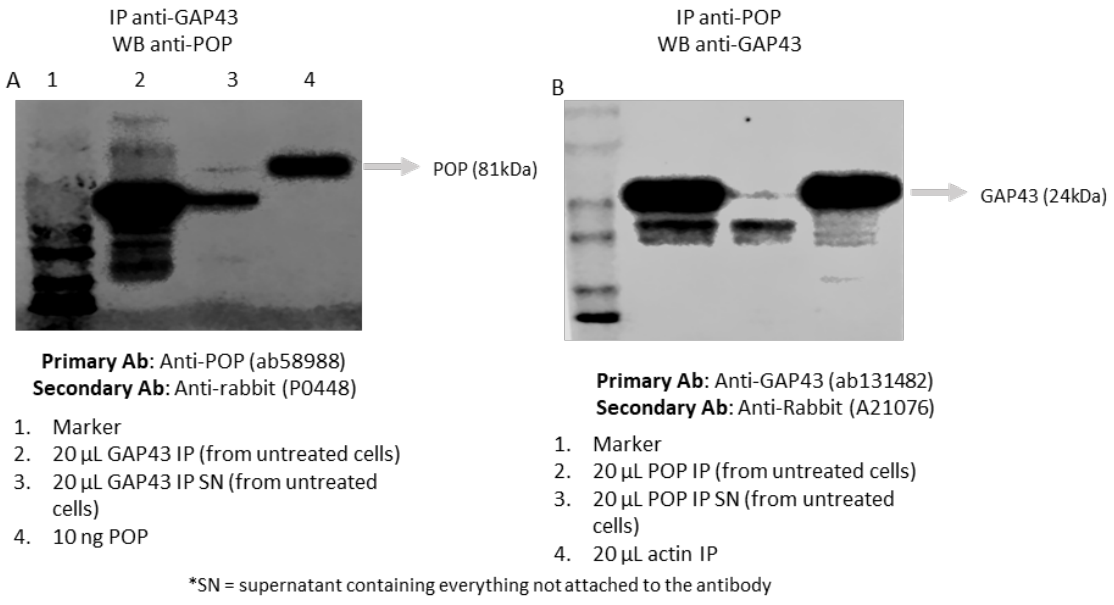

Figure 24. Western blots films of POP interactor A: Membrane incubated Anti-POP antibody obtained from anti-GAP43 IP. B: Membrane incubated Anti-GAP43 antibody ontained from anti-POP IP.

The interaction between POP and GAP43 protein was not observed, as depicted in Figure 24A and Figure 24B, because there are no bands at the molecular weight level where they should appear. . Even though In Figure 24A lane 3 a POP blurry lane appears, it is not clear enough to be considered as a positive result. GAP43 was not detected as shown in Figure 24B.

For the α-synuclein-POP interaction detection, it was performed an anti-POP IP and, after, detection POP in the WB (Figure 25). In Figure 25, the interaction between POP and α-synuclein protein was not observed. In Figure 25 lane 4 there is α-synuclein control and in lane 2 is not observed.

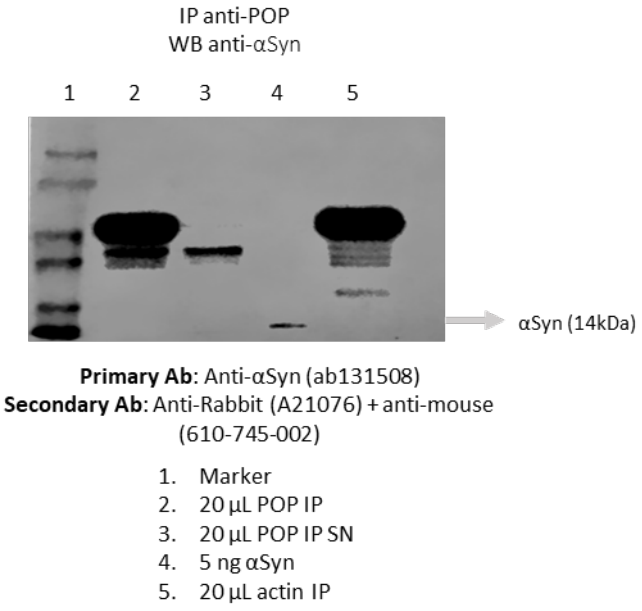

Figure 25. Western blots film of POP interactor α-synuclein. Membrane incubated Anti-α-synuclein antibody obtained from anti-POP IP.

Although several authors have previously described α-synuclein and GAP43 as POP interactors, the present study was not able to replicate this interaction because these interactions are perhaps weak and was not possible to detect it with the selected method.

2.4 Interactome analysis

There is the possibility that the POP protein may interact with other proteins that have not yet been described in the literature. Following the inconclusive results obtained in the POP co-IP experiments with the other POP interacting proteins described in the literature such as α-synuclein and GAP43, another type of experiment was carried out with the aim to find other possible protein interactors. This was carried out by means of an interactome analysis with liquid chromatography coupled to tandem mass spectrometry (LC-MS/MS), after POP-IP, to describe new possible POP interactors.

The POP interactome experiments using mass spectrometry were done in collaboration with the Proteomic's Unit of Centre for Genomic Regulation (CRG) in Barcelona. The POP-IP for this experiment was performed under very gentle conditions with the aim to preserve potential interactions of POP with other proteins and not to lose possible interactors during the IP washing step.

The interactome analyses were carried out using the SH-SY5Y cell extract. As a first step, a pilot experiment was performed to adjust the experimental conditions and check if the performance of the experimental conditions. This first experiment consisted in two IPs: one actin IP, as negative control, and other POP-IP (n=1). POP was identified with 24 peptides and coverage of 34.70 in the POP-IP, whereas the protein was not found in the negative control. Considering these positive results, the entire experiment was performed.

The second batch of samples to analyse consisted in triplicates of POP IPs and the negative control. POP was identified in all three POP IP triplicates with 14.17 and 16 peptides and coverage of 19.86, 24.08 and 22.82 respectively. POP was not found in any of the negative control IP triplicates. In these experiments, samples were analysed by means of liquid chromatography coupled to tandem mass spectrometry. A 1 hour LC gradient was used for the chromatographic separation and an Orbitrap Velos Pro was the detection tool used in the present work (detailed experimental protocol of experiment can be found in the Material and methods section of this thesis, section 5.2).

In these experiments, a list of 14 possible POP interactors was obtained:

- Cleavage and polyadenylation specificity factor subunit 5 (NUDT21)
- Tubulin beta chain (TUBB)
- Transportin-1 (TNPO1)
- Cleavage and polyadenylation specificity factor subunit 6 (CPSF6)
- Cleavage and polyadenylation specificity factor subunit 7 (CPSF7)
- Clathrin heavy chain 1 (CLTC)
- C-Jun-amino-terminal kinase-interacting protein 4 (SAPG9)
- Protein polybromo-1 (PBRM1)

- Tubulin beta-4B chain (TUBB4B)
- 60S ribosomal protein L7 (RPL7)
- 40S ribosomal protein S3 (RPS3)
- 60S ribosomal protein L6 (RPL6)
- Tubulin alpha-1C chain (TUBA1C)
- Heterogeneous nuclear ribonucleoprotein K (HNRNPK)

The proteins of this group of interactors were clustered using the STRING program, as shown in Figure 26.

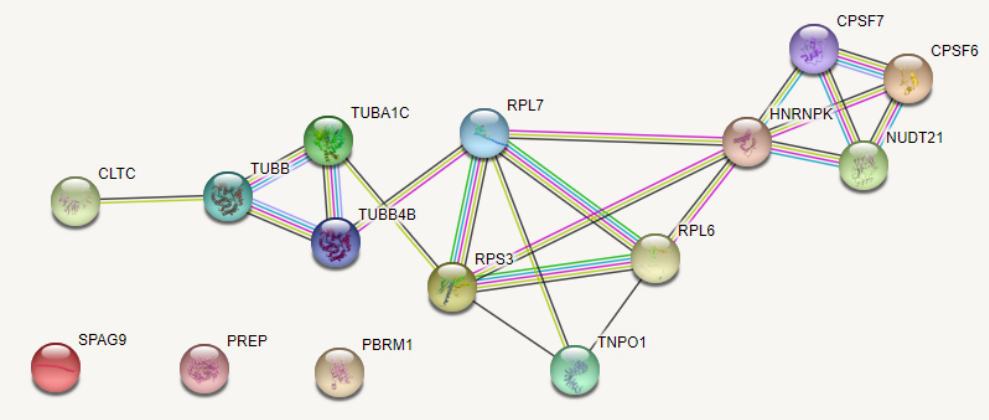

Figure 26. Cluster of protein found in LC-MS/MS analysis and their proposed interactions. Interactions reported in the literature are represented with blue and pink lines, other colours represent relationships such as co-expression or protein homology.

With the obtained results shown in Figure 26 and considering the available information in the literature, it was decided to study the possible interaction of POP with tubulin and clathrin by performing co-IPs using SH-SY5Y cell extracts.

2.5 Co-Immunoprecipitation tubulin and clathrin

Observing the results obtained the interactome analysis by means of mass spectrometry, it was selected to prioritize α-tubulin and clathrin proteins to study their possible interaction with POP protein because both are related in biological processes that involve vesicle trafficking (45), such as autophagy (42), or neuronal connectivity (114–116). It has been also reported the possible role of POP in these processes.

Repeated assemblies of α- and β-tubulin heterodimers comprise the structure of microtubules (MTs), which, together with microfilaments and intermediate filaments, form the cell cytoskeleton. Therefore, MTs are involved in a large number of cellular processes, including mitosis, cell motility, maintenance of cell shape, neurite growth, intracellular transport and vesicle secretion (117). Using co-localization and yeast two-hybrid assays, Schulz *et al*. demonstrated POP binding to the C-terminus region of α-tubulin (45). They also showed that POP inhibition promotes protein and peptide release in U-343 cells. Moreover, MTs are involved in PD, as demonstrated by observations of the interaction of tubulin with α-synuclein (118). These results support the hypothesis that POP participates in MT-associated processes, such as intracellular trafficking, protein secretion and axonal transport.

Co-IPs for α-tubulin and clathrin using SH-SY5Y cell extracts were carried out and in WB was detected the interactor protein (POP). The detailed experimental conditions can be found in Material and methods section of this thesis (section 5.3).

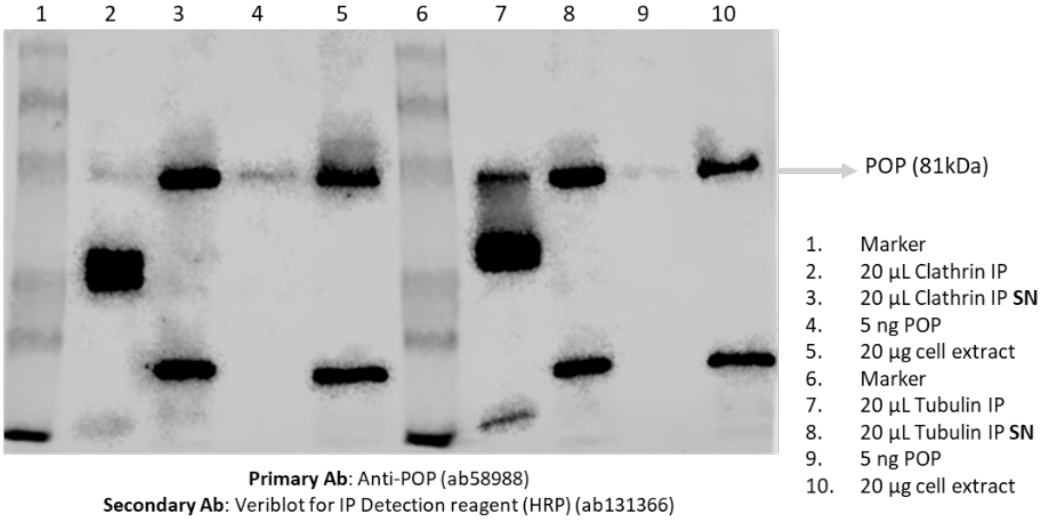

Figure 27. Western blots films of POP interactor. Membrane incubated Anti-POP antibody obtained from anti-clathrin IP and anti-α-tubulin IP.

As shown in Figure 27, interaction of POP with clathrin and tubulin was observed by Western blot assay. Although the band is too blurry, in lane 2 it is demonstrated that POP is detected in clathrin IP analysis. In lane 7, POP is also detected in the α-tubulin IP. The

success of clathrin IP experiments were confirmed during the incubation of this membrane with anti-clathrin antibody (Figure 28). The α-tubulin IP correct performance was not validated because tubulin and the heavy chain of the antibody have the same molecular weight.

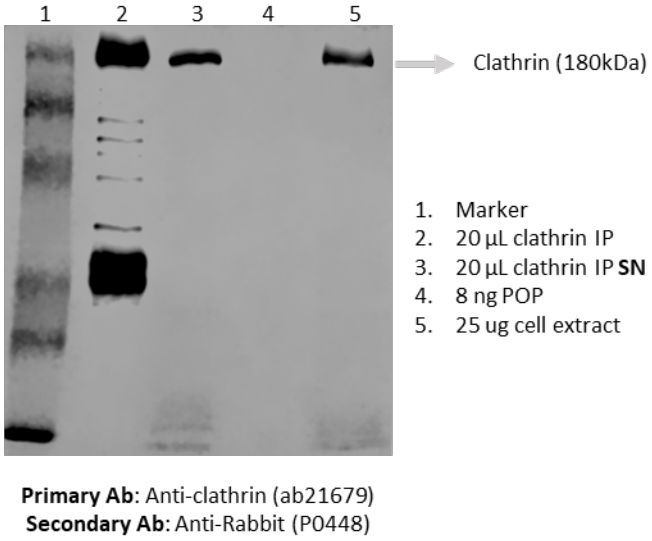

Figure 28. Western blot film of POP interactor. Membrane incubated with anti-clathrin antibody.

Another point that was addressed to better understand the mechanism of action of POP and its interaction with clathrin and α-tubulin was to incubate the POP inhibitor IPR166 in cell cultures to investigate whether these interactions can be modulated. These experiments were performed after co-IPs of α-tubulin or clathrin using SH-SY5Y cell extracts treated with or without IPR166 (or DMSO as a vehicle) for 1 h at 2 µM concentration. In the WB analysis, POP was the target protein.

In Figure 29, it can be observed that α-tubulin interacts with POP in basal conditions but differences are observed when POP is inhibited with IPR166 [2 µM]. In lane 2, it can be observed that co-IP tubulin-POP results are replicable. However, a blurry band appears when co-IP is performed with extracts from cells treated with 2 µM IPR166 (Figure 29, lane 5). This observation suggests that the POP-α-tubulin interaction is modulated by the inhibition of POP (however, more experiments need to be done).

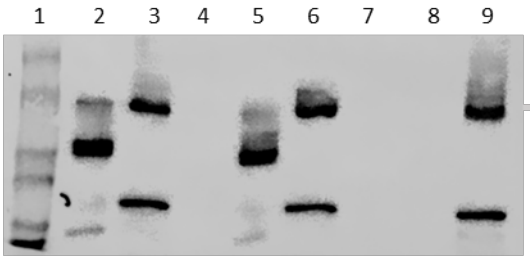

Primary Ab: Anti-POP (ab58988)
Secondary Ab: Veriblot for IP Detection reagent (HRP) (ab131366)

POP (81kDa)

1. Marker
2. 20 µL tubulin IP (non-treated cells)
3. 20 µL tubulin IP **SN** (non-treated cells)
4. -
5. 20 µL tubulin IP (cells treated with IPR166)
6. 20 µL tubulin IP **SN** (cells treated with IPR166)
7. -
8. 5 ng POP
9. 25 µg cell extract

Figure 29. Western blot film of POP interactor. Membrane incubated with anti-POP antibody after anti-α-tubulin IP.

As it can observed in Figure 30, clathrin interacts with POP in basal conditions (lane 2) and when POP is inhibited with IPR166 [2 µM] (Figure 30, lane 5).

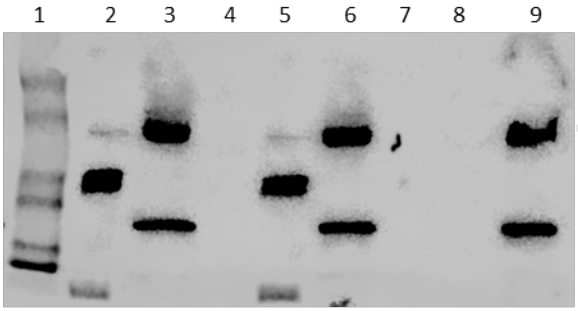

Primary Ab: Anti-POP (ab58988)
Secondary Ab: Veriblot for IP Detection reagent (HRP) (ab131366)

*SN = supernatant containing everything not attached to the antibody

POP (81kDa)

1. Marker
2. 20 µL clathrin IP (non-treated cells)
3. 20 µL clathrin IP SN (non-treated cells)
4. Blank
5. 20 µL clathrin IP (cells treated with IPR166)
6. 20 µL clathrin IP SN (cells treated with IPR166)
7. Blank
8. 5 ng POP
9. 25 µg cell extract

Figure 30. Western blot film of POP interactor. Membrane incubated with Anti-POP antibody obtained from anti-clathrin IP.

As mentioned before, an optimization of the α-tubulin-POP co-IP analysis was necessary to be able to detect α-tubulin in WB analysis and thus confirm its interaction with POP. The molecular weight of α-tubulin (50 kDa) is very similar to the molecular weight of the heavy chain used for antibodies in the Western blot analysis. Hence, it was

not possible to distinguish the band of α-tubulin from the heavy chain of the POP antibody. In the optimization process, a new secondary antibody was used. This antibody only recognizes the IgG light chain (Anti-rabbit IgG light chain (HRP), Abcam) in order to avoid the broad band that appears near to 50 kDa corresponding to the heavy chain corresponding to the antibody Figure 31A. It was expected to improve the sharpness of POP bands. By means this approach, it was possible to obtain bands with a significant improved resolution (Figure 31B).

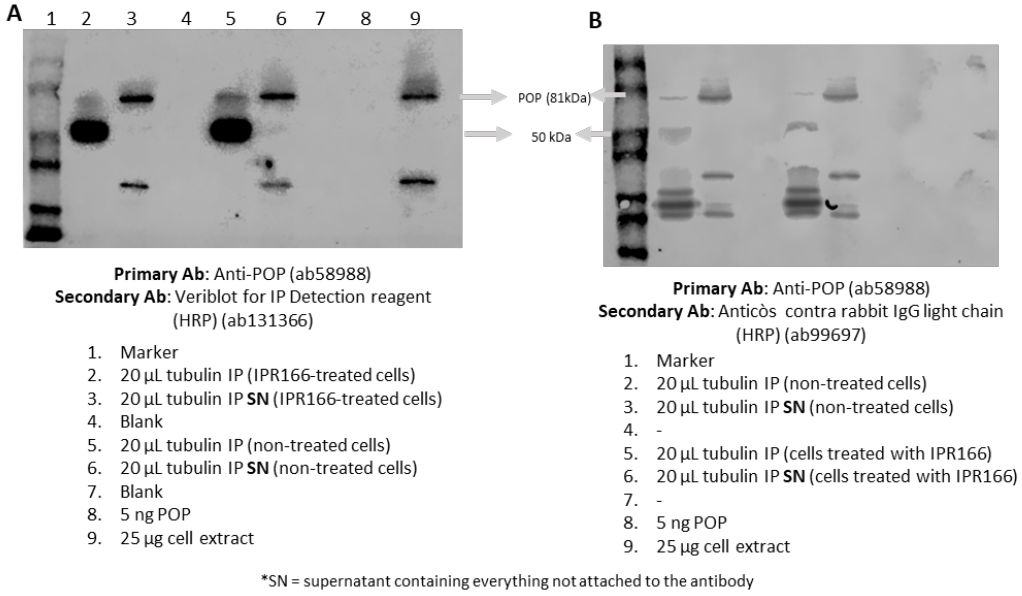

Figure 31. Western blot films of optimization of tubulin-POP co-IP analysis. **A**) Using secondary antibody that recognizes IgG heavy chain at 50kDa. **B**) Using secondary antibody that recognizes IgG light chain.

In order to confirm the existence of differences in the affinity between POP and α-tubulin in the presence or absence of the POP inhibitor IPR166, the previous experiment was repeated in triplicate. The light chain of the antibody (the lane that appears at 25 kDa) to normalize the signal of POP was used.

As it can be observed in Figure 32A and B, it is evidenced for the first time with statistical significance that POP interaction with tubulin is affected by the administration of IPR166 (mean 0,0101 ± SD 0,0006 in Control vs mean 0,0060 ± SD 0,0013 in IPR166 samples, p=0,0267) (Figure 32B). Despite using the band corresponding to the light chain

of the antibody for the normalization of the POP band is not the best approach, the incubation of the WB membrane with antibodies against other known tubulin interactors (concretely GAPDH and actin) did not work because no bands appeared. The reason why we are not able to detect these well-described tubulin protein interactors, we do not know it.

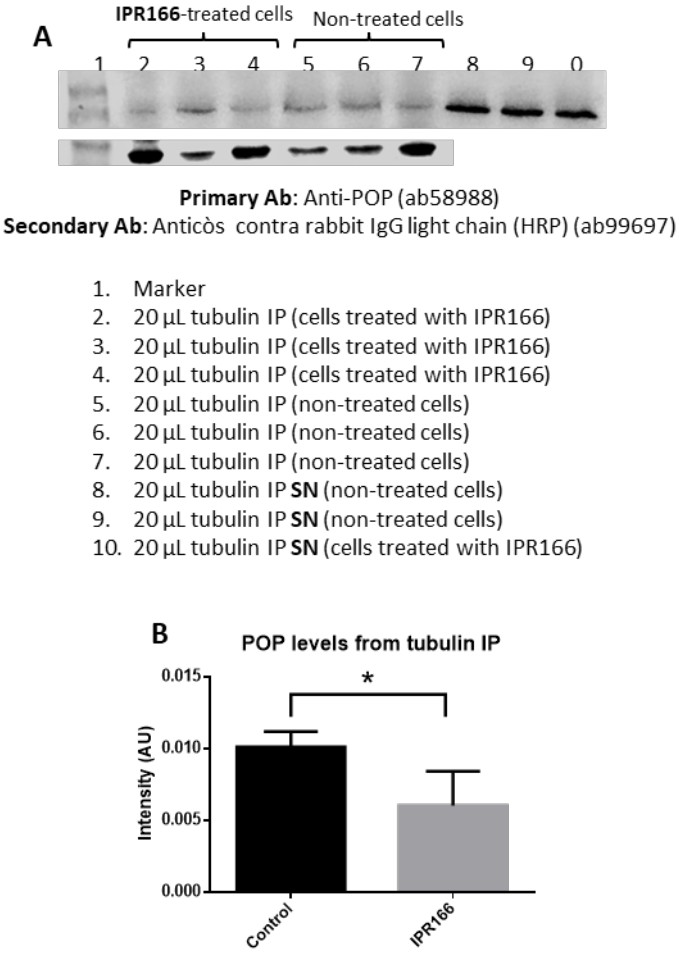

Figure 32. A) Western blot film of POP interactor. Membrane incubated with Anti-POP antibody obtained from anti-tubulin IP and **B**) the bar charts of the results: n=3 *p=0.0267 Control vs IPR166 treated (Student's t-test).

The results from the proteomic analysis that showed the interaction of POP with α-tubulin and clathrin were confirmed in co-IP experiments. However, with these two techniques it is not possible to discern whether it is a direct or indirect interaction. For that

purpose, other assays such as the surface plasmon resonance (SPR) or the Förster resonance energy transfer (FRET) should be performed.

With these results, it was possible to hypothesize that POP interaction with α-tubulin is affected by the presence of the POP inhibitor IPR166. Probably, its inhibition produces a conformational change of POP protein, therefore, in the interaction with the partner proteins. Nevertheless, co-IP assays are not the best approach to obtain quantitative results, for that purpose a SPR assay should be performed.

In POP IPs we had the problem that inhibited POP is not well recognized or properly immobilized by the used POP antibody as shown in Section 2.2 results. However, it has been demonstrated with these co-IPs that inhibited POP is also observed through α-tubulin or clathrin IP.

2.6 Other candidate POP interactors

As discussed in Chapter 1 of this thesis (section 1.2.4), differences in PP2A activity were observed when the cell cultures were incubated with the POP inhibitor IPR166. On the basis of this finding, it was decided to investigate whether the variation in activity was due to a direct interaction between these two proteins. A co-IP experiment was performed in order to assess the interaction between the two proteins using two different approaches: a) POP IP detecting PP2A by WB and b) the PP2A IP and detecting POP by WB. In both cases, however, it was found that there was not a direct interaction between these two proteins as shown in Figure 33.

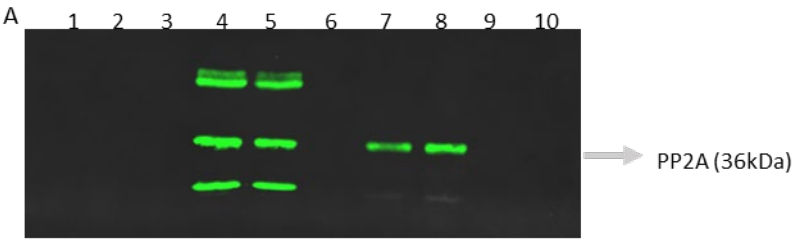

Primary Ab: Anti-PP2A (05-421)
Secondary Ab: Anti mouse Dylight 800 (610-745-002)

1. 20 µL POP-IP (from cells control)
2. 20 µL POP-IP (from cells treated with IPR166)
3. Blank
4. 20 µL PP2A-IP (from cells control)
5. 20 µL PP2A-IP (from cells treated with IPR166)
6. Blank
7. 20 µL POP-IP SN (from cells control)
8. 20 µL POP-IP SN (from cells treated with IPR166)
9. Blank
10. 5 ng POP

*SN = supernatant containing everything not attached to the antibody

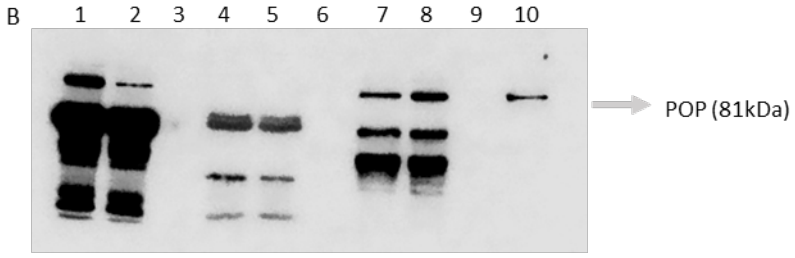

Primary Ab: Anti-POP (ab58988)
Secondary Ab: Anti-Rabbit (P0448)

1. 20 µL POP-IP (from cells control)
2. 20 µL POP-IP (from cells treated with IPR166)
3. Blank
4. 20 µL PP2A-IP (from cells control)
5. 20 µL PP2A-IP (from cells treated with IPR166)
6. Blank
7. 20 µL POP-IP SN (from cells control)
8. 20 µL POP-IP SN (from cells treated with IPR166)
9. Blank
10. 5 ng POP

*SN = supernatant containing everything not attached to the antibody

Figure 33. Western blot film of POP interactor. A) Membrane incubated with Anti-POP antibody obtained from anti-POP IP and anti-PP2A IP. B) Membrane incubated with Anti-PP2A antibody obtained from anti-POP IP and anti-PP2A IP.

As it can be observed in the Figure 33, there is not a direct interaction between POP and PP2A proteins.

On basis to the obtained results, it is concluded that the activation of PP2A activity by the POP inhibitor IPR166 is likely due to an indirect interaction between PP2A and POP since co-IP analysis suggest a lack of direct interaction between the two proteins. Moreover, in the interactome analysis study performed by mass spectrometry (results shown in section 2.3), PP2A protein was not result.

Following these experiments, a study conducted by Myöhänen *et al*. (104) demonstrated that the POP protein directly interacts with the c-subunit of the PP2A protein and other proteins that are part of the complex. They also showed that this interaction can be modulated with a POP inhibitor. This study was carried out using the co-IP technique using labelled proteins. They also emphasized that the POP protein can only bind from the N-terminal side and any protein anchoring from the C-terminal side of POP displays it inactive.

2.7 POP implication in autophagic processes

Savolainen *et al.* published in 2014 (42) that POP inhibition accelerates the clearance of protein aggregates via increased autophagy. As shown the proteomics data (Section 2.3) and co-IP results (Section 2.4) tubulin and clathrin are showed as POP interactors and it has been reported the involvement of both proteins in autophagy (119,120). Here, the role of POP in autophagy was investigated in the absence and the presence of POP inhibitor IPR166 (2 μM). These experiments were conducted under the advice and supervision of Professor Miquel Vila and Dr. Marta Martínez from the Neurodegenerative diseases group of the "Vall d'Hebron Research Institute" (VHIR).

Autophagy is an intracellular mechanism to degrade and recycle cytoplasmatic materials through lysosomes. This process removes misfolded or aggregated proteins, damaged organelles such as mitochondria, endoplasmic reticulum and peroxisomes, as well as intracellular pathogens. It is for these reasons that autophagy is generally considered as a survival mechanism although its deregulation has been linked to non-apoptotic cell death (121,122).

Autophagy is classified in three categories: macroautophagy, microautophagy and chaperone-mediated autophagy (123,124). The macroautophagy process consist of an isolation membrane (phagophore) that sequesters a small portion of the cytoplasm, including soluble materials and organelles to form an intermediate organelle with a double membrane called autophagosome. The autophagosome fuses with the lysosome to become an autolysosome and degrade the materials contained within it. Autophagosomes may fuse with endosomes before fusion with lysosomes (Figure 34A). Macroautophagy is the most common way of autophagy (125).

In microautophagy, the lysosome itself engulfs small components of the cytoplasm by inward invagination of the lysosomal membrane. Membrane dynamics of this mechanism is similar to the one that take place in the late-endosome (126) (Figure 34B). In the third type of autophagy, chaperone-mediated autophagy (CMA), targeted proteins labelled with KFERQ-like motif are recognized by cytosolic chaperone Hsc70 and are directly translocated across the lysosomal membrane by LAMP2A. Thus, it does not involve membrane reorganization (126) (Figure 34C).

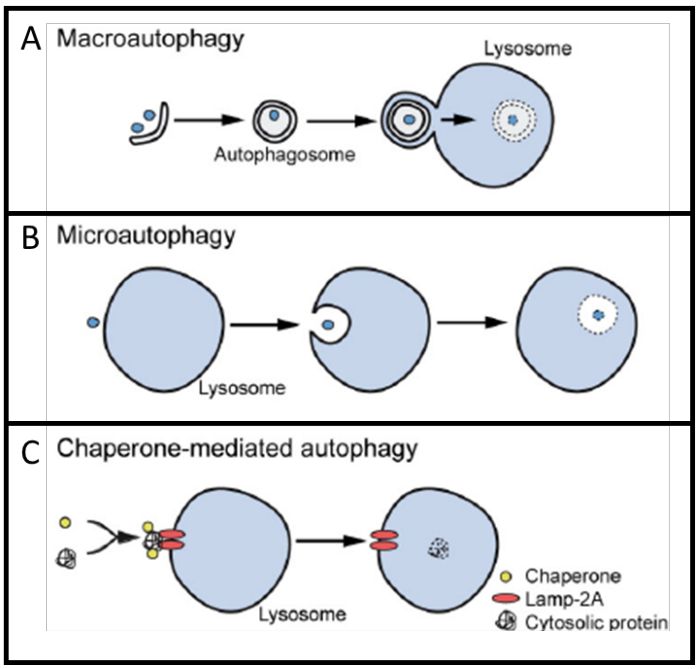

Figure 34. Scheme of types of autophagy. **A)** Macroautophagy involves the sequestration of cytosol and organelles by the autophagosome and then it fuses with a lysosome. **B)** Microautophagy implicates the degradation of cytoplasmic material that is directly invaginated by the lysosome. **C)** Chaperone-mediated autophagy entails the degradation of labelled protein with Hsp70 chaperone and this complex joins to the lysosomal receptor Lamp-2A receptor triggering the translocation to the lumen. (Image from reference (127)

Autophagy has a key role in preventing diseases such as cancer, neurodegeneration, cardiomyopathy, diabetes, liver disease, autoimmune diseases and infections because inhibits cellular senescence and cell surface antigen presentation, protects against genome instability and prevents necrosis since it causes the elimination of intracellular aggregates and damaged organelles (128–130). Effect of POP inhibitor IPR166 in macroautophagy (section 2.6.1) and CMA (section 2.6.2) was studied through the observation of differences in specific biomarker levels via Western blot.

2.6.1 Macroautophagy

The complex process of macroautophagy involves at least 16 proteins. However, LC_3 is the only one known to form a stable association with the membrane of autophagosomes (131). Concomitantly, a cytosolic form of LC_3 (LC_3-I) is conjugated to phosphatidylethanolamine to form LC_3-phosphatidylethanolamine conjugate (LC_3-II),

which is recruited to autophagosomal membranes. Detection of this conversion, using LC3 antibodies, is a useful biomarker to study macroautophagy.

In order to study the involvement of POP in macroautophagy the following experimental approach was used: stopping the autophagic flux using the lysosome inhibitor chloroquine in order to observe the LC3 accumulation in SH-SY5Y cells in the presence and absence of IPR166. Four experimental conditions were used using chloroquine at a concentration of 60 μM and POP inhibitor IPR166 at a concentration of 2 μM.

Figure 35 shows that autophagic flux is stopped when chloroquine was added (lanes 4 and 5) and it is not affected by POP inhibition with IPR166 (lanes 6 and 7) in SH-SY5Y cells as there was not an increase in LC3-II levels. Hence, it can also be concluded that the treatment of cells with POP inhibitor IPR166 are not increasing autophagy levels.

As a result, the hypothesis was focused on the possibility that POP inhibition with POP inhibitor IPR166 was modulating autophagic flux only when there was a cellular damage. This is because a dysregulation of the autophagy had been observed in the brains of PD patients and in animal model of PD (132) It has been demonstrated the clearance of α-synuclein aggregates are accelerated via increased macroautophagy in α-synuclein transgenic mice *in vitro* when they are treated with POP inhibitor KYP-2047 (42) In order to confirm this suggestion, a new experiment was conducted but by treating cells with non-competitive NMDA receptor antagonist MK-801, to induce schizophrenia-like molecular changes in the cells. SH-SY5Y cells were treated with MK-801 at 10 μM during 6h. Detailed experimental protocols of both experiments are in Material and methods section (section 5.5).

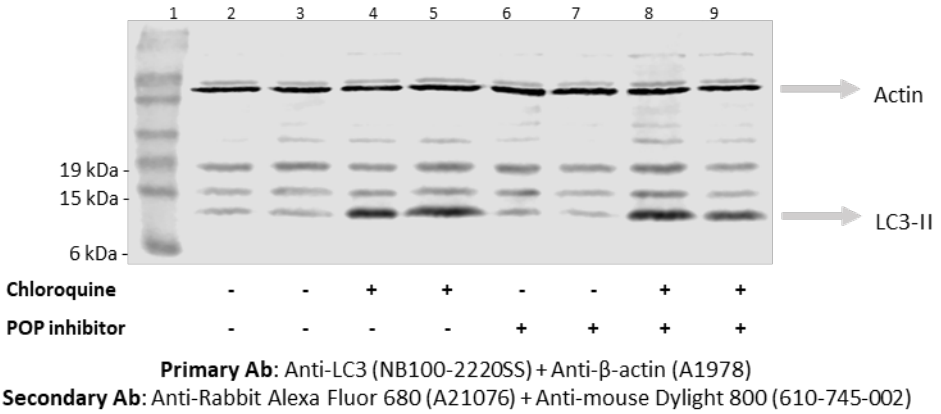

Primary Ab: Anti-LC3 (NB100-2220SS) + Anti-β-actin (A1978)
Secondary Ab: Anti-Rabbit Alexa Fluor 680 (A21076) + Anti-mouse Dylight 800 (610-745-002)

1. Marker
2. 20 µg SH extract: cells + 1% DMSO
3. 20 µg SH extract: cells + 1% DMSO
4. 20 µg SH extract: cells + 1% DMSO + 60 µM chloroquine
5. 20 µg SH extract: cells + 1% DMSO + 60 µM chloroquine
6. 20 µg SH extract: cells + 1% DMSO + 2 µM IPR166
7. 20 µg SH extract: cells + 1% DMSO + 2 µM IPR166
8. 20 µg SH extract: cells + 1% DMSO + 2 µM IPR166 + 60 µM chloroquine
9. 20 µg SH extract: cells + 1% DMSO + 2 µM IPR166 + 60 µM chloroquine

Figure 35. Western blot film of role of POP inhibition in macroautophagy. Membrane incubated with Anti-LC_3 antibody and anti-β-actin obtained from SH-SY_5Y cells extracts treated at different conditions.

As it can be observed in Figure 36, even if cells were treated with MK-801, POP inhibition with IPR166 was not affecting macroautophagy (lane 9 and 10), at least under the tested experimental conditions contrary to those results previously published by Savolainen, *et al.* (42). The possible causes of the fact that the results of our experiment do not agree with those published previously may be because, on the one hand, the published study used *in vivo* model that had altered α–synuclein levels.

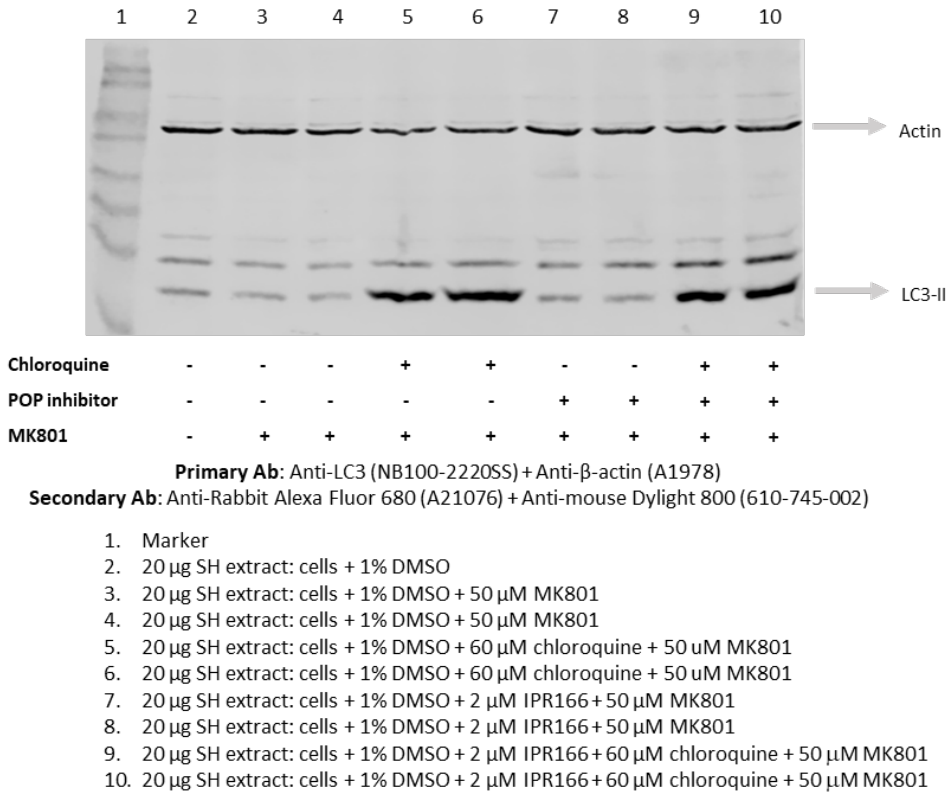

Figure 36. Western blot film of role of POP in macroautophagy. Membrane incubated with Anti-LC3 antibody and anti-β-actin obtained from SH-SY5Y cells extracts treated at different conditions.

In addition to that, in the *in vitro* model they used cells that were previously modified to express more or less POP, thus, not being comparable to the model used in this study. Another reason is that the POP inhibitor chosen is critical to the success of the experiment, as was later published (133). In Savolainen's *et al*. the molecule KYP-2047 was used, while the present study used IPR166.

2.6.2 Chaperone-mediated autophagy

Chaperone-mediated autophagy is a more selective form of autophagy than macroautophagy in which cytosolic proteins bearing a pentapeptide motif biochemically related to the KFERQ sequence (134). This protein is recognized by the heat shock protein family A member 8 (Hspa8) chaperone, delivered to the lysosomal membrane, and directly translocated across the lysosomal membrane by a protein complex containing lysosomal associated membrane protein 2a (LAMP-2A) (134).

It is known that α-synuclein aggregates are removed by this autophagic mechanism and considering previous references in which POP were related to α-synuclein aggregation (42), the possible involvement of POP in CMA was studied. This was carried out by treating SH-SY5Y cells with IPR166 at a concentration of 2 μM for 6h and quantifying the concentration levels of LAMP-2A by WB. Detailed experimental protocols are described in Material and methods section of this thesis (section 5.6).

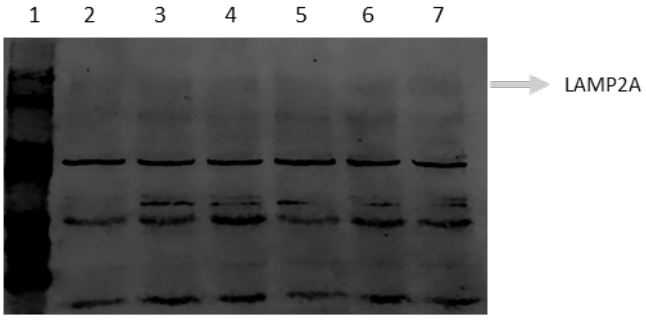

Primary Ab: Anti-LAMP2A (ab18528)
Secondary Ab: Anti-Rabbit Alexa Fluor 680 (A21076)

1. Marker
2. 40 μg SH extract: cells + 1% DMSO
3. 40 μg SH extract: cells + 1% DMSO
4. 40 μg SH extract: cells + 1% DMSO
5. 40 μg SH extract: cells + 1% DMSO + 2 μM IPR166
6. 40 μg SH extract: cells + 1% DMSO + 2 μM IPR166
7. 40 μg SH extract: cells + 1% DMSO + 2 μM IPR166

Figure 37. Western blot film of role of POP in chaperone-mediated autophagy. Membrane incubated with Anti-LAMP2A antibody obtained from SH-SY5Y cells extracts treated at different conditions.

As it can be seen in Figure 37no differences in LAMP-2A levels under these experimental conditions were observed as the LAMP-2A band was not completely defined.

In order to obtain a reliable conclusion from this experiment, it should be repeated changing the experimental conditions to try to obtain a clear band of LAMP-2A. One option to try to improve the experimental conditions would be to manipulate the cells to obtain a richer lysosomal fraction and thus increase the levels of LAMP-2A protein expression.

In 2020, it was reported by Myöhänen *et al.*(104) that POP regulates autophagy by interacting with protein PP2A and its endogenous inhibitor, protein phosphatase

methylesterase 1 (PME1), and activator protein phosphatase 2 phosphatase activator (PTPA), thus adjusting its activity and the levels of PP2A in the intracellular pool. They performed the experiments in HEK-293 and SH-SY5Y cell cultures after POP inhibition, POP deletion, and POP overexpression and restoration, and verified the results *in vivo* by using POP knock-out and wild-type mouse tissue where POP was restored or overexpressed, respectively. They observed that POP inhibition and deletion increased PP2A activity, leading to activation of death associated protein kinase 1 (DAPK1), beclin1 phosphorylation and induced autophagy while POP overexpression reduced this.

*CHAPTER 3: **Enhancing oral bioavailability and in vitro evaluation of MMP-9 inhibitors***

3.1 Introduction

MMP-9 is a gelatinase and one of the most complex proteases of MMP family for its different domains which is composed (71,72) . It has been described that various MMP-9 substrates are associated with several processes in CNS, such as epilepsy, Alzheimer and Parkinson disease (79).

Previous this work, it has developed a family of potent and selective gelatinase (MMP-2 and MMP-9) inhibitors which have the capacity to cross BBB. However, these inhibitors are proteolytically unstable in rat plasma and in *in vitro* microsomes studies, therefore, this means that the preclinical development of these compounds cannot be carried out since the studies are performed in rats. The present work is focused on the design and the synthesis of new lead candidates with a higher rat plasma stability while keeping the already achieved selectivity, potency and permeability to obtain a lead oral candidate to be able to carry out all its preclinical and clinical development.

For the development of peptides and proteins as new drugs the therapeutic administration is a key point, being the non-parenteral administration the preferred option This is particularly interesting for chronic diseases where repeated administrations are required although parenteral administration is the commonly used approach (135). Usually, the oral route, and others such as nasal or rectal, is the preferred one because parenteral administration of drugs have low patient compliance, as there is pain associated for the patient and it needs sterile and specific storage conditions, so the costs of manufacturing are usually very high. Therefore, the oral administration is mostly the preferred route of administration because is not invasive (136).

Parenteral administration of therapeutic peptides is the most indicated route because they have demonstrated poor oral bioavailability with a very low systemic circulation. It is well studied that peptides have fast renal clearance and are readily metabolized by plasma proteases. Moreover, another explanation is the enzymatic degradation caused by pH-mediated hydrolysis and poor permeability in the gastrointestinal tract (GIT) (136,137). Oral administrated drugs are usually metabolized by

hepatic metabolism. Therefore, drugs intended to be administered by this route must have a high hepatic metabolic stability to enter the systemic circulation and arrive at their pharmacological target (138). The hepatic metabolism is divided in three phases:

- Phase I – modification: addition of reactive groups by the action of variety of enzymes to convert the drugs in more active metabolites. Hydroxylation catalysed by cytochrome P450 is one of the most common modifications. Other reactions may occur by oxidation, reduction or hydrolysis, among others.
- Phase II – conjugation: the metabolites generated in phase I are conjugated with charged species to produce more polar metabolites to reduce their reactivity and facilitate its elimination.
- Phase III – further modification and excretion: the excretion of the generated metabolites.

In order to study the metabolic stability of oral drug candidates, the use of liver microsomes is one of the most used *in vitro* techniques. It is an experimental approach that allows to calculate the intrinsic clearance and to identify the metabolites formed for a given compound in a quickly and inexpensive manner (139). Liver microsomes are a pool of vesicles of the endoplasmic reticulum that contain drug-metabolizing enzymes, such as cytochromes, esterases or amidases, which are responsible for the phase I metabolism. They are also composed by phase II enzymes. In this stability assay, the addition of exogenous cofactors such as the nicotinamide adenine dinucleotide phosphate-oxidase (NADPH), a reducing agent involved in anabolic reactions, are required to stimulate the catalytic activity of both phase I and II enzymes (139). Furthermore, this *in vitro* tool allows comparing the metabolism of a drug in several species. In this regard, it is key to explore the stability of compounds under development in other species than human to choose the most appropriate and relevant species for the efficacy and toxicology evaluation of the molecule.

Plasma stability also plays an important role in drug discovery and development. This assay consists in the measurement of the degradation of drug candidates in plasma

from different species. Compounds which rapidly degrade in plasma generally show poor *in vivo* efficacy because the degradation implies a lower drug exposure of the therapeutic target. Moreover, the instability in plasma of the drug candidates can result in misleading *in vivo* data which can be difficult to interpret. The analysis of clinical samples from *in vivo* pharmacokinetic (PK) studies may be challenging, since degradation may continue upon plasma harvest.

Like the stability in liver microsomes, stability experiments can also be done using plasma from several animal species, which helps to select the most relevant animal model for the pre-clinical evaluation.

The company has developed a gelatinase inhibitor, compound IPR-179, which shows good potency (IC50 for gelatinases < 1 μM), selectivity (the IC50 values for MMP-1, MMP-3 and MMP-7 being higher than 10 μM), permeability (T>1%) and low cytotoxicity (88). This compound, however, has a reduced metabolic stability in rodents' plasma and low oral bioavailability in rodents (140). This compound has demonstrated good *in vitro* potency and selectivity for different gelatinases and other proteins and positive *in vitro* permeability in the GIT and BBB PAMPA assays. Moreover, *in vivo* several experiments with preclinical epilepsy models in rodents were performed. In these *in vivo* experiments, outstanding efficacy results were obtained after the parenteral administration of the compound. Furthermore, *ex vivo* analysis of the brain tissue of the IPR-179 treated animals revealed a significant reduction of the MMP-9 activity and positive BBB permeability after the administration of the compound. Also, several behavioural studies were performed with positive results (141). However, this candidate shows low microsomal stability and very low bioavailability after oral administration in rodents.

3.2 Design of new gelatinase inhibitor with improved microsomal and plasma stability

Over the past few years, Iproteos has been developed a library of MMP-9 inhibitors using computer aided drug design (CADD) *in silico* calculations. The most promising compounds have been synthesized and evaluated *in vitro* (88). The most potent and promising developed inhibitors are featured by having a hydroxamate moiety in their

structure, which acts as a warhead by coordinating the hydroxyl and carbonyl groups with the zinc atom located at the MMP's active site.

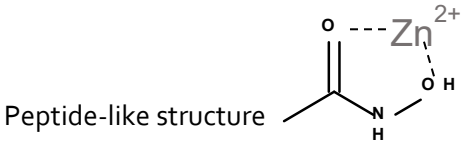

Figure 38. Scheme of zinc coordination with hydroxamic acid of peptide though hydroxyl and carbonyl groups.

After an optimization process of the compounds, a lead candidate with high potency, selectivity, BBB permeability, and low cytotoxicity was obtained: IPR-179 (Figure 39) (88). However, as explained, although this compound has shown a high efficacy in animal models of epilepsy, the compound was not orally available and showed limited plasma stability (in rodent).

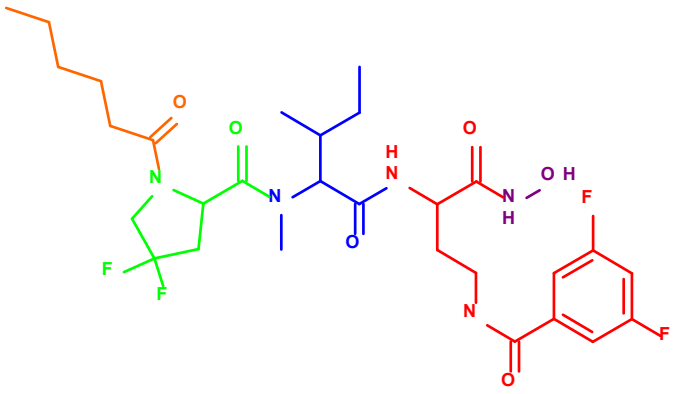

R-aa3-aa2-aa1-NHOH

Figure 39. Structure of IPR-179 compound

Previous studies have demonstrated that compound IPR-179 was not stable when incubated in rat liver microsomes, showing a high rate of degradation just after 5 minutes of incubation. In order to study which part of the molecule was more prone to metabolic cleavage by liver microsomes, the supernatant obtained after incubation of the drug with microsomes was analysed by means of mass spectroscopy to elucidate the structure of the different cleaved moieties. The results obtained showed two main fragments corresponding to the cleavage of the peptide bond between the 4,4-difluoroProline moiety (aa3) and the N-methylated Isoleucine (aa2) and a second cleavage between Dab side chain

and the aromatic moiety (3,5-difluorobenzoyl). For these reasons, it was decided to design and to synthesize analogues of IPR-179 compound modifying these two critical bonds to enhance proteolytic stability to improve its oral bioavailability (140).

Alongside microsomal stability enhancement, the proposed structures must preserve potency and selectivity for MMP-9, BBB permeability, low cytotoxicity and high stability in human serum.

The design and synthesis of these new analogues was started by Dr. Alexandra Bertran (140)

3.2.1 Design

New inhibitors preserved the hydroxamate moiety at the *C*-terminal part because good results were obtained when this warhead was used. Structural modifications of IPR-179 were divided in 4 strategies: 1, 2 and 3 were envisaged to ameliorate the cleavage between aa2 (NMeIle) and aa3 (4,4-difluoroProline) and strategy 4 was focused on increasing the proteolytic resistance at the Dab side chain. In **¡Error! No se encuentra el origen de la referencia.** are the sequences of the new structures proposed are shown. For patentability reasons, entire structures are not disclosed.

Summary of the main strategies followed:

1. *N*-terminal modification by use of alternative *N*-terminal tails (IPR-436, IPR-437, IPR-447, IPR-448, IPR-457 and IPR-458) because these modifications can protect the structure of the molecule from cleavage and improve its permeability.

2. Use of proline derivatives (IPR-424)

3. Replace *N*MeIle by other *N*Me amino acids (IPR-425, IPR-426, IPR-428, IPR-429, IPR-438, IPR-439)

4. Modification of aa1 position:

- Dab side chain modification: alternative aromatic moieties (IPR-430)
- Use of a Dab analogue (IPR-441)

Modifications in aa1 position to increase plasma stability were considered after research in the bibliography. Some investigations suggested structural rules to improve plasma stability of hydroxamate containing compounds. One of these new ideas is the use of less flexible compounds in position aa1 (142,143).

These design strategies were based on the results obtained by Bertran (140). Other attempted:

1. *N*-terminal modification by increasing length of the compound: add one or two additional amino acid
2. Use of D-Proline at aa3 position
3. Modification of aa1 position
    - Dab side chain modification: alternative aromatic moieties
        - Use of Dab analogue
        - Selective N-methylation at aa1

3.2.2 Synthesis

Compounds were synthesized by solid-phase peptide synthesis (SPPS) following the 9-fluorenyl-methoxycarbonyl/*tert*-butyl (Fmoc/*t*Bu) chemistry and using 2-chlorotrityl resin (2-CTC). The approach comprised the incorporation of a hydroxylamine linker to the solid support followed by the elongation peptide in a stepwise manner. Moreover, most of synthesized the compounds contain the Dab(Alloc) at the first position of sequences (aa1).

The removal of the Alloc protecting group and the formation of the amide bond by addition of the aromatic moiety was performed during the last stage of synthesis before the cleavage step. Detailed conditions are shown in Scheme and described in the Materials and methods section of this thesis (section 6.1).

Table 5. Sequences of IPR-179 analogues. In capital letters ("A"-"K") are indicated the structures that they cannot be shown for patentability reasons. Hex: Hexanoyl; 2PP:2-Propylpentanoyl; (2,2-diF)hex:2,2-difluorohexanoyl; TriFpentanoyl:5,5,5-Trifluoropentanoyl; NMe: N-Methyl; Pro(4,4diF):4,4-difluoroproline; Dab(3,5diFBz): diaminobutyryl(3,5-difluorobenzene).

R-aa3-aa2-aa1-NHOH				
Code	**R**	**aa³**	**aa²**	**aa¹**
IPR-179	Hex	Pro(4,4diF)	NMeIle	Dab(3,5diFBz)
IPR-424	2PP	Pro(4F)	NMeIle	"A"
IPR-425	2PP	Pro(4,4diF)	"B"	"A"
IPR-426	2PP	Pro	"C"	"A"
IPR-428	2PP	Pro	"D"	"E"
IPR-429	2PP	Pro(4F)	"G"	"A"
IPR-430	2PP	Pro	"D"	"H"
IPR-436	(2,2-diF)hex	Pro	NMeIle	"A"
IPR-437	(2,2-diF)hex	Pro	"I"	"A"
IPR-438	Hex	Pro(4,4diF)	"B"	"A"
IPR-439	2PP	Pro(4,4diF)	"B"	"A"
IPR-441	2PP	Pro	NMeIle	"J"
IPR-447	TriFpentanoyl	Pro	"B"	"A"
IPR-448	TriFpentanoyl	Pro(4,4diF)	"B"	"A"
IPR-456	2PP	Pro	NMeIle	"K"
IPR-457	TriFpentanoyl	Pro	"C"	"A"
IPR-458	Hex	Pro(4,4diF)	"C"	"A"

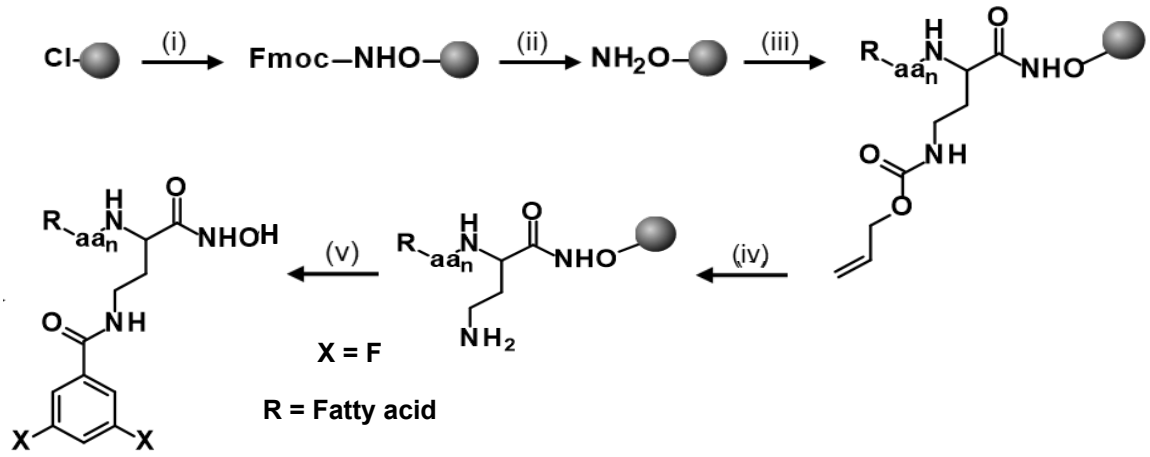

Scheme 1. Synthesis of compounds with hydroxamic acid and Dab (Alloc). (i) Fmoc-NHOH (0.6 eq), DIEA (5 eq), DCM, 24 h; (ii) 20% piperidine in DMF, 1 x 1 min + 2 × 5 min; (iii) (a) Fmoc-aa_n-OH (3 eq), oxime (3 eq), DIC (3 eq), DMF, 1h; (b) 20% piperidine in DMF, 1 x 1 min + 2 × 5 min; step (iii) is repeated until the length of peptide is achieved; (iv) Removal of the alloc group; Phenylsilane (10 eq), $Pd(PPh_3)_4$ (0.1 eq), DCM, 3 x 15 min; (v) a) Formation of the amide bond by addition of the aromatic moiety (3 eq), oxime (3 eq), DIC (3 eq), DMF, 1.5h. b) 5% TFA in DCM, 3 x 15 min.aromatic moiety (3 eq), oxime (3 eq), DIC (3 eq), DMF, 1.5h. b) 5% TFA in DCM, 3 x 15 min.

The obtained crudes were generally highly pure which then could be easily purified by reverse-phase chromatography (procedure described in section 6.3 from Materials and methods section of this thesis), obtaining a purity for the final product higher than 95% (HPLC, area/area) in all the cases. Using this strategy, the target compounds were obtained in high yields (>10 %).

For compounds IPR-441 and IPR-456, the synthesis strategy was modified. For the building blocks at aa1, the hydroxamate moiety was added at the end of the solid-phase synthesis in solution. After completing the synthesis of the two inhibitors in solid phase, these were cleaved from the 2-CTC resin obtaining the compounds with a carboxylic acid moiety at the *C*-terminal part. After cleavage, the transformation of the carboxylic acid to hydroxamate was performed in solution using the Hydroxylammonium chloride reagent.

3.3. *In vitro* enzymatic evaluation assays

Compounds IPR-224 and IPR-258 inhibition efficacy was initially evaluated for MMP-9. Later on, inhibition potency for MMP-1, MMP-2 and MMP-7 was evaluated.

The experimental conditions for the *in vitro* inhibition assays using MMP-1, MMP-2, MMP-7 and MMP-9 were set-up previously in the laboratory. Conditions for evaluation are described in the Materials and methods chapter of this thesis (section 6.5).

3.3.1. MMP-9 activity

Compounds were dissolved in DMSO as described in the Materials and methods chapter of this thesis (section 6.5.1). The half maximal inhibitory concentration (IC_{50}) of each compound was calculated by plotting the logarithm of each concentration tested for a given compound versus the inhibition percentage, which was calculated according to Equation 1. It must be take account that IC_{50} absolute values are dependent of the conditions of the assay. Hence, results cannot be compared from different laboratories since experimental conditions may differ. Therefore, a reference compound (Inhibitor 1) was always included in the assays as an internal control.

$$\%inhibition = \frac{F^{+}(t) - F^{-}(t)}{C^{+}(t) - C^{-}(t)} \text{ x } 100$$

Equation 1

Where:

F+ = average of fluorescence values in the presence of the enzyme and inhibitor (at a given concentration).

F- = average of fluorescence values in the presence of inhibitor (at a given concentration, without enzyme).

C+ = average of fluorescence values in the presence of enzyme (without inhibitor).

C- = average of fluorescence values (without enzyme and inhibitor).

The MMP-9 inhibitory activity of the compounds is detailed in **¡Error! No se encuentra el origen de la referencia.** .

3.3.2 MMP-2 activity

Once the MMP-9 enzymatic assay was completed, the *in vitro* potency of some compounds was investigated for MMP-2 (**¡Error! No se encuentra el origen de la referencia.**). Obtained results demonstrated that the evaluated inhibitors were selective

for MMP-9 as well as for MMP-2. Other groups had also failed in the design of MMP-9 high selective inhibitor because both enzymes have high structural homology on the catalytic active site (144). Although the inhibition of both enzymes are interesting because in epilepsy, MMP-2 is also upregulated.

The IC50 values for MMP-2 are detailed in Table 6. Inhibitor 1 compound was used as reference inhibitor.

Table 6. *In vitro* gelatinases MMP-9 and MMP-2 inhibitory activity (IC50, nM) for the compounds. Inhibitor 1 was used as reference inhibitor. N/E: Not evaluated.

ID	MMP-9 IC50 (nM)	MMP-2 IC50 (nM)
Inhibitor 1	33	-
IPR-179	304	610
IPR-424	596	14
IPR-425	268	14
IPR-426	168	14
IPR-428	389	N/E
IPR-429	>50000	N/E
IPR-430	30	N/E
IPR-436	200.5	44
IPR-437	233.5	44
IPR-438	498	42.8
IPR-439	856	N/E
IPR-441	>100000	>100000
IPR-447	427	42.8
IPR-448	1025	N/E
IPR-456	100000	N/E
IPR-457	>1000	N/E
IPR-458	>1000	N/E

Compounds twith an IC50 above 1 µM for MMP-9 were no further evaluated. Compounds IPR-441 and IPR-456 with "J" or "K" respectively in position aa1, showed low inhibitory potency for MMP-9. With these changes, the pharmacophore of the molecule changed notably and it couldn't access into protein catalytic site for inhibition. The same

problem was observed in the case of compound IPR-429 "G"in position aa2. Similar results were observed with IC50 MMP-2 results showing that it is very difficult to design a compound that only inhibits MMP-9. In general, if it is a good inhibitor for MMP-9, it will be a good inhibitor for MMP-2 too.

3.3.3 MMP-1 and MMP-7 activity

The experimental conditions for MMP-1 and MMP-7 inhibition evaluation are described in the Materials and methods chapter of this thesis (section 6.5.2).

The study of the inhibitory potency of compounds against other MMPs such as MMP-1 and MMP-7 was conducted in this section in order to define their selectivity profile for MMPs. Following this procedure, compounds IPR-425, IPR-436-439, IPR-447 showed IC50 values higher than 1 μM for MMP-1 and MMP-7 Table 7.

Table 7. Selectivity profile (MMP-1 and MMP-7) for compounds IPR-425, IPR-426, IPR-436, IPR-437, IPR-438, IPR-439 and IPR-447.

ID	MMP-1 IC50 (μM)	MMP-7 IC50 (μM)
IPR-425	3.8	2.2
IPR-426	13.4	39
IPR-436	13	5.1
IPR-437	11.6	6
IPR-438	4.3	7.7
IPR-439	2	2.3
IPR-447	1.1	4.1

3.3.4 In vitro evaluation of BBB permeability by PAMPA assay

The assessment of the potential BBB permeability of drugs targeting the CNS at early stages of the development is a key point to consider. In this regard, several *in vitro* tools have been developed to measure the permeability of compounds across the BBB. For example co-culture models where involve the use of two or more cell types, such as brain endothelial cells and astrocytes, that mimic the *in vivo* BBB (145). This is the case of dynamic *in vitro* BBB models which they use of microfluidic devices to create a more

physiologically relevant environment for the BBB (145) or multi-culture models with the use of two or more cell types (2D or 3D) that mimic the *in vivo* BBB (145). However, one of the most simple, inexpensive and popular models is the parallel artificial membrane permeability assay (PAMPA), a high-throughput screening method which allows to measure the *in vitro* potential BBB permeability of compounds by passive diffusion. A non-cell-based transport assay developed by Kansy, *et al.* (146).

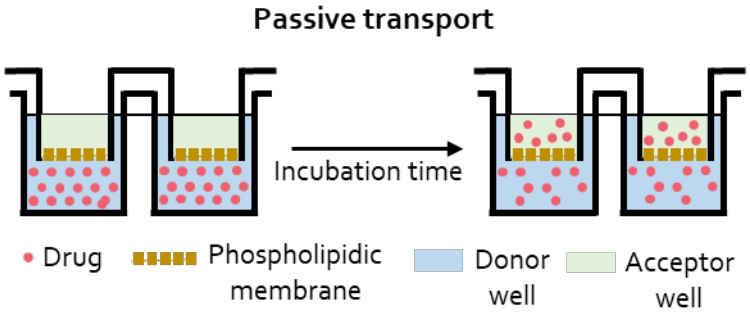

Figure 40. Schematic diagram of PAMPA model

PAMPA is a highly restrictive in *vitro* assay that allows to measure the permeability of drugs through an artificial phospholipid membrane that resemble the BBB. This is achieved by coating the filters of the PAMPA plate with a mixture of polar brain phospholipids. For this assay, propanolol was used as the positive transport control, whereas IPR-179 was selected as reference compound. The experimental procedure for the PAMPA assay is described in the Materials and methods section of this work (section 6.6.1). Briefly, the inhibitors were evaluated in a 96-well plate sandwich-like plate. The porous filter membrane of the plate was coated with mixture of a porcine polar brain lipid extract. For the transport evaluation, the drug candidates were dissolved in PAMPA buffer and isopropanol (15%) as a co-solvent at pH 7.4. The compounds were assayed at a concentration of 200 µM during 4 h at room temperature in a humidity saturated chamber. After that time, the content of donor and acceptor compartments was analysed by HPLC. The effective permeability (Pe) and percentage of transport (T%) were calculated according to Equation 2 and Equation 3:

Equation 2.

$$P_e = \frac{-218.3}{t} \times \log\left[1 - \frac{2C_A(t)}{C_D(t_0)}\right] \times 10^{-6}\ (cm/s)$$

Equation 3.

$$T\% = \left[1 - \frac{2C_A(t)}{C_D(t_0)}\right] \times 100$$

Where:

t = time (h)

$C_A(t)$ = compound concentration in the acceptor compartment at time t

$C_D(t_0)$ = compound concentration in the donor compartment at time 0.

Results of each compound are showing in Table 8. All of them showed promising results considering that transport values were above 5%. For this reason, all of these compounds were considered good candidates for further evaluation.

Table 8. Percentage of transport and effective permeability (Pe) after 4h in BBB-PAMPA model.

ID	BBB-PAMPA	
	Transport (%)	Pe (x10^{-6}) cm/s
IPR-179	14.3	8.0
IPR-425	18.9	11.3
IPR-426	8.7	4.5
IPR-436	20.1	12.2
IPR-437	11.7	6.3
IPR-438	27.4	19.2
IPR-439	28.9	20.7
IPR-447	5.6	2.8

3.3.5. Metabolic stability in rat liver microsomes

As mentioned before, the degradation of compounds by drug-metabolizing enzymes is a key point in drug development, in particular for the development of orally available drugs. In this thesis, the microsomal stability of compounds was tested using the experimental procedure described in the Materials and methods section (section 6.6.3). The conditions used in this assay had to be changed because two different lots of microsomes were used and their activity was different. Briefly, rat liver microsomes were incubated with the compounds under study at 1 μM (final concentration) in the presence of the cofactor NADPH. The stability of the compound was monitored for 60 min by HPLC-MS. Propranolol and IPR-179 were used as controls to compare the results between two conditions used in this assay.

The Napierian logarithm of the percentage of compound was plotted against incubation time. The elimination rate constant (k, Equation 4), the half-life time ($t_{1/2}$, Equation 5) and the intrinsic clearance (CLint, Equation 7) of each compound were calculated from the resulted degradation profile curve. CLint is the ability of the liver to remove drug in the absence of flow limitations and binding to cells or proteins in the blood.

Equation 4:

$$k = -g$$

Equation 5.

$$t_{1/2}\,(min) = \frac{0.693}{k}$$

Equation 6.

$$V(\mu L/mg) = \frac{volume\ of\ incubation\ (\mu L)}{protein\ in\ the\ incubation\ (mg)}$$

Equation 7:

$$CL_{int}(\mu L/\text{min/mg protein}) = \frac{V\ x\ 0.693}{t_{1/2}}$$

Where:

g = slope from a plot of ln [concentration] vs. incubation time.

k = negative value of g

V = µL volume of incubation per mg microsome protein

The half-life microsomal stability and the intrinsic clearance of the compounds selected for this experiment are shown in Table 9. As the objective is to increase the stability in rat microsomes of IPR-179, all the compounds that show a higher stability, were considered good candidates. Among them, the most stable compound was IPR-447, which have "B" instead of NMeIle in position aa2 and Trifluoropentanoyl instead of Hexanoyl at the N-terminal of the peptide. The addition of fluorenes in the fatty acid chain improves the stability.

Table 9. Stability of the molecules in rat liver microsomes in minutes. *: correspond to results obtained from the new protocol.

ID	t ½ (min)	CL_{int} (µL/min/mg)
IPR-179	0.9 / 16.73*	1540 / 82.8*
IPR-424	0.36	3826.6
IPR-425	0.75	1841.8
IPR-426	74.12*	18.7*
IPR-436	67.10*	20.6*
IPR-437	3.77	367.6
IPR-438	15.41*	90.0*
IPR-439	2.01	689.5
IPR-447	87.9*	15.8*
IPR-448	32.18*	43.1*

3.3.6. Evaluation in rat plasma stability

The stability of drug candidates in plasma is an important factor for *in vivo* experiments because it is an indicator that the drug will not be degraded before arriving to its target site. This experiment is performed in rat plasma because the efficacy of drugs in pre-clinical studies must be studied in this specie. The rat plasma stability was tested using the experimental procedure described in the Materials and methods section of this thesis (section 6.6.2). Briefly, rat plasma mixed with PBS (1:1) was incubated with the test compounds at 20 µM final. The stability of the compound was monitored for 10 min and analysed by HPLC-MS. Benfluorex, Verapamil and IPR-179 were used as controls in these experiments.

Table 10. Percentage of compound present in rat plasma at 10 minutes of experiment

ID	Plasma (10 min)
IPR-179	>21%
IPR-424	55%
IPR-425	93%
IPR-426	75%
IPR-428	0%
IPR-430	7%
IPR-436	46%
IPR-437	9%
IPR-438	88%
IPR-439	77%
IPR-441	97%
IPR-447	57%
IPR-448	38%

Results shown that the strategy of design compounds modifying the position aa1 adding a "J", improves the plasma stability, as we can observe in compound IPR-441 (**¡Error! No se encuentra el origen de la referencia.**), although it does not show MMP-9 inhibition (shown in section 3.3.1). The replacement of *N*MeIle by "B" notably increased the stability of the inhibitor in plasma, as shown in IPR-425, IPR-438 or IPR-439, it seems that it is also a good change. The use of "D" instead of *N*MeIle (IPR-428 or IPR-430) results in a total degradation of the compounds. The change of the hexanoyl by other fatty acids in N-terminal maintaining *N*MeIle in aa2 position, such as 2PP (IPR-424), 2,2-diF(hex) (IPR-436) and TriFpentanoyl (IPR-447) seems to increase the stability but in lower extend compared to others changes mentioned before.

3.3.7. Summary of *in vitro* results

Based on IPR-179 results, we compiled the *in vitro* results obtained from experiments performed in this chapter (MMP-9 and MMP-2 inhibition, selectivity for MMP-1, MMP-3 and MMP-7, BBB permeability, rat microsomal and plasma stability) to select the most promising analogues for further drug development experiments.

A summary of the *in vitro* results for the most relevant compounds is shown in **¡Error! No se encuentra el origen de la referencia.**:

Table 11. In vitro results of the most promising IPR-179 analogues. Gelatinase (MMP-9 and MMP-2) inhibitory activity, selectivity (MMP-1 and MMP-7), BBB-PAMPA assay, stability in rat liver microsomes and stability in rat plasma; N/E: Not evaluated; *Correspond to results obtained with new protocol (conditions explained in Section 3.3.5)

ID	MMP9 IC50 (nM)	MMP2 IC50 (nM)	MMP1 IC50 (μM)	MMP3 IC50 (μM)	MMP7 IC50 (μM)	PAMPA		Half-life in microsomes (min)	Degradation in rat plasma (10 min)
						% Transport	% Retention		
IPR-179	304	610	N/E	N/E	N/E	12.7	3.2	16.73*	>21%
IPR-424	596	14	N/E	N/E	N/E	N/E	N/E	0.36	55%
IPR-425	268	14	3.8	N/E	2.2	18.89	7.18	0.75	93%
IPR-426	168	14	13.4	N/E	39	8.71	-2.97	74.12*	75%
IPR-436	200.5	44	13	N/E	5.1	20.1	-0.43	67.10*	46%
IPR-437	233.5	44	11.6	N/E	6	11.7	-145.52	3.77	9%
IPR-438	498	42.8	4.3	N/E	7.7	27.43	-4.19	15.41*	88%
IPR-439	856	N/E	2	N/E	2.3	28.88	-38.71	2.01	77%
IPR-447	427	42.8	1.1	N/E	4.1	5.61	-38.07	87.9*	57%
IPR-448	1025	N/E	N/E	N/E	N/E	N/E	N/E	32.18*	38%

3.4. Pharmacokinetic study of IPR-426 and IPR-436

After evaluating the results of Table 11, compounds IPR-426 and IPR-436 (with this order of preference) were selected to perform the pharmacokinetic (PK) experiments in rats. PK experiments are necessary on drug development because provides data avbout drug exposure, potential tissue distribution, half-life, bioavailability and clearance rate. During the study these parameters were obtained by measuring drug concentration in plasma at several time points.

The PKs were performed at the CRO Eurofins-Advinus (India). The preliminary pharmacokinetic parameters of compounds IPR-426 and IPR-436 following iv and oral (po) administration were studied in male Sprague Dawley rats. A total of 6 (n=3/group, at a different dose for each group) male Sprague Dawley rats were used in the study for each compound. The drugs were administered acutely at a nominal concentration of 1 mg/kg for iv and 5 mg/kg for po. 2% Tween 80 in saline was used as vehicle in both groups. Blood samples were collected at 0, 0.083, 0.25, 0.5, 1, 2, 3, (iv only), 4, 6 (po only), 8, 12 and 24 hours, post-dose from each animal. Plasma was then extracted and analysed by LC-MS/MS.

In these studies, the following parameters were calculated:

- Area under the concentration time curve (AUC_{last})
- Peak plasma concentration (C_{max})
- Time to reach peak plasma concentration (T_{max})
- Clearance (CL)
- Volume of distribution at steady state (V_{ss})
- Half-life value ($T_{1/2}$)
- Mean residence time (MRT)
- Bioavailability (F)

3.4.1 IPR-426

Calculated pharmacokinetic parameters of compound IPR-426 are shown in **¡Error! No se encuentra el origen de la referencia.**. The plasma concentration-time profile after acute iv and po administration is shown in Figure 41.

Following single intravenous bolus administration of IPR-426 dose formulation to male Sprague Dawley rats (Actual dose: 0.94 mg/kg), the mean plasma clearance was found to be high (73.2 mL/min/kg) which is almost 1.33-fold higher than the normal hepatic blood flow in rats (55 mL/min/kg). The volume of distribution at steady state was found to be low which is almost half of the normal body water content of 0.7 L/kg in rats, suggesting that IPR-426 was confined to blood stream. The terminal plasma elimination half-life was found to be 0.219h. Following single oral gavage administration of IPR-426 dose formulation to male Sprague Dawley rats (Actual dose: 5.40 mg/kg), median time to reach peak plasma concentration (T_{max}) was found to be 0.75 h (0.50-1.00), suggesting rapid rate of absorption. The exposure (C_{max} and AUC_{last}) was found to be 4.34 ng/mL and 12.3 ng.h/mL, respectively. The absolute oral bioavailability of IPR-426 was found to be less than 1%.

Both iv and po dose formulations were analysed and found to be 94% and 108% compared to respective nominal concentrations.

Table 12. Pharmacokinetic parameters (mean ± SD; n=3) of IPR-426 following iv (dose: 0.94 mg/kg) and po (dose:5.40 mg/kg) administration of IPR-426 dose formulations in male Sprague Dawley rats. Co Back extrapolated concentration at time zero; [a]Tmax reported as median (min-max); [b] Actual doses and AUC_{last} of iv and po was used for bioavailability calculation; [c] n= 1 animal data (Rja2054); NR: Not reportable due to inadequate elimination phase.

Route	Actual Dose (mg/kg)	T_{max}[a] (h)	C_0/C_{max} (ng/mL)	AUC_{last} (ng.h/mL)	AUC_{inf} (ng.h/mL)	CL (mL/min/kg)	V_{SS} (L/kg)	$T_{1/2}$ (h)	%F[b]
iv	0.94	NA	2780 ± 1560	277 ± 192	278 ± 192	73.2 ± 36.7	0.348 ± 0.134	0.219 ± 0.0797	NA
po	5.40	0.5 (0.5-1.00)	4.34 ± 5.93	12.3 ± 16.7	NR	NA		1.63[c]	0.77

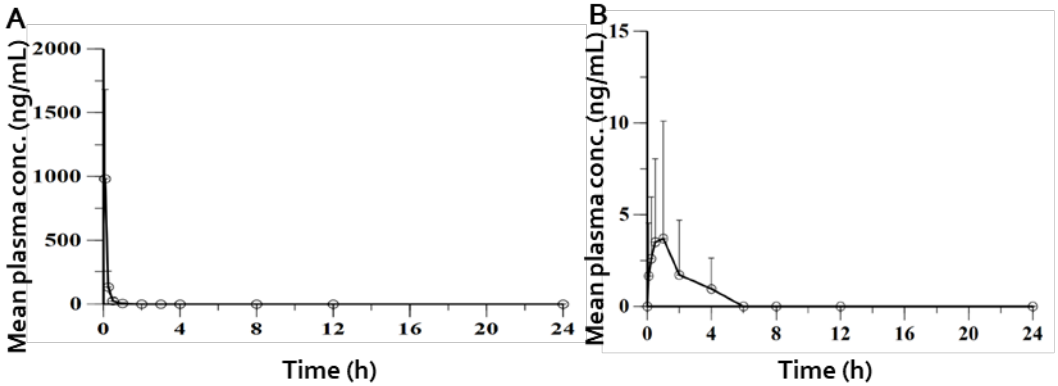

Figure 41. Mean plasma concentration-time profile following A: iv (dose: 0.94 mg/kg) and B: po (dose: 5.40 mg/kg) administration of IPR-426 in male Sprague Dawley rats.

The PK profile was determined first for the compound IPR-426 because it was the most promising compound according to the *in vitro* results obtained. However, after the PK results were obtained, it was concluded that IPR-426 was not a good candidate for oral administration because of the low exposure levels after po administration. Although the compound was detected early on, the volume of distribution at the steady stage (V_{SS}) was not calculated because the low bioavailability. In terms of the iv route, the results were worse than those registered for lead candidate IPR-179 (140).

Taking these results into account, it was decided to carry out the PK profile for the second most promising candidate, IPR-436.

3.4.2 IPR-436

Pharmacokinetic parameters of compound IPR-436 are shown in **¡Error! No se encuentra el origen de la referencia.**. The plasma concentration-time profile after acute iv and po administration is shown in Figure 42.

Following single iv bolus administration of IPR-426 dose formulation to male Sprague Dawley rats (Actual dose: 1.04 mg/kg), the mean plasma clearance was found to be high (268 mL/min/kg) which is almost 4.87-fold higher than the normal hepatic blood flow in rats (55 mL/min/kg) indicating extrahepatic elimination. The volume of distribution at steady state was found to be high which is almost 2.53-fold higher than the normal body water content of 0.7 L/kg in rats, suggesting a high extravascular distribution of IPR-436. The terminal plasma elimination half-life was found to be 0.233 h.

Following single po administration of IPR-436 dose formulation to male Sprague Dawley rats (Actual dose: 5.1 mg/kg), median time to reach peak plasma concentration (T_{max}) was found to be 0.25 h (0.25-0.5), suggesting rapid rate of absorption. The exposure (C_{max} and AUC_{last}) was found to be 8.55 ng/mL and 3.97 ng.h/mL, respectively. The absolute oral bioavailability of IPR-436 was found to be less than 1%.

Both iv and po dose formulations were analysed and found to be 104% and 102% compared to respective nominal concentrations.

Table 13. Pharmacokinetic parameters (mean ± SD; n=3) of IPR-436 following iv (dose: 1.04mg/kg) and po (dose:5.1 mg/kg) administration of IPR-436 dose formulations in male Sprague Dawley rats. Co Back extrapolated concentration at time zero; [a] Tmax reported as median (min-max); [b] Actual doses and AUC_{last} of iv and po was used for bioavailability calculation; NR: Not reportable due to inadequate elimination phase.

Route	Actual Dose (mg/kg)	T_{max}[a] (h)	C_o/C_{max} (ng/mL)	AUC_{last} (ng.h/mL)	AUC_{inf} (ng.h/mL)	CL (mL/min/kg)	V_{ss} (L/kg)	$T_{1/2}$ (h)	%F[b]
iv	1.04	NA	681 ± 157	65.0 ± 10.5	65.9 ± 10.8	268 ± 48.8	1.77 ± 0.45	0.233 ± 0.04	NA
po	5.1	0.25 (0.25-0.50)	8.55 ± 1.95	3.97 ± 1.00	NR	NA		NR	0.01

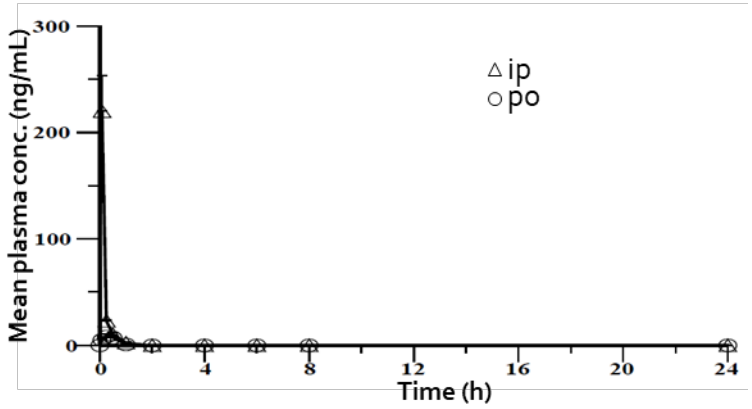

Figure 42. Mean plasma concentration-time profile following iv (dose: 1.04 mg/kg) and po (dose: 5.1 mg/kg) administration of IPR-436 in male Sprague Dawley rats.

The PK profile indicates that IPR-436 is neither a good candidate for po administration because the bioavailability (F) is very low (< 1%). It is neither a good candidate for iv administration as the results were also worse than that of the candidate IPR-179 (140).

These results indicate that *in vitro* tests are useful as a preliminary screening tool to select the best candidates, but the results obtained *in vivo* may not be equivalent to those previously obtained *in vitro*, since in *in vivo* there are many more complex and uncontrolled physiological factors that can affect.

Therefore, as we had not been succeeded in obtaining a good candidate for oral administration, and IPR-179 had been proved as a very effective compound *in vivo*, we started to make preliminary formulations for ip administration, although this was not our desired route of administration when the project started.

3.5. IPR-179 formula development for parenteral administration

Since the obtained results were not those desired in the PK experiments, the decision of the company was to halt the development of an orally available analogue for IPR-179 because the lack of success after several attempts. Compound IPR-179 has shown outstanding efficacy results in two preclinical animal epilepsy models (141) and the parenteral administration of this compound to humans could be acceptable because the lack of alternative drugs addressing epileptogenesis. In this regard, the next strategy was to find the optimal vehicle for parenteral administration. A good formulation of the drug can improve the bioavailability, efficacy, safety and patience compliance. The aim of this strategy was to find a vehicle able to dissolve the largest feasible amount of IPR-179 in the lower volume possible.

An excipient is a substance that has no medicinal properties and can be formulated with an active ingredient. It can enhance the physiological absorption of the drug such as enhancing the solubility or reducing viscosity (147–149). The FDA has a list of the excipients approved and their maximum volume of dosage for every administration method.

Three excipients with different properties were chosen; 5% polysorbate 80 (Tween 80) in water, 33% 2-hydroxypropyl)-β-cyclodextrin (HP-β-CD) in phosphate buffer saline (PBS) (pH=7,4) and 20% Polyethylene glycol 400 (PEG400) in saline buffer (0.9% NaCl). Moreover, the solubility was also tested in acetonitrile because is the solvent in which the molecule is dissolved during all molecule development experiments. The formulation with 5% tween 80 in saline was used as a reference since it had already been used and was intended to test if the solubility could be improved with other excipients. The other two excipients have been demonstrated to show high efficacy as drugs solubilizers in different studies (148,150). To calculate the maximum solubility of the compound IPR-1.79 in the selected excipients, different solutions were prepared. To 10 mg of the compound in solid state, successive volumes of 50 μL of the prepared excipient solution were added every hour, under constant magnetic stirring, until a clear solution was obtained. This process was repeated for each selected excipient formulation. Afterwards, magnetic stirring was continued for additional 48h at room temperature. Finally, the solution was filtered and analysed by HPLC in order to determine the maximum solubility. In Table 14 shows the composition of each formulation, the final concentration and the maximum solubility obtained.

¡Error! No se encuentra el origen de la referencia. shows that Tween 80 at 5% formula is the one with which the best solubility is obtained for the compound IPR-179. With 33% HP-β-CD formulation, the solubility obtained is better when it is compared to the reference ACN:H_2O formulation. Also, these results indicate the 20% PEG400 formula does not work well for the compound IPR-179. As this was a test and these are preliminary results, the formula could be optimised (by changing the HP-β-CD concentration or trying a similar one) to see if the solubility can be improved and, furthermore, it should be done in triplicate to confirm the results.

Table 14.: Composition, final concentration and maximum solubility obtained for each formulation.

Formulation	Excipient	Buffer	Final Concentration (mg/mL)	Maximum compound solubility (mg)
A	5% Tween 80	H_2O	50	3.69
B	33% HP-β-CD	PBS (pH=7,4)	14.2	1.05
C	20% PEG_{400}	Saline (0,9% NaCl)	11.11	0.28
D	50% ACN	H_2O	12.62	0.89

3.6. Summary of the chapter

The process of the lead optimization is a critical step in drug development because it is usually the final step for the optimization until reaching a preclinical candidate and it is usually challenging to identify a molecule that accomplishes all the required characteristics before starting the preclinical development. This thesis chapter was focused on the optimization of a compound to improve its metabolic stability in order to be a suitable preclinical candidate for oral administration. In previous work, it had been obtained IPR-179, which was a potent and selective MMP-9 inhibitor, able to cross the BBB and which had been proven effective in epileptogenesis *in vivo* model. However, it is not stable in *in vitro* microsomes, therefore, it should be developed for parenteral administration. To obtain a new candidate, new molecules had been designed and synthesized and had been tested in different *in vitro* assays to obtain the top candidates. Unfortunately, a good oral candidate has not been achieved because it must meet many requirements such as being a potent and selective MMP-9 inhibitor, being permeable to the BBB, being stable in plasma and stable in microsomes. Two candidates with the desired *in vitro* properties were obtained during this thesis, however, when *in vivo* PKs were performed in rats, it was demonstrated that they were not as good *in vivo* as the *in vitro* results pointed out.

CONCLUSIONS

The following lines present the main conclusions of this thesis. For consistency with the reported findings, conclusions are presented in line with the objectives stated in the introduction of this thesis.

1 The role of POP in Akt metabolic pathway:

1.a Mice brain extracts treated/untreated with POP inhibitor IPR19 were analysed in a *multiplex assay kit* to test the action POP inhibitor in total protein and phosphorylated Akt, GSK-3β, IGF-1R, IR, IRS-1, p70S6K and PRAS40 protein. It was observed that POP inhibitor IPR19 decreases PRAS40 phosphorylation level.

1.b To confirm the results obtained, it was tested the effects of POP inhibitor IPR166 in Akt, pAkt, PRAS40 and pPRAS40 in SH-SY5Y cells and in RPE cells cultures but not conclusive results were obtained. Overall, it seems that POP inhibition does not alter the targeted protein levels in these cellular models.

1.c It was also tested the effect of IPR166 on Akt, PRAS40 and S6 and their phosphorylated forms in brain extracts from two schizophrenia-like mice models. In the PI:C mice model, some differences were observed in Akt and S6 protein levels. PI:C mice treated with IPR166 have high levels of pAkt as those treated with vehicle, but when pS6 levels are analysed, it is observed that treatment with IPR166 reduces the phosphorylation level of this protein to levels like those registered for control animals. Thus, it seems that POP inhibition can restore pS6 levels in this schizophrenia model mice. The obtained results are not fully conclusive and more research in this area should be performed.

1.d It was tested the effect of IPR166 inhibitor in PP2A protein and it was observed that in presence of POP inhibitor, PP2A activity is higher than at basal conditions. On the other hand, it seems that IPR166 inhibitor does not affect the HDAC activity.

2 To identify the main protein interactions of POP:

2.a IP technique was optimized for POP from SH-SY5Y cells extracts.

2.b The co-IP technique used in the present work was not able to show GAP43 and a-synuclein are described as direct POP interactors.

2.c After POP interactome analysis by LC-MS/MS with IPR166 treated/untreated samples from SH-SY5Y, α-tubulin and clathrin were identified as interesting POP interactors. After these results, it was possible to validate by co-IP that clathrin interacts with POP in basal conditions and that POP is inhibited with IPR-166. Moreover, it was confirmed that POP interaction with tubulin is affected by the administration of IPR166.

2.d Direct interaction between POP and PP2A proteins has not been demonstrated by co-IP in the context of this thesis.

2.e The potential involvement of POP in macroautophagy and chaperone-mediated autophagy has not been observed in this thesis.

3 To obtain an optimized MMP-9 inhibitor for oral administration:

3.a Structural modifications on the structure of compound IPR-179 were carried out to improve the *in vitro* microsomal stability of the compound. A total of 16 IPR-179 analogues have been synthesized and their potency and selectivity have been evaluated *in vitro*. Changes in position aa1 of the compound causes a change in pharmacophore of the molecule and it couldn't access into protein catalytic for the inhibition.

3.b *In vitro* BBB permeability were tested of most promising compounds. All compound tested showed promising results considering that transport values were above 5%.

3.c *In vitro* microsomal and plasma stability were tested of most promising compounds. Some changes in position aa2 and aa3 position improves the microsomal and plasma stability.

3.d Compounds IPR-426 and IPR-436 were selected for an iv and oral pharmacokinetic study in rats. Unfortunately, neither of both compounds were found to produce significant drug levels in plasma upon oral administration of the compound.

MATERIALS AND METHODS

General Methods

1 Cell lines

1.1 SH-SY5Y cells

The SH-SY5Y cell line is a thrice cloned subline of the neuroblastoma cell line SK-N-SH (ATCC HTB-11) which was established in 1970 from a metastatic bone tumour from a 4-year-old cancer patient. The culture media used were Dulbecco's Modified Eagle Medium (DMEM) with high glucose (4500mg/mL) supplemented with 10% of inactivated fetal bovine serum, 1% L-Glutamine and 0.05% of penicillin and streptomycin.

1.1.1 Cell lysis

To obtain the cell extract samples for each experiment the following protocol was conducted. First, cells were detached from the wells using trypsin, washed once with DMEM and finally washed twice with PBS. Then, 75 µL RIPA buffer (without inhibitors) was added and incubated during 30 min in orbital agitation at 4ºC. Then, it was centrifuged at 10000 x g for 10 min at 4ºC and the pellet was discarded. Finally, it was performed a BCA protein quantification with a Pierce BCA Protein Assay Kit purchased from Thermo Fisher Scientific.

1.2. RPE cells

Retinal Pigment Epithelium (RPE) cells diverge from the optic vesicle during early embryonic development. This cell line was kindly provided by Dr. Neus Agell group from Hospital Clinic de Barcelona.

1.2.1 Cell lysis

To obtain the cell extract samples the following protocol was conducted. First, cells were detached from the wells using trypsin were washed once with DMEM and finally washed twice with PBS. Then, 75 µL Lysis buffer (67 mM Tris-HCl, 2% SDS, pH=6.8) was added and was incubated during 30 min in orbital agitation at 4ºC. Following this step, it was centrifuged at 10000 x g for 10 min at 4ºC and the pellet was discarded. Finally, it was

performed a BCA protein quantification with a Pierce BCA Protein Assay Kit purchased from Thermo.Fischer Scientific

2 Animals

2.1 C57/Bl6J mice model

Adult male C57BL/6J mice were injected ip with the vehicle (to) or IPR19 (5 mg/kg, 5% Tween80 in PBS) and at predetermined time points (0.5 and 6h). Animals were euthanized by cervical dislocation. Previous dislocation (6 min before), animals were anesthetized with chloral hydrate (400 mg/kg). Immediately after euthanizing, brains were excised. Brains were cut sagittally into two halves, frozen in dry ice and stored at -80°C until sample processing. 4 animals were used for each time point.

2.2 PCP mice model

Old male CD-1 mice were administered three doses of IPR-66 at 5 mg/kg, 2.5 mg/kg and 1mg/kg orally po diluted in Tween80 5% in saline or vehicle (5% Tween80 in saline) po 60 minutes before being euthanized. Cognitive deficit was induced by 3 mg/kg PCP given sc 30 min prior to euthanized. Previous dislocation (6 min before) animals were anesthetized with chloral hydrate (400 mg/kg). Immediately after euthanasia and brains were excised, were cut sagittally into two halves, frozen in dry ice and stored at -80°C until sample processing. 5 animals were used for each condition.

2.3 PI:C mice model

Female C57/BL6 mice on day 9.5 of pregnancy received intraperitoneal injection (ip) of polyinosinic:polycytidylic acid (7.5 mg/kg i.p.; Sigma-Aldrich) or saline. Offspring were separated from their mothers after three weeks. Subsequent experiments were performed in adult (8–10 weeks at the beginning) male mice. A single dose of IPR-166 at 5 mg/kg ip diluted in Tween80 5% in saline or vehicle (5% Tween80 in saline) ip was injected. The animals were euthanized 30 minutes post-treatment. Immediately after euthanasia, brains were excised and cut sagittally into two halves, frozen in dry ice and stored at -80°C until sample processing.

2.4 Mice brain homogenates

Half- brain from mouse was added in a vial containing two zirconium oxide beads. Then, 400 µL of cold PBS + 0.1% Tween80 or RIPA buffer was added. The disruption was performed with Precellis 24 tissue homogenizer, 2 cycles x 20 sec. After, the sample was transferred into an eppendorf, it was sonicated for 5 min at 4 °C and was incubated on ice for 15 min. Finally, it was centrifuged at 16000 x g for 30 min, at 4 °C and discard the pellet.

3 SDS-PAGE and Western Blot

3.1 SDS-PAGE

To separate the proteins according to their electrophoretic mobility, SDS-PAGE was performed. After incubation at 95°C for 5min, samples were loaded onto polyacrylamide (10%) gels. BenchMark Prestained molecular weight marker was purchased from Novex-Life technologies. Electrophoresis was accomplished at 150-180 V for 1,5 h approximately at room temperature.

3.2 Western blot

In order to detect POP protein in our samples, the electrophoretically separated proteins were transferred to a blotting membrane at a constant I = 300 mA for 1,5 h at 4 °C. After blocking the membranes with 10% Skim Milk Powder in TBS + 0,1% Tween 20 (TBSBT) for 1h at room temperature or overnight at 4°C and cleaning with PBS + 0,1% Tween 20, membranes were incubated with first antibody at the appropriate dilution. After first antibody and cleaning, second antibody was added at the membrane at the appropriate dilution were incubated with TBST buffer with 5% milk for 1h at room temperature. Finally, membranes were cleaned with TBST and the fluorescent signal was visualized using Odissey DLx from Li-Cor.

Statistics

Graphs and calculations were obtained with Prism software (version 5, GraphPad Inc).

Chapter 1

4.1 Multiplex assay of Akt pathway in mice brain samples

To identify the proteins from Akt pathway expressed in mice brain extract samples treated with IPR19, two different kits were selected for the simultaneous quantitative determination of total and phosphorylated protein. Specifically, it was selected Akt Total and Akt Phospho Magnetic 7-PLEX Panels from Novex-Life Technologies. The protocol followed was the provided by the supplier. The assay was performed in a 96-well plate format and analysed with a Luminex® 100™ instrument which monitors the spectral properties of the capture beads while simultaneously measuring the quantity of associated fluorophore. In these experiments, it was analyzed half-brain cortex homogenates from adult male C57/Bl6J mice treated with IPR19 (n=8) and untreated (vehicle)(n=8) in duplicate.

4.2 Akt and pAkt quantification in RPE cell line extract collection

RPE cells were treated with 2 µM IPR-166 or vehicle (1% DMSO) for 1 h. After, it was added EGF to a final concentration of 12nM into the cell media.

4.2.1 WB conditions

- Membrane: nitrocellulose, 0.2 µm
- Blocking: 5% BSA in TBST for 1 h at rt
- Primary antibody: TBST buffer with 5% BSA. Membrane was incubated overnight at 4ºC

- Against pAkt-Ser473 (4060S): Final dilution: 1/500.

- Against actin (A1978): Final dilution:1/200000

- Secondary antibody: TBST buffer with 5% milk. Membrane was incubated for 1h at room temperature.

- Against rabbit IgG (P0448): Final dilution: 1/2000.

- Against mouse IgG (Dylight 800, Thermo) 610-745-002): Final dilution: 1/10000

4.3 Akt and pAkt quantification in brain samples from PCP mouse model

For these experiments, it was used mice brain homogenates extracts samples from PCP mouse model.

4.3.1 WB conditions

- Membrane: nitrocellulose, 0.2 µm
- Blocking: 5% BSA in TBST for 1 h at rt
- Primary antibody: TBST buffer with 5% BSA. Membrane was incubated overnight at 4°C
  - Against Akt (9272S): Final dilution: 1/1000.
  - Against pAkt (4060S): Final dilution: 1/2000.
  - Against actin (A1978): Final dilution:1/200000
- Secondary antibody: TBST buffer with 5% milk. Membrane was incubated for 1h at room temperature.
  - Against rabbit IgG (Alexa Fluor 680, Thermo): Final dilution: 1/2000.
  - Against mouse IgG (Dylight 800, Thermo)): Final dilution: 1/10000

4.4 PP2A activity measurement and quantification

For this experiment, a PP2A Immunoprecipitation Phosphatase Assay Kit from Merck was used. Samples analysed were SH-SY5Y cell extracts. The cells were treated with 2 µM IPR-166 or vehicle (1% DMSO) for 1 h.

First, a PP2A- IP must be performed. For this reason, into an Eppendorf, it was added 100 µg protein from cell extract, 30 µL protein A agarose beads (Merck) and the corresponding antibody (optimized volumes):

a. Antibody against PP2A (05-421): 4 µL

b. Antibody against actin (A1978): 2 µL (Negative control)

Then, the assay buffer (50mM Tris-HCl, pH 7.0, 0.1mM $CaCl_2$) was added until a final volume of 500 µL and it was incubated for 90 min in orbital agitation at 4°C. Following, it was washed three times with 700 µL with TBS and once with Assay buffer.

After the IP was performed, PP2A activity measurement and quantification were carried out. Therefore, it was added 28 µL 1 mM phosphopeptide and 52 µL Assay Buffer (Final concentration: 350 µM) and it was incubated for 10 min at 30 ºC in agitation. After, it was added 25 µL/well (into a 96-well microtiter plate) with 100 µL Malaquite green and it was incubated for 10-15 min at RT. Finally, the absorbance was read at 650 nm.

The activity has been quantified using a phosphate standard curve that has been performed with dilutions of the phosphate standard available with the commercial kit.

4.5 HDAC activity assay

In order to carry out this experiment, HDAC Activity Assay Kit from Merck was used and the protocol provided was followed. HeLa Nuclear extracts were treated with 0.5 and 1 µM POP inhibitor IPR166 in triplicates. The following table list (**¡Error! No se encuentra el origen de la referencia.**) the additions required for the Assay.

Table 15. Summary of the assay conditions

Sample	Treatment	HeLa extract	Substrate	HDAC Developer
C+	10 µL Assay buffer (5% DMSO)	15 µL Hela Cell Nuclear Extract	25 µL	50 µL
C-	10 µL Assay buffer (5% DMSO)	15 µL Assay Buffer	25 µL	50 µL
1 µM IPR166	10 µL IPR166 in Assay Buffer (5% DMSO)	15 µL Hela Cell Nuclear Extract	25 µL	50 µL
1 µM IPR166 control	10 µL IPR166 in Assay Buffer (5% DMSO)	15 µL Assay Buffer	25 µL	50 µL
500 nM IPR166	10 µL IPR166 in Assay Buffer (5% DMSO)	15 µL Hela Cell Nuclear Extract	25 µL	50 µL
500 nM IPR166 control	10 µL IPR166 in Assay Buffer (5% DMSO)	15 µL Assay Buffer	25 µL	50 µL

Chapter 2

5.1 POP-IP optimization

5.1.1 SY-5YSY cell extract collection

Cells were treated with 2 µM IPR-166 or vehicle (1% DMSO) for 1 h. 1% of DMSO was only added to cell culture when it was performed the IP with cells treated with IPR166. In POP IPs in which proteomic analysis was performed, DMSO was not added to the culture.

5.1.2 IP

After some experiments to optimize the protocol, this is the final protocol of mixed IP method. Into an Eppendorf, 150 µg protein from cell extract or homogenized brain was added, 30 µL protein A agarose beads (Merck) and the corresponding antibody (optimized volumes):

a. Antibody against N-terminal domain of POP (ab58988-Abcam): 2 µL

b. Antibody against beta-propeller domain of POP (ab58993-Abcam): 3 µL

c. Antibody against actin (sc-47778-Santa Cruz Biotechnologies): 4 µL

Then, the assay buffer 50mM Tris-HCl, pH 7.0, 0.1mM $CaCl_2$ (TBS) was added until a final volume of 500 µL and it was incubated for 90 min in orbital agitation at 4ºC. Following, it was washed twice with 700 µL of Assay Buffer and it was added 20 µL Loading Buffer (containing 40% Laemmli Buffer 5x, 40% PBS, 20% DTT). Finally, the samples were incubated for 5 min at 95 ºC.

5.1.3. Western blot

- Membrane: nitrocellulose, 0.2 µm (GE Healthcare)
- Blocking: 5% BSA in TBST for 1 h at rt or overnight at 4ºC.
- Primary antibody: TBST buffer with 5% BSA. Membrane was incubated 1h at rt.
  - against POP (N-term) (ab58988): Final dilution: 1/5000.

• Secondary antibody: TBST buffer with 5% milk. Membrane was incubated for 1h at room temperature.

- Against rabbit IgG (P0448, Merck): Final dilution: 1/2000.

5.2. Interactome analysis

Two batchs of POP IPs from SH-SY5Y cell extracts were submitted to CRG proteomics Unit for proteomic analysis of POP interactome. The first batch consisted in one actin IP (as negative control) and one POP IP (n=1) in order to set up the experimental conditions. POP was identified with 24 peptides and a coverage of 34,70 in the POP IP whereas the protein was not found in the negative control.

The second batch of samples consisted in triplicates of the negative control IPs and the POP IPs. POP was identified in all three POP IP triplicates with 14, 17 and 16 peptides and a coverage of 19.86, 24.08 and 22.82 respectively. POP was not found in any of the negative control IP triplicates.

In the experiment, 45% of the samples were analysed by LC-MS/MS using 1-hour gradient in the Orbitrap Velos Pro (Thermo). As quality control, BSA controls were digested in parallel and ran between the samples to avoid carryover and assess the instrument performance. Results were searched against SwissProt human database (April 2018) using the search algorithm Mascot v2.5.1 (http://www.matrixscience.com/). Peptides have been filtered based on FDR and only peptides showing an FDR lower than 5% were retained. SAINT have been used to calculate protein fold change and p-value.

The protein cluster interactor was performed with STRING program.

5.3. Co-IP POP-Tubulin and POP-Clathrin

SH-SY5Y cell extract was used. The cells were treated with 2 µM IPR-166 or vehicle (1% DMSO) for 1 h. The detachment protocol was the same as in the other assays.

5.3.1 POP IP

Into an Eppendorf, 800-1000 µg protein from cell extract was added, 30 µL protein A agarose beads (Merck) and the corresponding antibody (optimized volumes):

a. Antibody against alpha tubulin (ab52866, Abcam): 3-4 µL

b. Antibody against clathrin heavy chain (ab21679, Abcam): 2 µL

c. Antibody against actin (sc-47778, Santa Cruz Biotechnology): 4 µL

Also, it was added 15 µL of IPR-166 (Co= 100 µM; Cf= 2 µM) into the Eppendorf containing the extract from the cells treated with the inhibitor and 15 µL of DMSO into the extract from non-treated cells. Then, the assay buffer (50mM Tris-HCl, pH 7.0, 0.1mM $CaCl_2$) was added until a final volume of 750 µL and it was incubated for 120 min in orbital agitation at 4ºC. Following, it was washed twice with 700 µL of Assay Buffer and it was added 20 µL Loading Buffer (containing 40% Laemmli Buffer 5x, 40% PBS, 20% DTT). Finally, the samples were incubated for 5 min at 95 ºC.

5.3.2 WB conditions

- Membrane: nitrocellulose, 0.2 µm (GE Healthcare)
- Blocking: 10% milk in TBST for 1h at RT or overnight at 4ºC
- Primary antibody – against POP (N-term) (ab58988, Abcam): Final dilution: 1/5000. TBST buffer with 5% milk. Membrane is incubated for 1h at rt.
- Secondary antibody – against rabbit IgG light chain - HRP (ab99697, Abcam): Final dilution: 1/2000. TBST buffer with 5% milk. Membrane is incubated for 1h at room temperature.

5.4 Co-IP POP-PP2A

SH-SY5Y cell extract was used. The cells were treated with 2 µM IPR-166 or vehicle (1% DMSO) for 21 h.

5.4.1 PP2A and POP IP

Into an Eppendorf, 100 µg protein from cell extract was added, 30 µL protein A agarose beads (Merck)(Merck)and the corresponding antibody (optimized volumes):

a. Antibody against PP2A (05-421, Merck): 4 µL

b. Antibody against POP (ab58988, Abcam): 2 µL

c. Antibody against actin (A1978, Sigma): 2 µL (Negative control)

Then, the assay buffer (50mM Tris-HCl, pH 7.0, 0.1mM $CaCl_2$) was added until a final volume of 500 µL and it was incubated for 90 min in orbital agitation at 4ºC. Following, it was washed three times with 700 µL with TBS and once with Assay buffer. Finally, it was added 20 µL Loading Buffer (containing 40% Laemmli Buffer 5x, 40% PBS, 20% DTT) and it was incubated for 5 min at 95 ºC.

5.4.2 WB conditions

- Membrane: nitrocellulose, 0.2 µm (GE Healthcare)
- Blocking: 10% milk in TBST for 1h at RT or overnight at 4ºC
- Primary antibody: TBST buffer with 5% milk. Membrane was incubated for 1h at room temperature.

  - Against POP (ab58988, Abcam): Final dilution: 1/5000.

  - Against PP2A (A1978, Merck): Final dilution: 1/800.

- Secondary antibody: TBST buffer with 5% milk. Membrane was incubated for 1h at room temperature.

  - Against rabbit IgG/HRP (P0448, Dako): Final dilution: 1/2000.

  - Against mouse IgG Dylight 800 (610-745-002, Thermo): Final dilution: 1/10000

5.5. Macroautophagy

5.5.1 SH-SY5Y cell extract collection

SH-SY5Y cell extract was used for this experiment. Four conditions were assayed with these cells. All of them with an incubation time of 6h:

a. Cells were treated with vehicle (1% DMSO) + vehicle 2 (H_2O)

b. Cells were treated with vehicle (1% DMSO) + 60 μM chloroquine.

c. Cells were treated with 2 μM IPR-166 + vehicle 2 (H_2O)

d. Cells were treated with 2 μM IPR-166 + 60 μM chloroquine.

The detachment protocol was the same as in the other assays.

5.5.2 Western Blot conditions

• Membrane: PVDF (GE Healthcare). These membranes were activated with a methanol.

• Blocking: 10% milk in TBST for 1h at RT or overnight at 4°C

• Primary antibody: TBST buffer with 5% milk. Membrane was incubated for 1h at room temperature.

- Against LC_3 (NB100-2220SS, Novus Biologicals): Final dilution: 1/2000.

- Against actin (A1978, Sigma): Final dilution: 1/200000.

• Secondary antibody: TBST buffer with 5% milk. Membrane was incubated for 1h at room temperature.

- Against rabbit IgG Alexa Fluor 680 (A21076, Thermo): Final dilution: 1/8000.

- Against mouse IgG Dylight 800 (610-745-002, Thermo): Final dilution: 1/10000

5.6 Chaperone-mediated autophagy

5.6.1 SH-SY5Y cell extract collection

SH-SY5Y cell extract was used for this experiment. The cells were treated with 2 µM IPR-166 or vehicle (1% DMSO) for 6 h. The detachment protocol was the same as in the other assays.

5.6.2 WB conditions

- Membrane: nitrocellulose, 0.2 µm
- Blocking: 10% milk in TBST for 1h at room temperature or overnight at 4°C
- Primary antibody: TBST buffer with 5% milk. Membrane was incubated for 1h at room temperature.

  - Against LAMP-2A (ab18528, Abcam): Final dilution: 1/1000.

  - Against actin (A1978, Sigma): Final dilution: 1/200000.

- Secondary antibody: TBST buffer with 5% milk. Membrane was incubated for 1h at room temperature.

  - Against rabbit IgG Alexa Fluor 680 (A21076, Thermo): Final dilution: 1/8000.

  - Against mouse IgG Dylight 800 (610-745-002, Thermo): Final dilution: 1/10000

Chapter 3

6.1 Solid-Phase Peptide Synthesis (SPPS)

6.1.1 General considerations for SPPS

All peptides were synthesized manually by SPPS following the Fmoc/tBu strategy (151) and using 2-chlorotrityl resin. Solid-phase peptide elongation and other solid-phase manipulations were done manually in polypropylene syringes, each fitted with a polyethylene porous disk. Solvents and soluble reagents were removed by suction. Washings between synthetic steps were done with DMF (3 x 1 min) and DCM (3 x 1 min)

using 5 mL of solvent/g resin each time. During couplings the mixture was allowed to react with intermittent manual stirring.

6.1.2 Colorimetric tests

Kaiser test

The Kaiser test,(152) also known as ninhydrin test, allowed the detection of primary amines and was used during solid-phase peptide chain assembly to monitor deprotection and coupling steps. The peptide-resin was washed with DCM and vacuum dried. A few peptide-resin beads were transferred to a small glass tube. Six drops of reagent solution A and 2 drops of reagent solution B were added to the tube and the mixture was heated at 110°C for 3 min. The formation of a blue colour on the beads or the supernatant was indicative of the presence of free amines and thus of an incomplete coupling, while a yellow coloration was characteristic of a negative test. The method was highly sensitive and a negative test assured a coupling rate higher than 99%.

Reagent solution A: 400 g of phenol were dissolved in 100 mL of absolute EtOH and the mixture was heated until complete dissolution of the phenol. 20 mL of 10 mM KCN (65 mg in 100 mL of H_2O) were added to 1000 mL of freshly distilled pyridine over ninhydrin. Both solutions were stirred for 45 min with 40 g of Amberlite MB-3 resin ion exchange resin, filtered, and combined.

Reagent solution B: 2.5 g of ninhydrin were dissolved in 50 mL of EtOH; the resulting solution was kept in flask protect from light.

Chloranil test

Chloranil test(153) detects secondary amines during solid-phase chain assembly and was used to evaluate couplings onto proline or *N*-methylated residues. The peptide-resin was washed with DCM and vacuum dried. A small portion of peptide resin beads was transferred to a small glass tub and 20 µl of a saturated solution of 2,3,5,6-tetrachloro-1,4-benzoquinone (chloranil) with toluene and 200 µl of acetone were added. The mixture was shaken at rt for 5 min. A blue-greenish colour was indicative of the presence of free

secondary amines and was thus considered a positive test. Negative samples appeared as yellow, amber or brown.

6.1.3 Initial conditioning of resin and coupling of the first amino acid

The initial conditioning of the resin and the coupling of the first amino acid were performed as follows. The 2-chlorotrityl resin was conditioned by swelling in DCM (15 min) and washings with DMF (3 x 30 s). The incorporation of the first amino acid was performed by adding Fmoc-aa-OH (0.6 eq) and DIEA (5 eq total, first add 1/3 and stir for 10 min, then add 2/3) to the resin in DCM for 40 min. After this, the unreacted points of the resin were capped with MeOH (0.8 mL/ g resin, 10 min). Finally, the resin was washed with DCM (5 x 1 min).

6.1.4 Initial conditioning of resin and coupling of the hydroxylamine linker

This procedure was performed to obtain hydroxamate-based peptide-like compounds in solid phase. The initial conditioning of the resin and the coupling of the hydroxylamine linker were performed as follows. The 2-CTC resin was conditioned by swelling in DCM (15 min) and washings with DMF (3 x 30s). The incorporation of hydroxylamine linker was performed by adding *N*-Fmoc-hydroxylamine (1.5 eq) and DIEA (10 eq) to the resin in DCM for 24 h (154). After this, the unreacted points of the resin were capped with MeOH (0.8 mL/ g resin, 10 min). Finally, the resin was washed with DCM (5 x 1 min).

6.1.5 Fmoc group removal

The Fmoc protecting groups were removed by treating the resin with 20% piperidine in DMF (3-4 mL/g resin, 1 x 1 min, 2 x 5 min).

Fmoc group quantification/resin loading capacity

Piperidine washes were collected and measured by UV spectroscopy (λ = 290 nm) to determine the loading capacity of the resin after the coupling of the first amino acid. The loading capacity was determined according to Equation 8:

Equation 8.

$$Z = \frac{A \times X}{\varepsilon \times Y \times l}$$

Where:

A: Absorbance

X: Volume of solvent (mL)

ε: Molar absorbance coefficient (5800 L· mol-1 · cm-1)

Y: Resin weight (g)

l: Length of the cell (cm)

Z: Loading of the resin

6.1.6 Peptide chain elongation

The coupling reactions were performed in DMF using Fmoc-amino acids (3 eq) and oxime (3 eq) in the presence of DIC (3 eq). The extent of the coupling reaction was controlled by the ninhydrin or chloranil test and re-couplings were judiciously performed. Then, Fmoc deprotection was carried out as described in section 6.1.5.

6.1.7 Deprotection of the alloc ester protecting groups

The alloc group was removed by adding phenylsilane (10 eq) and Tetrakis(triphenylphosphine) palladium(0) (0.1 eq) in DCM and stirred for 15 min. After this time, the reaction was filtered and the resin washed thoroughly. The same treatment was repeated two more times. The resin progressively turned darker. After the last treatment, the resin was washed thoroughly with DCM and DMF. The accomplishment of the reaction was monitored by the ninhydrin test.

6.1.8 Cleavage

The resin was washed several times with DCM and dried. Peptide-like compounds was cleaved from the resin using 5% TFA in DCM for 15 min. The same treatment was repeated two more times. The reaction mixture was filtered and the resin rinsed with 5% TFA/DCM. The same treatment was repeated two more times. The resin was washed in DCM (3 x 5 min) and all the filtrates and DCM washes were evaporated under nitrogen stirring and lyophilized.

6.2 Synthesis of hydroxamate-based peptide-like compounds from carboxylic acid derivatives in solution

The synthesis of the hydroxamate-based peptide-like compounds in solution from the carboxylic acid derivatives obtained by SPPS was previously optimized in the lab.

This procedure was done in solution by combining the following reagents:

- Hydroxylamine hydrochloride
- Coupling agents; HOAt and EDC.HCl,
- Base: NMM
- Solvents: DMF, DCM (1:1).

Reaction was performed at 0º C during 17h. Products were isolated and purified by reverse-phase column chromatography and analysed by HPLC and HPLC-MS.

6.3 Peptide purification

6.3.1 ISCO RF

The crude products obtained were purified by reverse-phase column chromatography using a Combi flash ISCO RF provided with dual UV detection using a high performance RediSep Rf Gold C18 column. Mobile phase: H2O (0.1% TFA) and ACN (0.1% TFA). Detection was performed at 220 nm.

6.4 Peptide characterization

6.4.1 Analytical HPLC

HPLC chromatograms were recorded on a Waters 2695 separation module equipped with a Waters 2996 photodiode array (PDA) detector and a column C18 XSelect CSH (50 mm x 4.6 mm, 3.5 µm, 100 Å, Waters Corporation) and recorded using Empower. Flow rate was 1.6 mL/min, mobile phase consisted in H2O (0.1% TFA) and ACN (0.1% TFA). Detection was performed at 220 nm.

6.4.2 Analytical HPLC-MS

HPLC-MS chromatograms were recorded on a Waters 2795 separation module system equipped with a Waters 2996 photodiode array detector, mass detector 3100 and a column C18 XSelect CSH (50 mm x 4.6 mm, 3.5 µm, 100 Å, Waters Corporation) and recorded using Masslynx software. Flow rate was 1.6 ml/min, column temperature: 50 °C, mobile phases consisted in: H2O (0.1% FA) and ACN (0.1% FA).

6.5 In vitro enzymatic assays

The enzymatic reactions were performed in 96-well plates. Positive (no inhibitor) and negative (no enzyme) controls were included in each enzymatic assay. All data were corrected by subtraction of their respective negative controls. All assays were conducted in triplicate at each point. The experimental conditions are described below.

6.5.1 MMP-2 and MMP-9

In vitro enzymatic assays were performed as previously described (155). The recombinant human MMP-9 and recombinant human MMP-2 were used in these assays at concentrations of 3.2 U/mL for MMP-9 and 4.5 U/mL for MMP-2, 100 µL total volume. For each assay, increasing concentrations of the compounds dissolved in DMSO were used. Subsequently, DQ-gelatin was added (final concentration: 20 µg/mL). The plate was then placed immediately in a fluorescence plate reader, and fluorescence was measured every 5 min for 1 h at rt. The excitation (ex) and emission (em) wavelengths were 483 nm and 525 nm, respectively.

6.5.2 MMP-1 and MMP-7

MMP-1 and MMP-7 were used at concentrations of 93 U/mL and 0.74 U/mL, respectively (100 µL total volume). For each assay, increasing concentrations of the

compounds dissolved in DMSO were used. Subsequently, MCA-Pro-Leu-Gly-Leu-Dap(Dnp)-Ala-Arg-NH_2 fluorogenic substrate was added (final concentration: 10 µM). The plate was then immediately incubated at rt for 4 h, after which it was placed in a fluorescence plate reader (ex 280 nm/em 360 nm).

6.6 ADME assays

6.6.1 Parallel artificial membrane permeability (PAMPA) assay

The in vitro permeability of the compounds was measured using the PAMPA assay as described previously (156). The compounds were studied at a concentration of 200 µM in buffer solution, which was prepared by adding 19.5 mL of H_2O to 0.5 mL of PAMPA system solution and adjusted at pH 7.4 using a 0.5 M NaOH. During the assay, a final concentration of 15% 1-propanol was used as a cosolvent to enhance the solubility of the compounds under study. The PAMPA sandwich was separated and each acceptor well was filled with 200 µL of buffer solution and each donor well was filled with 200 µL of the compound of interest in buffer solution. PAMPA plate filters were coated with 4 µL of a mixture of Polar brain lipid extracts (20 mg/mL). The PAMPA sandwich was incubated at rt in a saturated humidity atmosphere under orbital agitation at 100 rpm for 4 h. After incubation, the content of the acceptor and donor compartments was analysed by HPLC (detection at 220 nm).

6.6.2 Metabolic stability in rat plasma

The determination of the stability of the compounds in rat plasma was performed according to the protocol described by Chen *et al*. (157).

For each compound, the sample was prepared as following, 15 µL of compound at 800 µM in DMSO were dissolved in 585 µL of Plasma:PBS (1:1) obtaining a final peptide concentration of 20 µM. The samples were incubated at 37°C with orbital agitation (50 rpm). At selected time points (0, 10min), 100 µl aliquots were extracted and precipitated on 300 µl of cold acetonitrile. Samples were immediately cooled down to 4°C and kept at that temperature for 30 minutes. After this step, samples were centrifuged at 3000 rpm at

4ºC for 15 minutes. The supernatant was analysed by HPLC-MS to detect the compound. The experiment of each compound was done in duplicate.

6.6.3 Metabolic stability in rat liver microsomes

The study of the stability in rat liver microsomes was done after supplier (Corning) protocol optimization for metabolic stability determinations. Compounds were incubated at 1 µM concentration (cosolvent: 0.2% DMSO), as recommended by the microsomes supplier for metabolic stability determinations. This is consistent with tissue concentration levels reached after oral dosing but is not so high as to saturate the metabolizing enzymes.

A 1/2 dilutions from stock solutions was made for the following reagents:

- NADPH regenerating system solution A
- NADPH regenerating system solution B
- Rat liver microsomes (stock solution 20 mg/mL)

After, a mixture of the reagents it was combined the following chemicals:

1. 776.75 µL of water
2. 200 µL 0.5 M potassium phosphate pH 7.4 (100 µM final concentration)
3. 12.5 µL NADPH regenerating system solution A dilution
4. 2.5 µL NADPH regenerating system solution B dilution
5. 2 µL of substrate in DMSO (the stock solution of the compound was 500 µM. 1 µM final concentration)

The resulting mixture was warmed to 37°C for 5 minutes. 6.25 µL (62.5 µg, stock dilution was 10 mg/mL) of rat liver microsomes were added. The mixture was immediately vortexed and incubated at 37°C with orbital agitation (100 rpm). After 0, 5, 10, 20, 60 minutes, 100 µL of the sample were withdraw and 100 µL of acetonitrile were added to the extracted sample, mixing and placing it on ice afterwards. After finishing the experiment, the extracted samples were centrifuged at 20000 rpm (4°C) for 20 minutes. The

supernatant was withdrawn from the protein pellet and placed in a HPLC vial. The experiment was done in duplicate.

The supernatant was analysed by HPLC-MS. All stability tests were performed in duplicates.

6.7 Pharmacokinetic study

Pharmacokinetic studies were performed externally by the CRO Advinus (India). Compounds IPR-426 and IPR-436 were administered intravenous (iv) and oral (po) administration in male Sprague Dawley rats. A total of 6 (n=3/group) rats were used in the study for each compound. Drugs were administered acutely at a nominal concentration of 1 mg/kg for iv and 5 mg/kg for po and oral administration using 2% Tween 80 in saline as vehicle in iv groups.

Blood samples were collected at 0.083 (iv only), 0.25, 0.5, 1, 2, 4, 6, 8, 24 and 48 h post-dose from each animal. At each time point, approximately 200 µL of blood was withdrawn and transferred to a labelled microfuge tube containing 200 mM K2EDTA solution (20 µL per mL of blood). Following sampling, equal volume of heparinized saline was injected into the catheter. Blood was processed to collect plasma and stored below -60°C until bioanalysis. The plasma samples were analysed using a LC-ESI-MS/MS.

ANNEX I
Product characterization
and
HPLC Chromatograms

Product Characteritzation

2PP-Pro(4F)-*N*MeIle-"A"-NHOH (IPR-424)

MW: 641.7

Purity: 97%

HPLC, t_R (gradient 40-100% ACN): 1.83 min

HPLC-MS, $[M + H]^+$: 642.5

2PP-Pro(4,4diF)-"B"-"A"-NHOH (IPR-425)

MW: 623.4

Purity: >99%

HPLC, t_R (gradient 40-100% ACN): 2.032 min

HPLC-MS, $[M + H]^+$: 624.5

2PP-Pro-"C"-"A"-NHOH (IPR-426)

MW: 581.3

Purity: >99%

HPLC, t_R (gradient 40-100% ACN): 1.397 min

HPLC-MS, $[M + H]^+$: 582.5

2PP-Pro-"D"-"E"-NHOH (IPR-428)

MW: 637.4

Purity: >99%

HPLC, t_R (gradient 40-100% ACN): 1.613

HPLC-MS, $[M + H]^+$: 638.5

2PP-Pro(4F)-"G"-"A"-NHOH (IPR-429)

MW: 652.4

Purity: 50%

HPLC, t_R (gradient 40-100% ACN): 2.836min

HPLC-MS, $[M + H]^+$: 653.6

2PP-Pro-"D"-"H"-NHOH (IPR-430)

MW: 683.2

Purity: 98%

HPLC, t_R (gradient 40-100% ACN): 1.886 min

HPLC-MS, $[M + H]^+$: 684.5

(2,2-diF)Hex-Pro- *N*MeIle -"A"-NHOH (IPR-436)

MW: 631.3

Purity: >99%

HPLC, t_R (gradient 40-100% ACN): 1.766 min

HPLC-MS, $[M + H]^+$: 632.5

(2,2-diF)Hex-Pro- "I"-"A"-NHOH (IPR-437)

MW: 603.3

Purity: 98%

HPLC, t_R (gradient 40-100% ACN): 1.213

HPLC-MS, $[M + H]^+$: 604.5

Hex-Pro(4,4diF)-"B"-"A"-NHOH (IPR-438)

MW: 631.6

Purity: >99%

HPLC, t_R (gradient 40-100% ACN): 2.171

HPLC-MS, $[M + H]^+$: 632.5

2PP-Pro(4,4diF)-"B"-"A"-NHOH (IPR-439)

MW: 659.7

Purity: >99%

HPLC, t_R (gradient 40-100% ACN): 1.715 min

HPLC-MS, $[M + H]^+$: 660.5

2PP-Pro-*N*Melle-"J"-NHOH (IPR-441)

MW: 635.7

Purity: >99%

HPLC, t_R (gradient 40-100% ACN): 2.93 min

HPLC-MS, $[M + H]^+$: 636.6

TriFpentanoyl-Pro- "B"-"A"-NHOH (IPR-447)

MW: 635.4

Purity: >99%

HPLC, t_R (gradient 40-100% ACN): 1.370 min

HPLC-MS, $[M + H]^+$: 636.7

TriFpentanoyl-Pro(4,4diF)-"B"-"A"-NHOH (IPR-448)

MW: 638.6

Purity: 99%

HPLC, t_R (gradient 40-100% ACN): 1.580 min

HPLC-MS, $[M + H]^+$: 639.4

2PP-Pro-*N*MeIle-"K"-NHOH (IPR-456)

MW: 659.2

Purity: Not available

HPLC, t_R (gradient 40-100% ACN): Not available

HPLC-MS, $[M + H]^+$: 660.3

TriFpentanoyl-Pro-"C"-"A"-NHOH (IPR-457)

MW: 593.2

Purity: 98%

HPLC, t_R (gradient 20-80% ACN): 2.201 min

HPLC-MS, $[M + H]^+$: 594.5

Hex-Pro(4,4diF)- "C"-"A"-NHOH (IPR-458)

MW: 589.3

Purity: >99%

HPLC, t_R (gradient 40-100% ACN): 1.167 min

HPLC-MS, $[M + H]^+$: 590.6

HPLC Chromatograms

2PP-Pro(4F)-*N*Melle-"A"-NHOH (IPR-424)

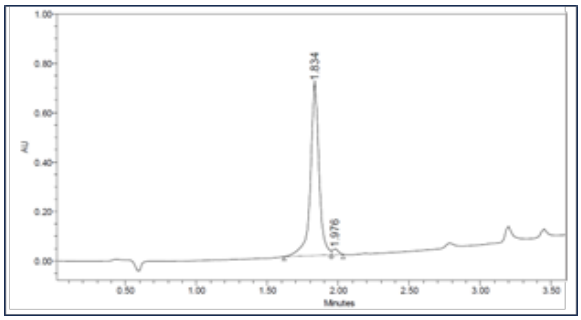

2PP-Pro(4,4diF)-"B"-"A"-NHOH (IPR-425)

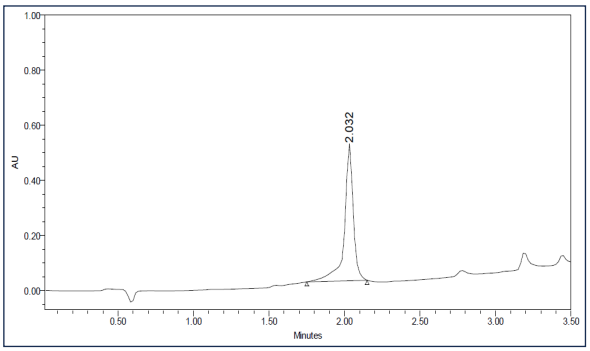

2PP-Pro-"C"-"A"-NHOH (IPR-426)

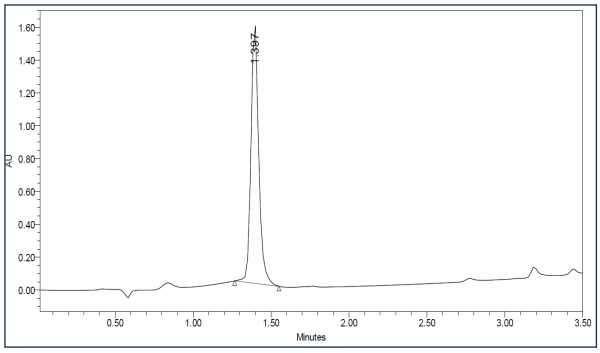

2PP-Pro-"D"-"E"-NHOH (IPR-428)

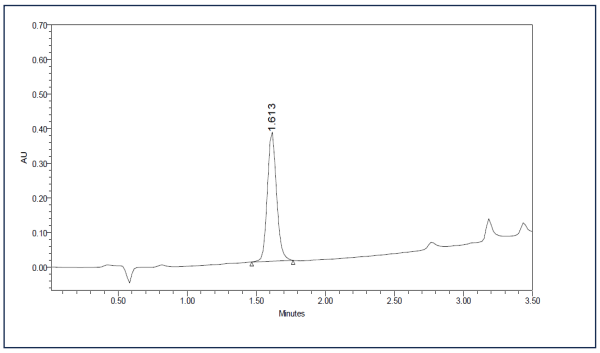

2PP-Pro(4F)-"G"-"A"-NHOH (IPR-429)

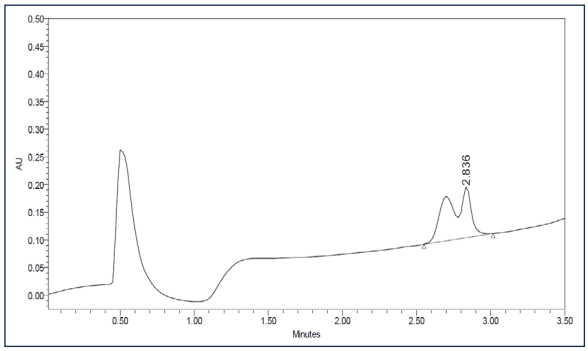

2PP-Pro-"D"-"H"-NHOH (IPR-430)

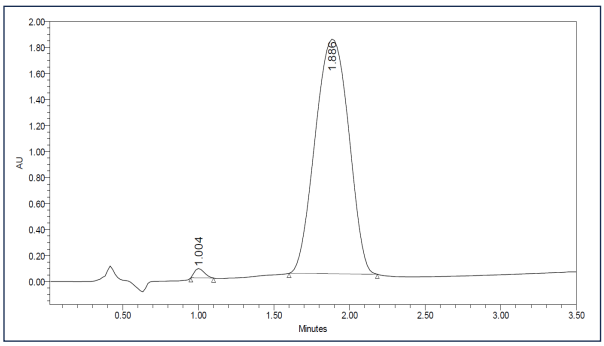

(2,2-diF)Hex-Pro- *N*MeIle -"A"-NHOH (IPR-436)

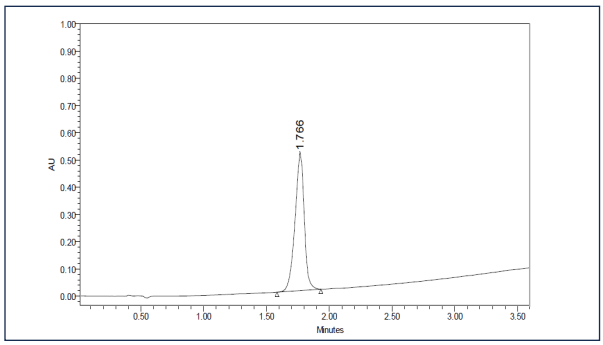

(2,2-diF)Hex-Pro- "I"-"A"-NHOH (IPR-437)

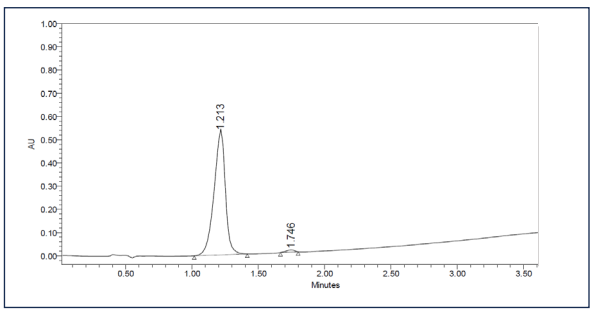

Hex-Pro(4,4diF)-"B"-"A"-NHOH (IPR-438)

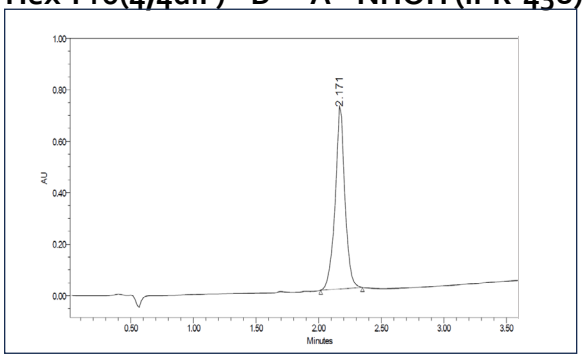

2PP-Pro(4,4diF)-"B"-"A"-NHOH (IPR-439)

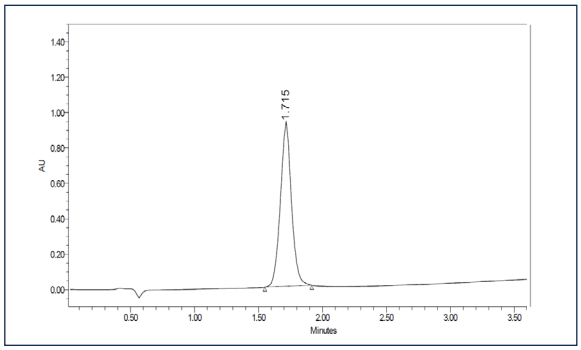

2PP-Pro-*N*Melle-"J"-NHOH (IPR-441)

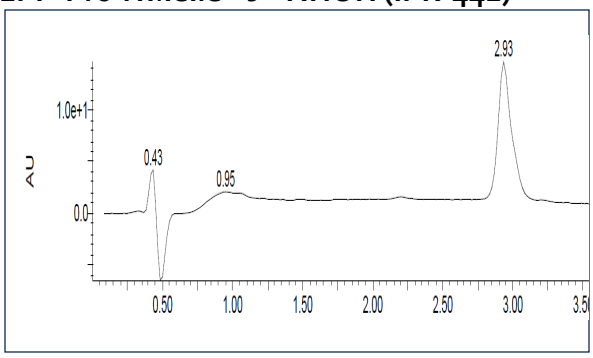

TriFpentanoyl-Pro- "B"-"A"-NHOH (IPR-447)

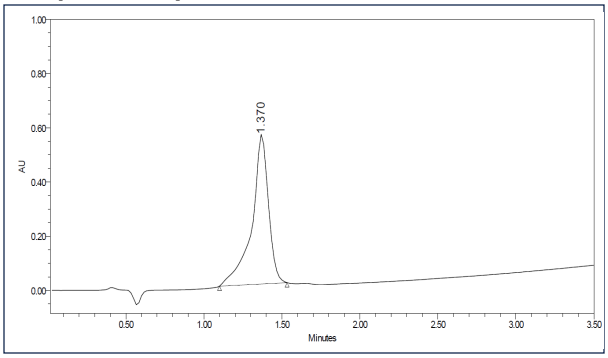

TriFpentanoyl-Pro(4,4diF)-"B"-"A"-NHOH (IPR-448)

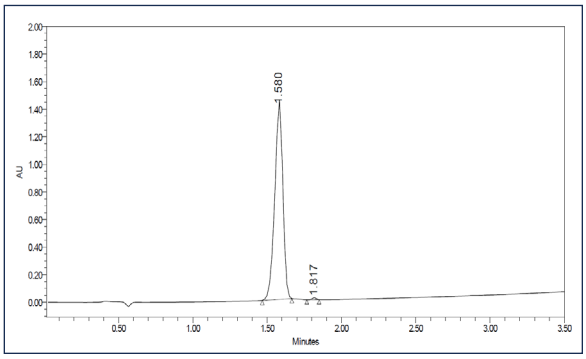

2PP-Pro-*N*Melle-"K"-NHOH (IPR-456)

Not Available

TriFpentanoyl-Pro-"C"-"A"-NHOH (IPR-457)

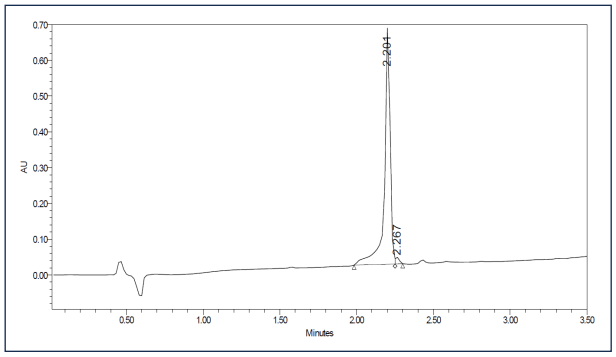

Hex-Pro(4,4diF)- "C"-"A"-NHOH (IPR-458)

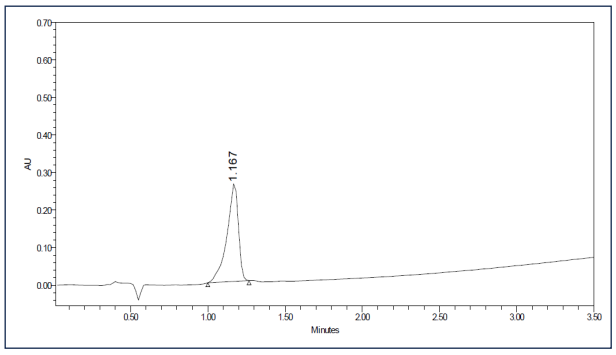

ANNEX II
Publication

ISSN: 2469-5866

Trallero et al. Int J Brain Disord Treat 2019, 5:029
DOI: 10.23937/2469-5866/1410029
Volume 5 | Issue 1
Open Access

International Journal of
Brain Disorders and Treatment

REVIEW ARTICLE

The Role of Prolyl Oligopeptidase in Microtubule-Associated Processes and Cognitive Impairment

***Nuria Trallero*[#]*, Ariadna Anunciación-Llunell*[#]*, Roger Prades and Teresa Tarragó*[*]**

Iproteos S.L., Barcelona, Spain

***Corresponding author:** *Teresa Tarragó, Iproteos S.L., Barcelona, Spain*

Abstract

Prolyl oligopeptidase (POP) is a cytosolic serine protease with prominent expression in the brain. Inhibition of this enzyme leads to cognition-enhancing and neuroprotective effects in animal models with cognitive deficits. However, the biological function of POP remains unknown. Although in the past it was though that its catalytic activity was responsible for its physiological role, lately it has been hypothesized that POP is involved in the inositol pathway and that it interacts with several proteins, including α-tubulin, thereby implying that its function may be related to protein-protein interactions. In this review, we analyze the destabilization of microtubules in neurological diseases such as schizophrenia, Parkinson's, Alzheimer's and Huntington's disease. Given the interaction of POP with α-tubulin, we discuss the relevance of this protease in the modulation of synaptic processes. In this context, we also examine the potential of POP as a promising target for the treatment of cognitive impairment.

Keywords

Microtubules, Neurological disease, Prolyl oligopeptidase, Protein-protein interaction, Synapsis

Prolyl Oligopeptidase Overview

Prolyl oligopeptidase (POP, EC3.4.21.26), also known as prolyl endopeptidase, is a cytosolic serine protease (81 kDa) that hydrolyzes post-proline bonds of small peptides (less than 30 residues long). It was discovered in the human uterus in the early 1970s [1] and was first described as an oxytocin-hydrolyzing enzyme and further characterized as a peptidase that cleaves small substrates involved in learning and mnemonic processes, such as substance P, neurotensin, arginine-vasopressin and thyrotropin-releasing hormone, among others [2]. Some studies described that the administration of a POP inhibitor increases the levels of substance P and arginine-vasopressin in the hippocampus and frontal cortex [3]. However, it has been proposed that the hydrolytic activity of POP does not drive its physiological role, which remains elusive. In this regard, given that POP interacts with other proteins and it modulates the inositol triphosphate pathway, several alternative hypotheses have been put forward to explain POP function [4]. Despite further research is needed to elucidate the exact role of this enzyme *in vivo*, in this review, we focus on the known POP interactors and their relevance in POP function Regarding structure, POP is a monomeric protein that has an overall cylindrical shape formed by two domains. The catalytic domain is a typical α/β-hydrolase, whereas the structural domain is a seven-bladed β-propeller, which acts as an empty cylinder, restricting the size and orientation of the substrate [5,6] (Figure 1). Although the enzymatic mechanism of POP is still not fully understood, electron microscopy, NMR and X-ray crystallography studies have unveiled a state of equilibrium between open and closed conformations of this enzyme in solution. This equilibrium can be modulated by direct active site POP inhibitors [5,7].

POP is ubiquitously expressed in the human body, but there is an increased concentration in the central nervous system (CNS) [8,9]. In this regard, this enzyme is expressed in cortical and hippocampal glutamatergic neurons, in γ-aminobutyric acid (GABA) ergic and cholinergic interneurons of the thalamus and cortex, and in Purkinje cells [10,11]. Moreover, after an inflammatory insult, POP expression is elevated in microglia and astrocytes [12].

Citation: Trallero N, Anunciación-Llunell A, Prades R, Tarragó T (2019) The Role of Prolyl Oligopeptidase in Microtubule-Associated Processes and Cognitive Impairment. Int J Brain Disord Treat 5:029. doi.org/10.23937/2469-5866/1410029

Accepted: June 27, 2019: **Published:** June 29, 2019

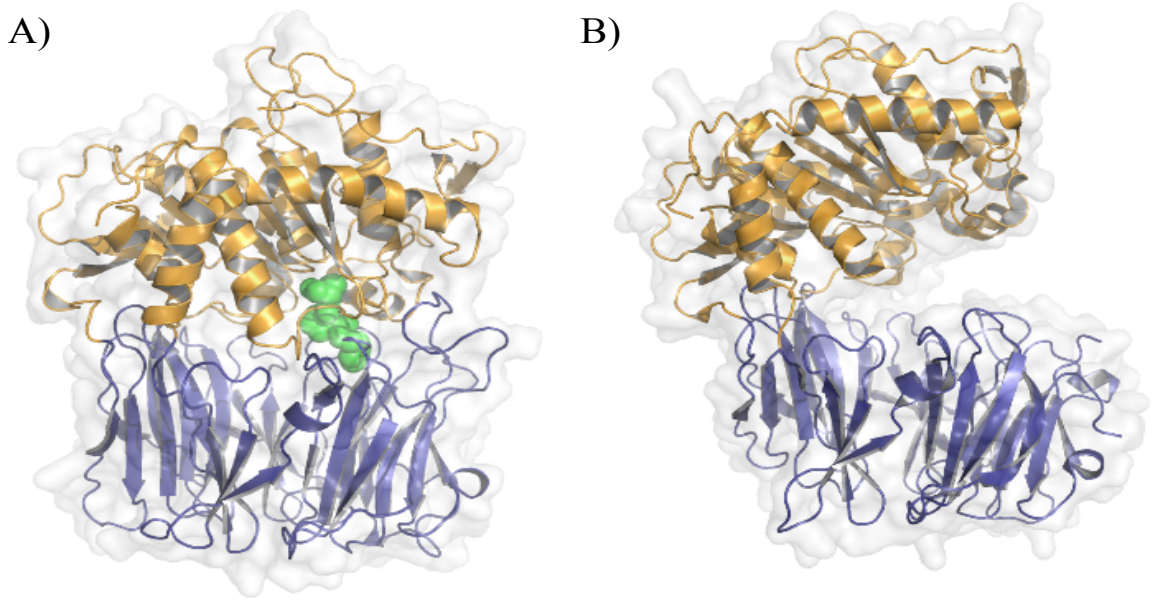

Figure 1: POP conformations in solution. A) Closed conformation of porcine POP (PDB ID: 1QFS) covalently bound to inhibitor Z-pro-prolinal (ZPP), the first POP inhibitor to be designed. β-propeller is shown in blue, α/β-hydrolase domain in orange and ZPP in green; B) Open conformation of Aemonas punctate POP (PDB ID: 3IUJ).

Given the expression of POP in the CNS, its involvement in neurodegenerative and neuropsychiatric diseases has been addressed. Several studies report that POP activity is altered in patients with Alzheimer's disease (AD), Lewy body dementia, Parkinson's disease (PD), Huntington's disease (HD), and schizophrenia, among others [9]. POP activity has also been found to be altered in the serum of patients with mood disorders, such as depression and bipolar disorder [13]. However, care must be taken when interpreting these studies since many of them measured POP in plasma or post-mortem brain samples. In addition, experimental data show that POP inhibition has neuroprotective, anti-amnesic and cognition-enhancing properties in scopolamine-treated rats, whereas it decreases extracellular acetylcholine concentrations in the cortex and hippocampus of these animals [14,15]. The cognition-enhancing properties of POP inhibitors have been further demonstrated in other animal models with cognitive impairment [16-18] and in healthy human volunteers [19-22]. Furthermore, in cortical and cerebellar granule cells, POP inhibitors exert neuroprotective effects [23,24]. Three of these inhibitors, namely S-17092, JTP-4819 and Z-321, reached clinical stages for the treatment of AD [19-22]. However, unfortunately, the development of these drugs did not progress beyond these stages.

Involvement of Prolyl Oligopeptidase in Protein-Protein Interactions

The presence of POP in the cytosol, together with its conformational dynamics and capacity to interact with other proteins, has led to the hypothesis that its biological function is related to protein-protein interactions. This notion was first put forward by Schulz, et al. in 2005, who proposed that POP regulates a number of cell functions independently of its peptidase activity [25]. In addition, it has been observed that POP inhibitors induce changes in the tertiary structure of the enzyme and can modify its interactome. The main POP interactors described in the literature are the cytosolic proteins α-synuclein, glyceraldehyde-3-phosphate dehydrogenase (GAPDH), growth-associated protein 43 (GAP43) and α-tubulin.

α-synuclein

The abnormal fibrillary aggregation of α-synuclein protein in the cytoplasm of neurons and glia is the main characteristic of synucleinopathies, including PD, Lewy body dementia and multiple-system atrophy, among others [26]. The contribution of POP to enhancing α-synuclein aggregation was reported for the first time by Brandt, et al. in 2008 [27]. Since then, it has been shown that POP co-localizes with α-synuclein in the substantia nigra of PD patients [28] and later that the two proteins directly interact. This interaction was revealed through microscale thermophoresis and surface plasmon resonance studies [29]. In addition, POP inhibition reverses α-synuclein aggregation and promotes autophagy-the catabolic pathway used for clearing insoluble α-synuclein oligomers and fibrils [30]. These findings suggest that modulation of the α-synuclein-POP interaction using POP inhibitors could provide a new approach for the treatment of synucleinopathies.

GAPDH

GAPDH is a glycolytic enzyme involved in energy production pathways. However, this protein also participates in other non-glycolytic processes, including

programmed cell death [30]. In this regard, it has been shown that GAPDH translocation and accumulation in the nucleus serves as an initiation signal for apoptosis [31,32]. Puttonnen, et al. and some years later Matsuda, et al. reported that POP inhibitors prevent GAPDH translocation into the nucleus under oxidative stress [33,34]. Later on, using co-localization, co-immunoprecipitation and proximity ligation experiments, Matsuda, et al. confirmed the interaction of POP with GAPDH [33]. This information strongly supports the notion that POP mediates GAPDH nuclear translocation and, consequently, that it may be involved in the regulation of apoptosis.

GAP43

Among other CNS-related functions, GAP43 is involved in growth cone formation and axon guidance [35,36], although the underlying molecular mechanism is still not well understood. Valproic acid, carbamazepine and lithium treatment induce an increase in the average spread area of growth cones in sensory neuron cultures, and this increase is reversed by the administration of POP inhibitors [37]. This finding suggests that POP is also related to growth cone development. In this regard, Di Daniel, et al. proposed that this function of POP might be explained by its interaction with GAP43. They demonstrated binding between POP and GAP43 using co-immunoprecipitation and yeast two-hybrid assays [38]. Years later, this study was questioned by Szeltner, et al. who reported partial co-localization of POP and GAP43, without strong physical binding. In this regard, those authors reported a weak and transient interaction between the two proteins, as demonstrated by a glutaraldehyde cross-linking assay [39]. Despite this contradiction, it is plausible that POP participates in growth cone development via direct or indirect interaction with GAP43.

α-tubulin

Repeated assemblies of α- and β-tubulin heterodimers comprise the structure of microtubules (MTs), which, together with microfilaments and intermediate filaments, form the cell cytoskeleton. Therefore, MTs are involved in a large number of cellular processes, including mitosis, cell motility, maintenance of cell shape, neurite growth, intracellular transport and vesicle secretion [40]. Using co-localization and yeast two-hybrid assays, Schulz, et al. demonstrated POP binding to the C-terminus region of α-tubulin [25]. They also showed that POP inhibition promotes protein and peptide release in U-343 cells. These results suggest that POP participates in MT-associated processes, such as intracellular trafficking, protein secretion and axonal transport.

Prolyl Oligopeptidase and Microtubules as Key Players in Synaptic Processes

Since several POP inhibitors have been demonstrated to improve memory and cognition in animals, the possible implication of POP in synaptic function has been studied using alternative approaches.

Firstly, in the same publication that proposed POP interaction with GAP43, the authors also generated POP knockout (KO) mice. These animals were used to demonstrate that the absence of POP causes a decrease in the number of collapsed growth cones and an increase in their spread area in explants when compared with wild-type (WT) mice [38]. Likewise, they observed that WT mouse explants treated with valproic acid, carbamazepine or lithium (all of them considered mood stabilizers) also show a decrease in the number of growth cones. However, treatment with POP inhibitors reversed the effect of these three mood stabilizers. Höfling, et al. also determined that POP KO mice show an increased expression of polysialylated-neural cell adhesion molecule (PSA-NCAM) [41], which has been associated with enhanced brain plasticity [42]. Alternatively, D'Agostino, et al. used POP gene trap mice to study the involvement of POP in synapsis. They observed that these mice present reduced hippocampal long-term potentiation, impaired learning and memory processes related to the hippocampus, decreased spine density in the hippocampus, especially in the CA1 region, and reduced GAP43 expression [43].

Given these observations, it is plausible that POP participates in the modulation of neuronal synapses. Although the molecular mechanisms underlying such modulation are not well understood, the interaction POP-GAP43 and POP-α-tubulin could provide an explanation. Here we outline some basic ideas about α-tubulin and, consequently, MT involvement in synaptic processes and in neurological diseases associated with POP dysregulation.

As mentioned previously, MTs are the major component of the cell cytoskeleton, and as such they are present in all eukaryotic cell types. The key properties of MTs are their dynamic behavior and directionality. The orientation of α- and β-tubulin heterodimers that make up the MT structure is particularly important for the polarity and stability of these cytoskeletal components. The (-) end of a MT has an exposed α-tubulin subunit, whereas the (+) end-where MT elongation takes placehas an exposed β-tubulin. Regarding neuronal MTs, which are characterized by the formation of the bundles required for the growth and maintenance of neurites [40,44], it has been described that axonal MTs are uniformly directed, with (+) ends orientated to axon tips, whereas in dendrites, MTs present mixed orientations (Figure 2). An additional difference between the MTs of axons and dendrites is their predominant microtubule-associated proteins (MAPs). Tau is found mostly in axons, while MAP2 predominates in dendrites. Despite these variations, there is general consensus that MT dynamics play a key role in ensuring the correct function

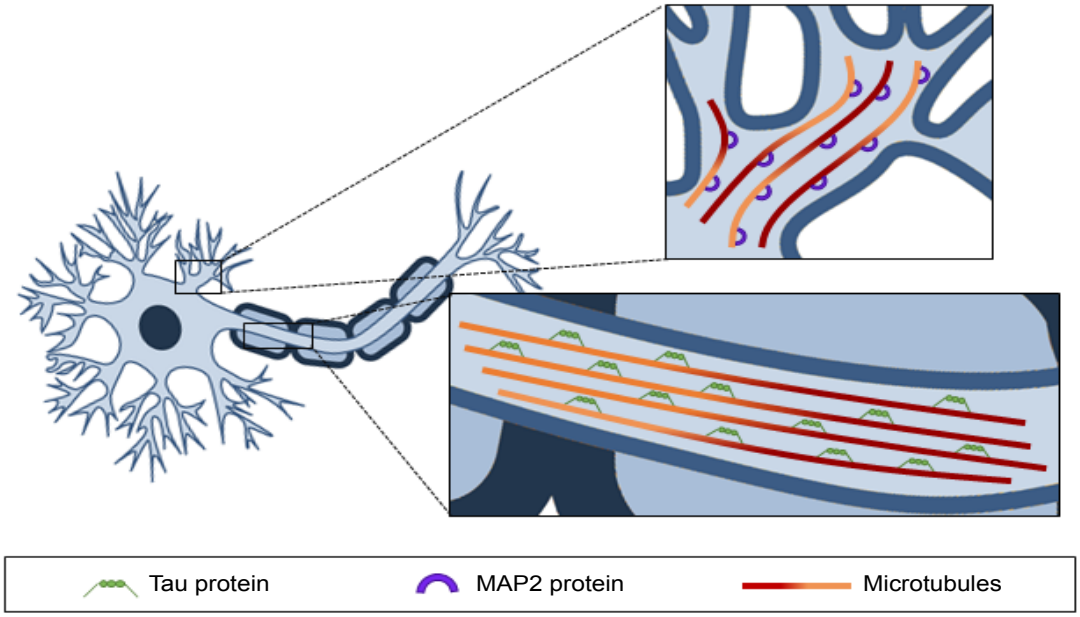

Figure 2: Microtubule distribution along axons and dendrites. MTs are oriented uniformly in axons and Tau protein is the predominant MAP, whereas in dendrites MTs show a mixed orientation and MAP2 protein is bound to them.

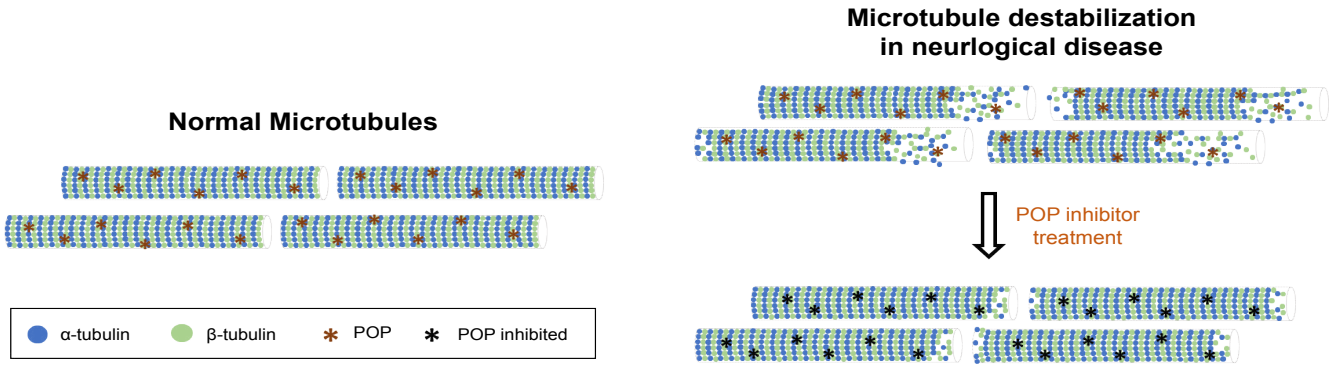

Figure 3: Destabilization of microtubules in neurological diseases. The diagram shows the difference in MT conformation between healthy subjects and patients with neurological diseases. The hypothetical recovery of the normal MT structure after POP inhibition is also shown.

of axons and dendrites, and consequently, in memory, learning and other cognitive processes. Indeed, MTs, in cooperation with other proteins, are involved in the regulation of intracellular cargo trafficking in axons and dendrites, as well as in the modulation of dendritic spine morphology and synaptic plasticity [45,46].

Neurodegenerative diseases are commonly characterized by a decrease in MT mass, as well as disrupted polarity patterns and impaired axonal transport, which are caused, in part, by a reduction in MT stability [40,47]. These findings support the notion that the modulation of MT dynamics could provide a potential therapy through which to improve the cognitive impairment associated with neurological diseases. Given the reported interaction between α-tubulin and POP and the implication of these proteins in synaptic processes, it cannot be ruled out that POP, and therefore POP inhibition, regulates MT dynamics (Figure 3). However, the interaction between POP and α-tubulin and the possible implication of this protease in MT stability requires further attention.

Prolyl Oligopeptidase in Neurological Diseases

POP has been proposed to be a promising target for the cognitive impairment present in some CNS diseases, including schizophrenia, PD and AD, among others. This proposal has come about on the basis of three main observations: i) The brains of individuals with these conditions present altered levels of POP [13]; ii) The hypothesized implication of POP in spine density and formation [38,41-43] and; iii) The promising discoveries about molecules that interact with POP [25,29,33,38].

Schizophrenia

According to the WHO, schizophrenia is a neuropsychiatric disease that affects more than 1% of the population worldwide. Individuals with this condition can

manifest three types of symptoms: Positive, negative and cognitive. Several antipsychotics for the treatment of positive and negative symptoms are available on the market. However, to date, no drug has been approved to treat cognitive impairment. POP emerged as a promising target to tackle the cognitive symptoms of schizophrenia [48]. Successful results regarding this indication were published by Prades, et al. In that study, three distinct mouse models of schizophrenia-which were based on the administration of subchronic phencyclidine (PCP) or acute dizocilpine (MK801), and on maternal immune activation induced by polyinosinic: Polycytidylic (PIC) during pregnancy-were treated with the POP inhibitor IPR19. Those authors showed that this inhibitor reversed the impaired cognitive symptomatology in a number of cognition tests that evaluate working and visual memory [49]. Therefore, it was concluded that POP inhibition exerts cognition-enhancing effects in animal models of schizophrenia.

Patients with schizophrenia show alterations in dendritic spines. These abnormalities have been observed in multiple brain regions, specifically in layer 3 of the neocortex, where pyramidal cells present a lower density of the smallest spines. It has been hypothesized that these spine deficits appear during early childhood and adolescence, probably as a result of disturbances in molecular mechanisms such as spine formation, pruning, and/or maintenance [50,51]. POP inhibitors may be able to restore dendritic spine deficits and therefore contribute to improving cognitive symptomatology.

Parkinson's disease

PD is a neurodegenerative disorder characterized by loss of neurons in the substantia nigra and an accumulation of Lewy bodies, which comprise aggregated forms of α-synuclein. As previously mentioned, α-synuclein co-localizes and interacts with POP in the substantia nigra [28,29]. Nevertheless, no differences in POP activity or expression between PD and control subjects have been observed [28].

MTs are involved in PD, as demonstrated by observations of the interaction of tubulin with α-synuclein [52]. In addition, α-synuclein has been linked to MT stabilization, although the mechanism of action is not well understood. It has been proposed that α-synuclein is a MAP and that it therefore modulates the stabilization, polymerization and dynamics of MTs. Another hypothesis is that the interaction between α-synuclein and GSK-3β modulates Tau phosphorylation and consequently MT stabilization. Nevertheless, these two hypotheses are not necessarily exclusive [53].

Myöhänen, et al. demonstrated that POP is involved in α-synuclein aggregation. In this regard, those authors showed that POP inhibitor KYP-2047 stimulates the clearance of α-synuclein aggregates by enhancing macroautophagy in the A30P transgenic mouse model of PD [30].

Alzheimer disease

The hallmark of AD is the accumulation of misfolded β-amyloid peptide plaques in the extracellular space, as well as the aggregation of phosphorylated Tau protein in neurons-a process that results in neurofibrillary tangles. The brains of AD patients show altered expression and activity of POP, and this protease has also been observed to co-localize with β-amyloid protein both intra- and extracellularly in this organ [9,29]. Tau protein co-localizes with POP inside cells in AD and control brains [26].

MTs are involved in the development of AD, as demonstrated by their reduced length and density [54], which indicate a possible alteration of synaptic processes. In this regard, in early stages of AD, β-amyloid alters changes in dendritic spine shape, whereas in later stages the cellular response to β-amyloid toxicity leads to a reduction in MT density and length and to the loss of dendritic spines [55].

Huntington's disease

HD is an inherited neurodegenerative disorder characterized by motor, psychiatric and cognitive deficits [56]. Cognitive impairment is one of the earliest symptoms of this disease. HD is caused by an abnormal CAG repeat expansion within exon 1 of the human huntingtin gene (HTT) [57], which encodes the huntingtin protein. Mutated huntingtin forms oligomers and globular intermediates that lead to aggregates, which in turn promote neuronal dysfunction and neurodegeneration [58].

HD is another example of a pathological process in which POP activity is decreased in brain samples of patients respect to controls [59]. Therefore, HD presents abnormalities in MTs and the cytoskeleton, most of these abnormalities being related to MAP dysregulation. Post-mortem HD brain samples present hyperphosphorylated Tau aggregates, a phenomenon observed in AD [60]. Dendritic atrophy induced by the dysregulation of MAP2, probably caused by splicing altered events, has also been reported [61].

Future Perspectives

Patients with neurological disorders, including AD, PD, HD and schizophrenia, present altered POP expression patterns. Moreover, the last two decades have brought about the design and testing of inhibitors of this serine protease for the treatment of the cognitive impairment related to these pathologies. POP inhibitors have widely demonstrated *in vitro* and *in vivo* cognition-enhancing and neuroprotective properties. However, although some of these drug candidates reached clinical stages, the biological mechanisms underlying the effects of POP are still unclear. Even though, the catalytic activity of the protease has been traditionally proposed as the function responsible for the biological

activity of POP, a new promising hypothesis attribute the *in vivo* functionalities of this protease to its involvement in key physiologically relevant protein-protein interactions.

One of the most promising POP interactors is α-tubulin, a component of the heterodimer that forms the MT structure. In this regard, several neurological diseases are characterized by alterations in the stability and formation of MTs, as well as deficits in spine density.

On the basis of the findings reviewed herein, POP emerges as potential new target for the treatment of the cognitive impairment associated with some neurological diseases and psychiatric diseases. Research efforts should now be channeled into studying the binding of POP to α-tubulin, the potential involvement of POP in the cytoskeleton and neurite growth, and the effect of POP inhibitors as MT stabilizers.

Notes

N.T., A.A-Ll, R.P. and T.T. are employees of Iproteos, S.L. T.T. is founder of Iproteos, S.L.

Author Contributions

N.T. and A.A-Ll. drafted the manuscript, R.P. and T.T. revised the manuscript. All the contributors revised, gave their approval to the final version of the manuscript, and agreed to be accountable for all aspects of the work.

References

1. Walter R, Shlank H, Glass JD, Schwartz IL, Kerenyi TD (1971) Leucylglycinamide released from oxytocin by human uterine enzyme. Science 173: 827-829.
2. Kovács GL, De Wied D (1994) Peptidergic modulation of learning and memory processes. Pharmacol Rev 46: 269-291.
3. Toide K, Shinoda M, Fujiwara T, Iwamoto Y (1997) Effect of a Novel Prolyl Endopeptidase Inhibitor, JTP-4819, on Spatial Memory and Central Cholinergic Neurons in Aged Rats. Pharmacol Biochem Behav 56: 427-434.
4. Williams RSB, Eames M, Ryves WJ, Viggars J, Harwood AJ (1999) Loss of a prolyl oligopeptidase confers resistance to lithium by elevation of inositol (1,4,5) trisphosphate. EMBO J 18: 2734-2745.
5. Millet O, Tarragó T, Gairí M, Kotev M, López A, Giralt E, et al. (2016) Active-Site-Directed Inhibitors of Prolyl Oligopeptidase Abolish Its Conformational Dynamics. Chembiochem 17: 913-917.
6. Fülöp V, Böcskei Z, Polgar L (1998) Prolyl oligopeptidase: An unusual beta-propeller domain regulates proteolysis. Cell 94: 161-170.
7. López A, Vilaseca M, Madurga S, Varese M, Tarragó T, et al. (2016) Analyzing slowly exchanging protein conformations by ion mobility mass spectrometry: Study of the dynamic equilibrium of prolyl oligopeptidase. J Mass Spectrom 51: 504-511.
8. Wilk S (1983) Prolyl endopeptidase. Life Sci 33: 2149-2147.
9. Goossens F, De Meester I, Vanhoof G, Scharpé S (1996) Distribution of prolyl oligopeptidase in human peripheral tissues and body fluid. Eur J Clin Chem Clin Biochem 34: 17-22.
10. Myöhänen TT, Kääriäinen TM, Jalkanen AJ, Piltonen M, Männistö PT (2009) Localization of prolyl oligopeptidase in the thalamic and cortical projection neurons: A retrograde neurotracing study in the rat brain. Neurosci Lett 450: 201-205.
11. Myöhänen TT, Venäläinen JI, Garcia-Horsman JA, Piltonen M, Männistö PT (2008) Cellular and subcellular distribution of rat brain prolyl oligopeptidase and its association with specific neuronal neurotransmitters. J Comp Neurol 507: 1694-1708.
12. Natunen TA, Gynther M, Rostalski H, Jaako K, Jalkanen AJ (2019) Extracellular prolyl oligopeptidase derived from activated microglia is a potential neuroprotection target. Basic Clin Pharmacol Toxicol 124: 40-49.
13. García-Horsman JA, Männistö PT, Venäläinen JI (2007) On the role of prolyl oligopeptidase in health and disease. Neuropeptides 41: 1-24.
14. Yoshimoto T, Kado K, Matsubara F, Koriyama N, Kaneto H, et al. (1987) Specific inhibitors for prolyl endopeptidase and their anti-amnesic effect. J Pharmacobiodyn 10: 730-735.
15. Jalkanen AJ, Leikas JV, Forsberg MM (2014) Prolyl oligopeptidase inhibition decreases extracellular acetylcholine levels in rat hippocampus and prefrontal cortex. Neurosci Lett 579: 110-113.
16. Schneider JS, Giardiniere M, Morain P (2002) Effects of the prolyl endopeptidase inhibitor S 17092 on cognitive deficits in Chronic low dose MPTP-treated monkeys. Neuropsychopharmacology 26: 176-182.
17. Toide K, Shinoda M, Miyazaki A (1998) A novel prolyl endopeptidase inhibitor, JTP-4819. Its behavioral and neurochemical properties for the treatment of Alzheimer's disease. Rev Neurosci 9: 17-29.
18. Kato A, Fukunari A, Sakai Y, Nakajima T (1997) Prevention of amyloid-like deposition by a selective prolyl endopeptidase inhibitor, Y-29794, in senescence-accelerated mouse. J Pharmacol Exp Ther 283: 328-335.
19. Umemura K, Kondo K, Ikeda Y, Kobayashi T, Urata Y, et al. (1997) Pharmacokinetics and safety of JTP-4819, a novel specific orally active prolyl endopeptidase inhibitor, in healthy male volunteers. Br J Clin Pharmacol 43: 613-618.
20. Morain P, Robin JL, De Nanteuil G, Jochemsen R, Heidet V, et al. (2000) Pharmacodynamic and pharmacokinetic profile of S 17092, a new orally active prolyl endopeptidase inhibitor, in elderly healthy volunteers. A phase I study. Br J Clin Pharmacol 50: 350-359.
21. Umemura K, Kondo K, Ikeda Y, Nishimoto M, Hiraga Y, et al. (1999) Pharmacokinetics and safety of Z-321, a novel specific orally active prolyl endopeptidase inhibitor, in healthy male volunteers. J Clin Pharmacol 39: 4462-4470.
22. Morain P, Boeijinga PH, Demazières A, De Nanteuil G, Luthringer R (2007) Psychotropic profile of S 17092, a prolyl endopeptidase inhibitor, using quantitative EEG in young healthy volunteers. Neuropsychobiology 55: 176-183.
23. Katsube N, Sunaga K, Aishita H, Chuang DM, Ishitani R (1999) ONO-1603, a potential antidementia drug, delays age-induced apoptosis and suppresses overexpression of glyceraldehyde-3-phosphate dehydrogenase in cultured central nervous system neurons. J Pharmacol Exp Ther 288: 6-13.
24. Katsube N, Sunaga K, Chuang DM, Ishitani R (1996) ONO-

1603, a potential antidementia drag, shows neuroprotective effects and increases m3-muscarinic receptor mRNA levels in differentiating rat cerebellar granule neurons. Neurosci Lett 214: 151-154.

25. Schulz I, Zeitschel U, Rudolph T, Ruiz-Carrillo D, Rahfeld JU, et al. (2005) Subcellular localization suggests novel functions for prolyl endopeptidase in protein secretion. J Neurochem 94: 970-979.

26. Spillantini MG, Crowther RA, Jakes R, Hasegawa M, Goedert M (1998) Alpha-Synuclein in filamentous inclusions of Lewy bodies from Parkinson's disease and dementia with lewy bodies. Proc Natl Acad Sci U S A 95: 6469-6473.

27. Brandt I, Gérard M, Sergeant K, Devreese B, Baekelandt V, et al. (2008) Prolyl oligopeptidase stimulates the aggregation of α-synuclein. Peptides 29: 1472-1478.

28. Hannula MJ, Myöhänen TT, Tenorio-Laranga J, Männistö PT, Garcia-Horsman JA (2013) Prolyl oligopeptidase colocalizes with α-synuclein, β-amyloid, tau protein and astroglia in the post-mortem brain samples with Parkinson's and Alzheimer's diseases. Neuroscience 242: 140-150.

29. Savolainen MH, Yan X, Myöhänen TT, Huttunen HJ (2015) Prolyl oligopeptidase enhances α-Synuclein dimerization via direct protein-protein interaction. J Biol Chem 290: 5117-5126.

30. Savolainen MH, Richie CT, Harvey BK, Männistö PT, Maguire-Zeiss KA, et al. (2014) The beneficial effect of a prolyl oligopeptidase inhibitor, KYP-2047, on alpha-synuclein clearance and autophagy in A30P transgenic mouse. Neurobiol Dis 68: 1-15.

31. Saunders PA, Chalecka-Franaszek E, Chuang DM (1997) Subcellular distribution of glyceraldehyde-3-phosphate dehydrogenase in cerebellar granule cells undergoing cytosine arabinoside-induced apoptosis. J Neurochem 69: 1820-1828.

32. Ishitani R, Tanaka M, Sunaga K, Katsube N, Chuang DM (1998) Nuclear localization of overexpressed glyceraldehyde-3-phosphate dehydrogenase in cultured cerebellar neurons undergoing apoptosis. Mol Pharmacol 53: 701-707.

33. Matsuda T, Sakaguchi M, Tanaka S, Yoshimoto T, Takaoka M (2013) Prolyl oligopeptidase is a glyceraldehyde-3-phosphate dehydrogenase-binding protein that regulates genotoxic stress-induced cell death. Int J Biochem Cell Biol 45: 850-857.

34. Puttonen KA, Lehtonen Š, Raasmaja A, Männistö PT (2006) A prolyl oligopeptidase inhibitor, Z-Pro-Prolinal, inhibits glyceraldehyde-3-phosphate dehydrogenase translocation and production of reactive oxygen species in CV1-P cells exposed to 6-hydroxydopamine. Toxicol Vitr 20: 1446-1454.

35. Oestreicher AB, De Graan PNE, Gispen WH, Verhaagen J, Schrama LH (1997) B-50, the growth associated protein-43: Modulation of cell morphology and communication in the nervous system. Prog Neurobiol 53: 627-686.

36. Aigner L, Caroni P (1993) Depletion of 43-kD growth-associated protein in primary sensory neurons leads to diminished formation and spreading of growth cones. J Cell Biol 123: 417-429.

37. Harwood AJ, Mudge AW, Cheng L, Williams RSB (2002) A common mechanism of action for three mood-stabilizing drugs. Nature 417: 292-295.

38. Di Daniel E, Glover CP, Grot E, Chan MK, Sanderson TH, et al. (2009) Prolyl oligopeptidase binds to GAP-43 and functions without its peptidase activity. Mol Cell Neurosci 41: 373-382.

39. Szeltner Z, Morawski M, Juhász T, Szamosi I, Liliom K, et al. (2010) GAP43 shows partial co-localisation but no strong physical interaction with prolyl oligopeptidase. Biochim Biophys Acta - Proteins Proteomics 1804: 2162-2176.

40. Matamoros AJ, Baas PW (2016) Microtubules in health and degenerative disease of the nervous system. Brain Res Bull 126: 217-225.

41. Höfling C, Kulesskaya N, Jaako K, Peltonen I, Männistö PT, et al. (2016) Deficiency of prolyl oligopeptidase in mice disturbs synaptic plasticity and reduces anxiety-like behaviour, body weight, and brain volume. Eur Neuropsychopharmacol 26: 1048-1061.

42. Uryu K, Butler AK, Chesselet MF (1999) Synaptogenesis and ultrastructural localization of the polysialylated neural cell adhesion molecule in the developing striatum. J Comp Neurol 405: 216-232.

43. Diano S, Jeong JK, Kim JD, D'Agostino G, Calignano A, et al. (2012) Prolyl endopeptidase-deficient mice have reduced synaptic spine density in the CA1 region of the hippocampus, impaired LTP, and spatial learning and memory. Cereb Cortex 23: 2007-2014.

44. Conde C, Cáceres A (2009) Microtubule assembly, organization and dynamics in axons and dendrites. Nat Rev Neurosci 10: 319-332.

45. Pellegrini L, Wetzel A, Grannó S, Heaton G, Harvey K (2017) Back to the tubule: Microtubule dynamics in Parkinson's disease. Cell Mol Life Sci 74: 409-434.

46. Camera P, Defilippi P, Jaworski J, Spangler SA, Gouveia SM, et al. (2009) Dynamic microtubules regulate dendritic spine morphology and synaptic plasticity. Neuron 61: 85-100.

47. Brunden KR, Lee VMY, Smith AB, Trojanowski JQ, Ballatore C (2017) Altered microtubule dynamics in neurodegenerative disease: Therapeutic potential of microtubule-stabilizing drugs. Neurobiol Dis 105: 328-335.

48. López A, Mendieta L, Prades R, Royo S, Tarragó T, et al. (2013) Peptide POP inhibitors for the treatment of the cognitive symptoms of schizophrenia. Future Med Chem 5: 1509-1523.

49. Prades R, Munarriz-Cuezva E, Urigüen L, Gil-Pisa I, Gómez L, et al. (2017) The prolyl oligopeptidase inhibitor IPR19 ameliorates cognitive deficits in mouse models of schizophrenia. Eur Neuropsychopharmacol 27: 180-191.

50. Glausier JR, Lewis DA (2013) Dendritic spine pathology in schizophrenia. Neuroscience 251: 90-107.

51. MacDonald ML, Alhassan J, Newman JT, Richard M, Gu H, et al. (2017) Selective loss of smaller spines in Schizophrenia. Am J Psychiatry 174: 586-594.

52. Zhou RM, Huang YX, Li XL, Chen C, Shi Q, et al. (2010) Molecular interaction of α-synuclein with tubulin influences on the polymerization of microtubule in vitro and structure of microtubule in cells. Mol Biol Rep 37: 3183-3192.

53. Carnwath T, Mohammed R, Tsiang D (2018) The direct and indirect effects of α-synuclein on microtubule stability in the pathogenesis of parkinson's disease. Neuropsychiatr Dis Treat 14: 1685-1695.

54. Cash AD, Aliev G, Siedlak SL, Nunomura A, Fujioka H, et al. (2003) Microtubule reduction in Alzheimer's disease and aging is independent of τ filament formation. Am J Pathol 162: 1623-1627.

55. Pchitskaya EI, Zhemkov VA, Bezprozvanny IB (2018) Dynamic microtubules in Alzheimer's disease: Association with dendritic spine pathology. Biochem 83: 1068-1074.

56. Ross CA, Aylward EH, Wild EJ, Langbehn DR, Long JD, et al. (2014) Huntington disease: Natural history, biomarkers and prospects for therapeutics. Nat Rev Neurol 10: 204-216.

57. Gusella JF, Wexler NS, Conneally PM, Naylor SL, Anderson MA, et al. (1983) A polymorphic DNA marker genetically linked to Huntington's disease. Nature 306: 234-238.

58. Arrasate M, Finkbeiner S (2012) Protein aggregates in Huntington's disease. Exp Neurol 238: 1-11.

59. Mantle D, Falkous G, Ishiura S, Blanchard PJ, Perry EK (1996) Comparison of proline endopeptidase activity in brain tissue from normal cases and cases with Alzheimer's disease, Lewy body dementia, Parkinson's disease and Huntington's disease. Clin Chim Acta 249: 129-139.

60. Barker RA, Cisbani G, Spillantini MG, Vuono R, de Silva R, et al. (2015) The role of tau in the pathological process and clinical expression of Huntington's disease. Brain 138: 1907-1918.

61. Cabrera JR, Lucas JJ (2017) MAP2 splicing is altered in Huntington's disease. Brain Pathol 27: 181-189.

BIBLIOGRAPHY

1. World Health Organization (WHO). Neurological Disorders. 2021.

2. Daneman, Richard; Alexander P. The Blood-Brain Barrier. Dev Med Child Neurol. 1961;

3. Banks WA. From blood–brain barrier to blood–brain interface: new opportunities for CNS drug delivery. Nat Rev Drug Discov. 2016 Apr 22;15(4):275–92.

4. Li G, Shao K, Umeshappa CS. Recent progress in blood-brain barrier transportation research. In: Brain Targeted Drug Delivery System. Elsevier; 2019. p. 33–51.

5. Soni S, Ruhela RK, Medhi B. Nanomedicine in central nervous system (CNS) disorders: A present and future prospective. Vol. 6, Advanced Pharmaceutical Bulletin. Tabriz University of Medical Sciences; 2016. p. 319–35.

6. Dong X. Current Strategies for Brain Drug Delivery. Theranostics. 2018;8(6):1481–93.

7. Zhao X, Chen R, Liu M, Feng J, Chen J, Hu K. Remodeling the blood–brain barrier microenvironment by natural products for brain tumor therapy. Acta Pharm Sin B. 2017 Sep;7(5):541–53.

8. Drag M, Salvesen GS. Emerging principles in protease-based drug discovery. Nat Rev Drug Discov. 2010 Sep;9(9):690–701.

9. Lewis DA, Lieberman JA. Catching Up on Schizophrenia. Neuron. 2000 Nov;28(2):325–34.

10. World Health Organitzation. Schizophrenia [Internet]. 2022 [cited 2023 Jun 10].

11. https://www.nimh.nih.gov/health/topics/schizophrenia.

12. http://www.who.int/mental_health/management/schizophrenia/en/.

13. Harvey PD, Bosia M, Cavallaro R, Howes OD, Kahn RS, Leucht S, et al. Cognitive dysfunction in schizophrenia: An expert group paper on the current state of the art. Schizophr Res Cogn. 2022 Sep;29:100249.

14. Keefe RSE. Neurocognitive Effects of Antipsychotic Medications in Patients With Chronic Schizophrenia in the CATIE Trial. Arch Gen Psychiatry. 2007 Jun 1;64(6):633.

15. Joshi YB, Thomas ML, Braff DL, Green MF, Gur RC, Gur RE, et al. Anticholinergic Medication Burden–Associated Cognitive Impairment in Schizophrenia. American Journal of Psychiatry. 2021 Sep 1;178(9):838–47.

16. Horan WP, Green MF. Treatment of social cognition in schizophrenia: Current status and future directions. Schizophr Res. 2019 Jan;203:3–11.

17. McCutcheon RA, Keefe RSE, McGuire PK. Cognitive impairment in schizophrenia: aetiology, pathophysiology, and treatment. Mol Psychiatry. 2023 Jan 23;

18. López A, Mendieta L, Prades R, Royo S, Tarragó T, Giralt E. Peptide POP inhibitors for the treatment of the cognitive symptoms of schizophrenia. Future Med Chem. 2013;5(13):1509–23.

19. Kroken RA, Løberg EM, Drønen T, Grüner R, Hugdahl K, Kompus K, et al. A Critical Review of Pro-Cognitive Drug Targets in Psychosis: Convergence on Myelination and Inflammation. Front Psychiatry. 2014;5.

20. Männisto PT, Vanäläinen J, Jalkanen A, García-Horsman JA. Prolyl oligopeptidase: A potential target for the treatment of cognitive disorders. Drug News Perspect. 2007;20(5):293.

21. Tenorio-Laranga J, T. Mannisto P, Arturo Garcia-Horsman J. Hunting for Peptide Substrates of Prolyl Oligopeptidase: Classical Versus Non-Classical Bioactive Peptides. CNS Neurol Disord Drug Targets. 2011 May 1;10(3):319–26.

22. Rea D, Fulop V. Prolyl Oligopeptidase Structure and Dynamics. CNS Neurol Disord Drug Targets. 2011 May 1;10(3):306–10.

23. Szeltner Z, Polgár L. Structure, function and biological relevance of prolyl oligopeptidase. Curr Protein Pept Sci. 2008 Feb;9(1):96–107.

24. Walter R, Shlank H, Glass JD, Schwartz IL, Kerenyi TD. Leucylglycinamide released from oxytocin by human uterine enzyme. Science (1979). 1971;173(3999):827–9.

25. Jalkanen AJ, Savolainen K, Forsberg MM. Inhibition of prolyl oligopeptidase by KYP-2047 fails to increase the extracellular neurotensin and substance P levels in rat striatum. Neurosci Lett. 2011 Sep 15;502(2):107–11.

26. Matsuda T, Sakaguchi M, Tanaka S, Yoshimoto T, Takaoka M. Prolyl oligopeptidase is a glyceraldehyde-3-phosphate dehydrogenase-binding protein that regulates genotoxic stress-induced cell death. International Journal of Biochemistry and Cell Biology. 2013 Apr;45(4):850–7.

27. Fülöp, V., Böcskei, Z. & Polgar L. Prolyl oligopeptidase: an unusual beta-propeller domain regulates proteolysis. Cell. 1998;94(2):161–170.

28. Polgir L. Structural relationship between lipases and peptidases of the prolyl oligopeptidase family. Vol. 311, Chztobcr. European Biochemical Societies; 1992.

29. Tarragó T, Martín-Benito J, Sabidó E, Claasen B, Madurga S, Gairí M, et al. A new side opening on prolyl oligopeptidase revealed by electron microscopy. FEBS Lett. 2009 Oct 20;583(20):3344–8.

30. López A, Vilaseca M, Madurga S, Varese M, Tarragó T, Giralt E. Analyzing slowly exchanging protein conformations by ion mobility mass spectrometry: study of the dynamic equilibrium of prolyl oligopeptidase. Journal of Mass Spectrometry. 2016;51(7):504–11.

31. Wilk S. Prolyl endopeptidase. Life Sci. 1983;33(22):2149–2147.

32. Goossens F, De Meester I, Vanhoof G, Scharpé S. Distribution of Prolyl Oligopeptidase in Human Peripheral Tissues and Body Fluids. Clin Chem Lab Med [Internet]. 1996;34(1).

33. Myöhänen TT, García-Horsman JA, Tenorio-Laranga J, Männistö PT. Issues About the Physiological Functions of Prolyl Oligopeptidase Based on Its Discordant Spatial Association With Substrates and Inconsistencies Among mRNA, Protein Levels, and Enzymatic Activity. Journal of Histochemistry & Cytochemistry. 2009 Sep 26;57(9):831–48.

34. Matsuda T, Sakaguchi M, Tanaka S, Yoshimoto T, Takaoka M. Prolyl oligopeptidase is a glyceraldehyde-3-phosphate dehydrogenase-binding protein that regulates genotoxic stress-induced cell death. Int J Biochem Cell Biol. 2013 Apr;45(4):850–7.

35. García-Horsman JA, Männistö PT, Venäläinen JI. On the role of prolyl oligopeptidase in health and disease. Neuropeptides. 2007;41(1):1–24.

36. Jalkanen AJ, Leikas J V., Forsberg MM. Prolyl oligopeptidase inhibition decreases extracellular acetylcholine levels in rat hippocampus and prefrontal cortex. Neurosci Lett. 2014;579:110–3.

37. Prades R, Munarriz-Cuezva E, Urigüen L, Gil-Pisa I, Gómez L, Mendieta L, et al. The prolyl oligopeptidase inhibitor IPR19 ameliorates cognitive deficits in mouse models of schizophrenia. European Neuropsychopharmacology [Internet]. 2017 Feb;27(2):180–91.

38. Babkova K, Korabecny J, Soukup O, Nepovimova E, Jun D, Kuca K. Prolyl oligopeptidase and its role in the organism: attention to the most promising and clinically relevant inhibitors. Future Med Chem. 2017 Jun;9(10):1015–38.

39. Yiannopoulou KG, Anastasiou AI, Zachariou V, Pelidou SH. Reasons for Failed Trials of Disease-Modifying Treatments for Alzheimer Disease and Their Contribution in Recent Research. Biomedicines. 2019 Dec 9;7(4):97.

40. Di Daniel E, Glover CP, Grot E, Chan MK, Sanderson TH, White JH, et al. Prolyl oligopeptidase binds to GAP-43 and functions without its peptidase activity. Molecular and Cellular Neuroscience. 2009;41(3):373–82.

41. Szeltner Z, Morawski M, Juhász T, Szamosi I, Liliom K, Csizmók V, et al. GAP43 shows partial co-localisation but no strong physical interaction with prolyl oligopeptidase. Biochim Biophys Acta Proteins Proteom. 2010;1804(12):2162–76.

42. Savolainen MH, Richie CT, Harvey BK, Männistö PT, Maguire-Zeiss KA, Myöhänen TT. The beneficial effect of a prolyl oligopeptidase inhibitor, KYP-2047, on alpha-synuclein clearance and autophagy in A30P transgenic mouse. Neurobiol Dis. 2014;68:1–15.

43. Hannula MJ, Myöhänen TT, Tenorio-Laranga J, Männistö PT, Garcia-Horsman JA. Prolyl oligopeptidase colocalizes with α-synuclein, β-amyloid, tau protein and astroglia in the post-mortem brain samples with Parkinson's and Alzheimer's diseases. Neuroscience. 2013;242:140–50.

44. Brandt I, Gérard M, Sergeant K, Devreese B, Baekelandt V, Augustyns K, et al. Prolyl oligopeptidase stimulates the aggregation of α-synuclein. Peptides (NY). 2008 Sep;29(9):1472–8.

45. Schulz I, Zeitschel U, Rudolph T, Ruiz-Carrillo D, Rahfeld JU, Gerhartz B, et al. Subcellular localization suggests novel functions for prolyl endopeptidase in protein secretion. J Neurochem. 2005;94(4):970–9.

46. B Williams RS, Cheng L, Mudge AW, Harwood AJ. A common mechanism of action for three mood-stabilizing drugs [Internet]. 2002. Available from: www.nature.com

47. Li Z, Wu F, Zhang X, Chai Y, Chen D, Yang Y, et al. Valproate attenuates endoplasmic reticulum stress-induced apoptosis in SH-SY5Y cells via the AKT/GSK3β signaling pathway. Int J Mol Sci. 2017 Feb 8;18(2).

48. Duan L, Ying G, Danzer B, Perez RE, Shariat-Madar Z, Levenson V V., et al. The prolyl peptidases PRCP/PREP regulate IRS-1 stability critical for rapamycin-induced feedback activation of PI3K and AKT. Journal of Biological Chemistry. 2014 Aug 1;289(31):21694–705.

49. Wang L, Zhou K, Fu Z, Yu D, Huang H, Zang X, et al. Brain Development and Akt Signaling: the Crossroads of Signaling Pathway and Neurodevelopmental Diseases. Vol. 61, Journal of Molecular Neuroscience. Springer New York LLC; 2017. p. 379–84.

50. Crino PB. The mTOR signalling cascade: paving new roads to cure neurological disease. Nat Rev Neurol. 2016 Jul 24;12(7):379–92.

51. Emamian ES. AKT/GSK3 signaling pathway and schizophrenia. Frontiers in Molecular Neuroscience. 2012. p. 1–12.

52. Zheng W, Wang H, Zeng Z, Lin J, Little PJ, Srivastava LK, et al. The possible role of the Akt signaling pathway in schizophrenia. Vol. 1470, Brain Research. 2012. p. 145–58.

53. Eteläinen TS, Silva MC, Uhari-Väänänen JK, De Lorenzo F, Jäntti MH, Cui H, et al. A prolyl oligopeptidase inhibitor reduces tau pathology in cellular models and in mice with tauopathy. Sci Transl Med. 2023 Apr 12;15(691).

54. Männisto PT, Vanäläinen J, Jalkanen A, García-Horsman JA. Prolyl oligopeptidase: A potential target for the treatment of cognitive disorders. Drug News Perspect. 2007;20(5):293.

55. Millet O, Tarragó T, Gairí M, Kotev M, López A, Giralt E, et al. Active-Site-Directed Inhibitors of Prolyl Oligopeptidase Abolish Its Conformational Dynamics. ChemBioChem. 2016;17(10):913–7.

56. Tarrago T, Kichik N, Seguí J, Giralt E. The Natural Product Berberine is a Human Prolyl Oligopeptidase Inhibitor. ChemMedChem. 2007 Mar 12;2(3):354–9.

57. Mariaule G, De Cesco S, Airaghi F, Kurian J, Schiavini P, Rocheleau S, et al. 3-Oxo-hexahydro-1 *H* -isoindole-4-carboxylic Acid as a Drug Chiral Bicyclic Scaffold: Structure-Based Design and Preparation of Conformationally Constrained Covalent and Noncovalent Prolyl Oligopeptidase Inhibitors. J Med Chem. 2016 May 12;59(9):4221–34.

58. Guardiola S, Prades R, Mendieta L, Brouwer AJ, Streefkerk J, Nevola L, et al. Targeted Covalent Inhibition of Prolyl Oligopeptidase (POP): Discovery of Sulfonylfluoride Peptidomimetics. Cell Chem Biol. 2018 Aug;25(8):1031-1037.e4.

59. López A, Tarragó T, Giralt E. Low molecular weight inhibitors of Prolyl Oligopeptidase: a review of compounds patented from 2003 to 2010. Expert Opin Ther Pat. 2011 Jul 3;21(7):1023–44.

60. Bakker A V, Jung S, Spencer RW, Vinick FJ, Faraci WS. Slow tight-binding inhibition of prolyl endopeptidase by benzyloxycarbonyl-prolyl-prolinal. Biochemical Journal. 1990 Oct 15;271(2):559–62.

61. YOSHIMOTO T, KAWAHARA K, MATSUBARA F, KADO K, TSURU D. Comparison of Inhibitory Effects of Prolinal-Containing Peptide Derivatives on Prolyl Endopeptidases from Bovine Brain and Flavobacterium1. The Journal of Biochemistry. 1985 Oct;98(4):975–9.

62. Abramowitz N, Schechter I, Berger A. On the size of the active site in proteases II. Carboxypeptidase-A. Biochem Biophys Res Commun. 1967 Dec;29(6):862–7.

63. Schechter I, Berger A. On the size of the active site in proteases. I. Papain. Biochem Biophys Res Commun. 1967 Apr;27(2):157–62.

64. Li M, Chen C, Davies DR, Chiu TK. Induced-fit Mechanism for Prolyl Endopeptidase. Journal of Biological Chemistry. 2010 Jul;285(28):21487–95.

65. Shinoda M, Matsuo A, Toide K. Pharmacological studies of a novel prolyl endopeptidase inhibitor, JTP-4819, in rats with middle cerebral artery occlusion. Eur J Pharmacol. 1996 Jun;305(1–3):31–8.

66. Toide K, Iwamoto Y, Fujiwara T, Abe H. JTP-4819: a novel prolyl endopeptidase inhibitor with potential as a cognitive enhancer. J Pharmacol Exp Ther [Internet]. 1995 Sep;274(3):1370–8.

67. Peltonen I, Jalkanen AJ, Sinervä V, Puttonen KA, Männistö PT. Different Effects of Scopolamine and Inhibition of Prolyl Oligopeptidase on Mnemonic and Motility Functions of Young and 8- to 9-Month-Old Rats in the Radial-Arm Maze. Basic Clin Pharmacol Toxicol. 2010 Apr;106(4):280–7.

68. Katsube N, Sunaga K, Aishita H, Chuang DM, Ishitani R. ONO-1603, a potential antidementia drug, delays age-induced apoptosis and suppresses overexpression of glyceraldehyde-3-phosphate dehydrogenase in cultured central nervous system neurons. J Pharmacol Exp Ther. 1999;288(1):6–13.

69. Schneider JS, Giardiniere M, Morain P. Effects of the prolyl endopeptidase inhibitor S 17092 on cognitive deficits in Chronic low dose MPTP-treated monkeys. Neuropsychopharmacology. 2002;26(2):176–82.

70. Morain P, Boeijinga PH, Demazières A, De Nanteuil G, Luthringer R. Psychotropic profile of S 17092, a prolyl endopeptidase inhibitor, using quantitative EEG in young healthy volunteers. Neuropsychobiology. 2007;55(3–4):176–83.

71. Kim YS, Joh TH. Matrix Metalloproteinases, New Insights into the Understanding of Neurodegenerative Disorders. Biomol Ther (Seoul). 2012 Mar 31;20(2):133–43.

72. Rivera S, Khrestchatisky M, Kaczmarek L, Rosenberg GA, Jaworski DM. Metzincin Proteases and Their Inhibitors: Foes or Friends in Nervous System Physiology? Journal of Neuroscience [Internet]. 2010 Nov 17;30(46):15337–57.

73. Cui N, Hu M, Khalil RA. Biochemical and Biological Attributes of Matrix Metalloproteinases. In: Progress in Molecular Biology and Translational Science [Internet]. 2017. p. 1–73.

74. Loffek S, Schilling O, Franzke CW. Biological role of matrix metalloproteinases: a critical balance. European Respiratory Journal. 2011 Jul 1;38(1):191–208.

75. Sorsa T, Tjäderhane L, Salo T. Matrix metalloproteinases (MMPs) in oral diseases. Oral Dis. 2004 Nov;10(6):311–8.

76. Perucca P, Scheffer IE, Kiley M. The management of epilepsy in children and adults. Medical Journal of Australia. 2018 Mar;208(5):226–33.

77. Clossen BL, Reddy DS. Novel therapeutic approaches for disease-modification of epileptogenesis for curing epilepsy. Biochimica et Biophysica Acta (BBA) - Molecular Basis of Disease. 2017 Jun;1863(6):1519–38.

78. Pitkänen A, Lukasiuk K. Mechanisms of epileptogenesis and potential treatment targets. The Lancet Neurology. 2011.

79. Rempe RG, Hartz AM, Bauer B. Matrix metalloproteinases in the brain and blood–brain barrier: Versatile breakers and makers. Journal of Cerebral Blood Flow & Metabolism. 2016 Sep 20;36(9):1481–507.

80. Vandooren J, Van Den Steen PE, Opdenakker G. Biochemistry and molecular biology of gelatinase B or matrix metalloproteinase-9 (MMP-9): The next decade. Crit Rev Biochem Mol Biol. 2013;48(3):222–72.

81. Pijet B, Stefaniuk M, Kostrzewska-Ksiezyk A, Tsilibary PE, Tzinia A, Kaczmarek L. Elevation of MMP-9 Levels Promotes Epileptogenesis After Traumatic Brain Injury. Mol Neurobiol. 2018;

82. Bronisz E, Kurkowska-Jastrzębska I. Matrix Metalloproteinase 9 in Epilepsy: The Role of Neuroinflammation in Seizure Development. Vol. 2016, Mediators of Inflammation. 2016. p. 1–14.

83. Overall CM, Kleifeld O. Validating matrix metalloproteinases as drug targets and anti-targets for cancer therapy. Nature Reviews Cancer. 2006.

84. Vandenbroucke RE, Libert C. Is there new hope for therapeutic matrix metalloproteinase inhibition? Nat Rev Drug Discov. 2014 Dec 7;13(12):904–27.

85. Zhang H, Chang M, Hansen CN, Basso DM, Noble-Haeusslein LJ. Role of Matrix Metalloproteinases and Therapeutic Benefits of Their Inhibition in Spinal Cord Injury. Neurotherapeutics. 2011 Apr 1;8(2):206–20.

86. Rao B. Recent Developments in the Design of Specific Matrix Metalloproteinase Inhibitors aided by Structural and Computational Studies. Curr Pharm Des. 2005 Feb 1;11(3):295–322.

87. Cathcart JM, Cao J. MMP Inhibitors: Past, present and future. Front Biosci (Landmark Ed). 2015 Jun 1;20:1164–78.

88. Bertran A, Khomiak D, Konopka A, Rejmak E, Bulska E, Seco J, et al. Design and synthesis of selective and blood-brain barrier-permeable hydroxamate-based gelatinase inhibitors. Bioorg Chem. 2020 Jan;94:103365.

89. Emamian ES, Hall D, Birnbaum MJ, Karayiorgou M, Gogos JA. Convergent evidence for impaired AKT1-GSK3β signaling in schizophrenia. Nat Genet. 2004 Feb 25;36(2):131–7.

90. Millward TA, Zolnierowicz S, Hemmings BA. Regulation of protein kinase cascades by protein phosphatase 2A. Trends Biochem Sci. 1999 May;24(5):186–91.

91. Williams RSB, Cheng L, Mudge AW, Harwood AJ. A common mechanism of action for three mood-stabilizing drugs. Nature. 2002 May;417(6886):292–5.

92. Peltonen I, Männistö PT. Effects of Diverse Psychopharmacological Substances on the Activity of Brain Prolyl Oligopeptidase. Basic Clin Pharmacol Toxicol. 2011 Jan;108(1):46–54.

93. Schulz I, Zeitschel U, Rudolph T, Ruiz-Carrillo D, Rahfeld JU, Gerhartz B, et al. Subcellular localization suggests novel functions for prolyl endopeptidase in protein secretion. J Neurochem. 2005 Aug;94(4):970–9.

94. Griffith OW. Mechanism of action, metabolism, and toxicity of buthionine sulfoximine and its higher homologs, potent inhibitors of glutathione synthesis. J Biol Chem. 1982 Nov 25;257(22):13704–12.

95. Wu H, Wang X, Gao Y, Lin F, Song T, Zou Y, et al. NMDA receptor antagonism by repetitive MK801 administration induces schizophrenia-like structural changes in the rat brain as revealed by voxel-based morphometry and diffusion tensor imaging. Neuroscience. 2016 May;322:221–33.

96. Zhang L. Migration of retinal pigment epithelial cells is EGFR PI3K AKT dependent. Frontiers in Bioscience. 2013;S5(2):S398.

97. Sabbah DA, Hajjo R, Sweidan K. Review on Epidermal Growth Factor Receptor (EGFR) Structure, Signaling Pathways, Interactions, and Recent Updates of EGFR Inhibitors. Curr Top Med Chem. 2020 May 19;20(10):815–34.

98. Castañé A, Santana N, Artigas F. PCP-based mice models of schizophrenia: differential behavioral, neurochemical and cellular effects of acute and subchronic treatments. Psychopharmacology (Berl). 2015 Nov 7;232(21–22):4085–97.

99. Gumusoglu SB, Stevens HE. Maternal Inflammation and Neurodevelopmental Programming: A Review of Preclinical Outcomes and Implications for Translational Psychiatry. Biol Psychiatry. 2019 Jan;85(2):107–21.

100. Bergdolt L, Dunaevsky A. Brain changes in a maternal immune activation model of neurodevelopmental brain disorders. Prog Neurobiol. 2019 Apr;175:1–19.

101. Meyer U, Feldon J. To poly(I:C) or not to poly(I:C): Advancing preclinical schizophrenia research through the use of prenatal immune activation models. Neuropharmacology. 2012 Mar;62(3):1308–21.

102. Canetta S, Brown A. Prenatal infection, maternal immune activation, and risk for schizophrenia. Transl Neurosci. 2012 Jan 1;3(4).

103. Nestler EJ, Hyman SE. Animal models of neuropsychiatric disorders. Nat Neurosci. 2010 Oct 27;13(10):1161–9.

104. Svarcbahs R, Jäntti M, Kilpeläinen T, Julku UH, Urvas L, Kivioja S, et al. Prolyl oligopeptidase inhibition activates autophagy via protein phosphatase 2A. Pharmacol Res. 2020 Jan;151:104558.

105. Gottlicher M. Valproic acid defines a novel class of HDAC inhibitors inducing differentiation of transformed cells. EMBO J. 2001 Dec 17;20(24):6969–78.

106. Brandt I, Gérard M, Sergeant K, Devreese B, Baekelandt V, Augustyns K, et al. Prolyl oligopeptidase stimulates the aggregation of α-synuclein. Peptides (NY). 2008;29(9):1472–8.

107. Lambeir AM. Interaction of Prolyl Oligopeptidase with α-Synuclein. CNS Neurol Disord Drug Targets. 2011 May 1;10(3):349–54.

108. Wavreille ASM. Src homology 2 domain proteins binding specificity: from combinatorial chemistry to cell-permeable inhibitors. 2006.

109. Spillantini MG, Crowther RA, Jakes R, Hasegawa M, Goedert M. alpha-Synuclein in filamentous inclusions of Lewy bodies from Parkinson's disease and dementia with lewy bodies. Proc Natl Acad Sci U S A. 1998;95(11):6469–73.

110. Brandt I, Gérard M, Sergeant K, Devreese B, Baekelandt V, Augustyns K, et al. Prolyl oligopeptidase stimulates the aggregation of α-synuclein. Peptides (NY) [Internet]. 2008 Sep;29(9):1472–8.

111. Savolainen MH, Yan X, Myöhänen TT, Huttunen HJ. Prolyl oligopeptidase enhances α-Synuclein dimerization via direct protein-protein interaction. Journal of Biological Chemistry. 2015;290(8):5117–26.

112. Oestreicher AB, de Graan PNE, Gispen WH, Verhaagen J, Schrama LH. B-50, the growth associated protein-43: Modulation of cell morphology and communication in the nervous system. Prog Neurobiol. 1997;53(6):627–86.

113. Aigner L, Caroni P. Depletion of 43-kD growth-associated protein in primary sensory neurons leads to diminished formation and spreading of growth cones. Journal of Cell Biology. 1993;123(2):417–29.

114. Höfling C, Kulesskaya N, Jaako K, Peltonen I, Männistö PT, Nurmi A, et al. Deficiency of prolyl oligopeptidase in mice disturbs synaptic plasticity and reduces anxiety-like behaviour, body weight, and brain volume. European Neuropsychopharmacology. 2016;26(6):1048–61.

115. Uryu K, Butler AK, Chesselet MF. Synaptogenesis and ultrastructural localization of the polysialylated neural cell adhesion molecule in the developing striatum. Journal of Comparative Neurology. 1999;405(2):216–32.

116. Diano S, Jeong JK, Kim JD, D'Agostino G, Calignano A, Liu ZW, et al. Prolyl Endopeptidase-Deficient Mice Have Reduced Synaptic Spine Density in the CA1 Region of the Hippocampus, Impaired LTP, and Spatial Learning and Memory. Cerebral Cortex. 2012;23(8):2007–14.

117. Matamoros AJ, Baas PW. Microtubules in health and degenerative disease of the nervous system. Brain Res Bull. 2016;126(Pt 3):217–25.

118. Zhou RM, Huang YX, Li XL, Chen C, Shi Q, Wang GR, et al. Molecular interaction of α-synuclein with tubulin influences on the polymerization of microtubule in vitro and structure of microtubule in cells. Mol Biol Rep. 2010;37(7):3183–92.

119. Mackeh R, Perdiz D, Lorin S, Codogno P, Poüs C. Autophagy and microtubules – new story, old players. J Cell Sci. 2013 Mar 1;126(5):1071–80.

120. Rong Y, Liu M, Ma L, Du W, Zhang H, Tian Y, et al. Clathrin and phosphatidylinositol-4,5-bisphosphate regulate autophagic lysosome reformation. Nat Cell Biol. 2012 Sep 12;14(9):924–34.

121. Dikic I, Elazar Z. Mechanism and medical implications of mammalian autophagy. Nat Rev Mol Cell Biol. 2018 Jun 4;19(6):349–64.

122. Klionsky DJ. Autophagy revisited: A conversation with Christian de Duve. Autophagy. 2008 Aug 16;4(6):740–3.

123. Hansen M, Rubinsztein DC, Walker DW. Autophagy as a promoter of longevity: insights from model organisms. Nat Rev Mol Cell Biol. 2018 Sep 13;19(9):579–93.

124. Kaushik S, Cuervo AM. The coming of age of chaperone-mediated autophagy. Nat Rev Mol Cell Biol. 2018 Jun 6;19(6):365–81.

125. Levine B, Kroemer G. SnapShot: Macroautophagy. Cell. 2008 Jan;132(1):162.e1-162.e3.

126. Yim WWY, Mizushima N. Lysosome biology in autophagy. Cell Discov. 2020 Feb 11;6(1):6.

127. Aburto MR, Hurlé JM, Varela-Nieto I, Magariños M. Autophagy During Vertebrate Development. Cells. 2012 Aug 2;1(3):428–48.

128. Glick D, Barth S, Macleod KF. Autophagy: Cellular and molecular mechanisms. Journal of Pathology. 2010.

129. Mizushima N. Autophagy: Process and function. Genes and Development. 2007.

130. Mizushima N, Komatsu M. Autophagy: Renovation of Cells and Tissues. Cell [Internet]. 2011 Nov;147(4):728–41.

131. Tanida I, Ueno T, Kominami E. LC3 and Autophagy. In 2008. p. 77–88.

132. Lynch-Day MA, Mao K, Wang K, Zhao M, Klionsky DJ. The Role of Autophagy in Parkinson's Disease. Cold Spring Harb Perspect Med. 2012 Apr 1;2(4):a009357–a009357.

133. Kilpeläinen TP, Hellinen L, Vrijdag J, Yan X, Svarcbahs R, Vellonen KS, et al. The effect of prolyl oligopeptidase inhibitors on alpha-synuclein aggregation and autophagy cannot be predicted by their inhibitory efficacy. Biomedicine & Pharmacotherapy. 2020 Aug;128:110253.

134. Catarino S, Pereira P, Girão H. Molecular control of chaperone-mediated autophagy. Lane JD, Korolchuk VI, Murray JT, editors. Essays Biochem. 2017 Dec 12;61(6):663–74.

135. Ratnaparkhi M P, Pandya CSP. PEPTIDES AND PROTEINS IN PHARMACEUTICALS. Int J Curr Pharm Res. 2011;

136. Ibraheem D, Elaissari A, Fessi H. Administration strategies for proteins and peptides. Int J Pharm. 2014 Dec;477(1–2):578–89.

137. Zhou XH, Po ALW. Peptide and protein drugs: II. Non-parenteral routes of delivery. Int J Pharm [Internet]. 1991 Sep;75(2–3):117–30.

138. Zeng M, Yang L, He D, Li Y, Shi M, Zhang J. Metabolic pathways and pharmacokinetics of natural medicines with low permeability. Drug Metabolism Reviews. 2017.

139. Coe KJ, Koudriakova T. Metabolic stability assessed by liver microsomes and hepatocytes. Methods in Pharmacology and Toxicology. 2014;

140. Alexandra Bertran-Junqué. Design and synthesis of selective MMP-9 inhibitors for the treatment of epilepsy. Universitat de Barcelona; 2018.

141. Broekaart DWM, Bertran A, Jia S, Korotkov A, Senkov O, Bongaarts A, et al. The matrix metalloproteinase inhibitor IPR-179 has antiseizure and antiepileptogenic effects. Journal of Clinical Investigation. 2021 Jan 4;131(1).

142. Flipo M, Charton J, Hocine A, Dassonneville S, Deprez B, Deprez-Poulain R. Hydroxamates: Relationships between structure and plasma stability. J Med Chem. 2009;

143. Hermant P, Bosc D, Piveteau C, Gealageas R, Lam B, Ronco C, et al. Controlling Plasma Stability of Hydroxamic Acids: A MedChem Toolbox. J Med Chem [Internet]. 2017 Nov 9;60(21):9067–89. Available from: http://pubs.acs.org/doi/10.1021/acs.jmedchem.7b01444

144. Lukacova V, Zhang Y, Mackov M, Baricic P, Raha S, Calvo JA, et al. Similarity of Binding Sites of Human Matrix Metalloproteinases. Journal of Biological Chemistry. 2004 Apr 2;279(14):14194–200.

145. Bagchi S, Chhibber T, Lahooti B, Verma A, Borse V, Jayant RD. In-vitro blood-brain barrier models for drug screening and permeation studies: an overview . Drug Des Devel Ther. 2019 Oct;Volume 13:3591–605.

146. Kansy M, Senner F, Gubernator K. Physicochemical High Throughput Screening: Parallel Artificial Membrane Permeation Assay in the Description of Passive Absorption Processes. J Med Chem. 1998 Mar 1;41(7):1007–10.

147. Kalepu S, Nekkanti V. Insoluble drug delivery strategies: review of recent advances and business prospects. Acta Pharm Sin B. 2015 Sep;5(5):442–53.

148. Love Kumar Soni SSSRKM. Development of parenteral formulation of poorly water soluble drugs: the role of novel mixed-solvency concept. Asian J Pharm. 2017 Jan;11.

149. Wen H, Jung H, Li X. Drug Delivery Approaches in Addressing Clinical Pharmacology-Related Issues: Opportunities and Challenges. AAPS J. 2015 Nov 15;17(6):1327–40.

150. European Medicines Agency. Cyclodextrins used as excipients. Report published in support of the 'Questions and answers on cyclodextrins used as excipients in medicinal products for human use.' 2017.

151. Lloyd-Williams P, Albericio F, Giralt E. Chemical Approaches to the Synthesis of Peptides and Proteins. CRC Press LCC. 1995;95–130.

152. Kaiser E, Colescott RL, Bossinger CD, Cook PI. Color test for detection of free terminal amino groups in the solid-phase synthesis of peptides. Anal Biochem. 1970 Apr;34(2):595–8.

153. Christensen TA. Test for Monitoring Coupling Completness in Solid Phase Peptide Synthesis Using Chloranil. acta Chem sca. 1979;33:163–766.

154. Mellor SL, McGuire C, Chan WC. N-Fmoc-aminooxy-2-chlorotrityl polystyrene resin: A facile solid-phase methodology for the synthesis of hydroxamic acids. Tetrahedron Lett. 1997 May;38(18):3311–4.

155. Vandooren J. Gelatin degradation assay reveals MMP-9 inhibitors and function of O-glycosylated domain. World J Biol Chem. 2011;2(1):14.

156. Di L, Kerns EH, Fan K, McConnell OJ, Carter GT. High throughput artificial membrane permeability assay for blood–brain barrier. Eur J Med Chem. 2003 Mar;38(3):223–32.

157. Di L, Kerns EH, Hong Y, Chen H. Development and application of high throughput plasma stability assay for drug discovery. Int J Pharm [Internet]. 2005 Jun;297(1–2):110–9.